No guts, no reef: understanding the microbiome, genetic diversity, and phylogenetic relationships of the Puerto Rican long-spined black sea urchin, *Diadema antillarum*, a keystone species of the Caribbean reef

By:

Alejandro J. Mercado Capote

A thesis submitted in partial fulfillment of the requirements for the degree of

MASTER OF SCIENCE
in
BIOLOGY

UNIVERSITY OF PUERTO RICO
MAYAGÜEZ CAMPUS

2020

Approved by:

Juan Carlos Martínez Cruzado, Ph.D. President, Graduate Committee	Date
Audrey Majeske, Ph.D. Member, Graduate Committee	Date
Nikolaos V. Schizas, Ph.D. Member, Graduate Committee	Date
Taras K. Olesyk, Ph.D. Member, Graduate Committee	Date
Rosa I. Román Pérez, Ph.D. Representative, Office of Graduate Studies	Date
Ana V. Vélez Díaz, M.S. Chair, Department of Biology	Date

Abstract

In this paper we describe the gut microbiome of the Puerto Rican keystone sea urchin *Diadema antillarum*. We also used next generation sequencing of the c*ytochrome b* region to examine the phylogenetic relationships among the different samples. The gut microbial communities were mostly populated with Proteobacteria, in which a large proportion were in the class Alphaproteobacteria, followed by classes Betaproteobacteria and Gammaproteobacteria. Firmicutes, Clostrodiales and Tenericutes were other represented phyla in the gut tissue samples of *D. antillarum*. Within Tenericutes, only several animals were harboring the species *Candidatus hepatoplasma*. There is reason to suspect that all these bacteria do not represent a threat to the sea urchin except for the Firmicutes. *Clostridium* are a known type of highly virulent bacteria that could potentially be the main cause behind the great *Diadema antillarum* die off. Bioinformatic and statistical analysis using pairwise chi-square analysis also reveal that anthropogenic activities can impact the microbiome. Current strength and relative position on the island may also play a role on defining the microbiome. The sea urchins living upstream have a statistically different composition that animals living downstream. These findings paint a clearer picture of the Puerto Rican *D. antillarum* population that can aid in the efforts to restore former numbers of these animals.

Alejandro J Mercado Capote 2020 ©

Resumen

En este artículo se describe el microbioma intestinal del erizo de mar vital puertorriqueño *Diadema antillarum*. Se utilizo la secuenciación de próxima generación para amplificar y examinar la región del *citocromo b* para poder determinar las relaciones filogenéticas entre las diferentes muestras. Las comunidades microbianas intestinales del erizo estaban pobladas en su mayoría por *Proteobacteria*, que eran una gran proporción la clase *Alphaproteobacteria*, seguida de las clases *Betaproteobacteria* y *Gammaproteobacteria. Firmicutes, Clostrodiales* y *Tenericutes* fueron otros filos representados en las muestras de tejido intestinal de *D. antillarum*. Dentro de los Tenericutes, solo varios animales albergaban la especie *Candidatus hepatoplasma*. Hay motivos para sospechar que todas estas bacterias no representan una amenaza para el erizo de mar a excepción de los Firmicutes. Adentro de la clase Clostridum hay bacterias altamente virulentes que podrían ser la causa principal de la muerta del erizo de mar *D. antillarum*. El análisis bioinformático y estadístico mediante el análisis de chi-cuadrado por pares también revela que las actividades antropogénicas pueden afectar el microbioma. La fuerza actual y la posición relativa en la isla también pueden influir en la definición del microbioma. Los erizos de mar que viven río arriba tienen una composición estadísticamente diferente a la de los animales que viven río abajo. Estos hallazgos pintan una imagen más clara de la población puertorriqueña de *D. antillarum* que puede ayudar en los esfuerzos para restaurar los números anteriores de estos animales.

Alejandro J Mercado Capote 2020 ©

Acknowledgements

Foremost, I would like to express my genuine gratitude to my committee members for the continuous support I received throughout my academic career at University Mayagüez at Puerto Rico. I want to thank my advisor Prof. Audrey Majeske for her incredible insights, persistence, motivation, and communication. Her guidance was essential throughout the entire life of the project and this project would have not been possible without her. I want to extend my thanks to Prof. Juan Carlos Martinez Cruzado for his guidance and patience from the very beginning. My sincere thanks to Prof. Taras Olesyk who was an essential member that helped the entire project through his invaluable knowledge, and experience. Also, Prof. Nikolaos Schizas who provided meaningful suggestions and guidance through the entire process. Lastly, Professor Heidy Morales who was there at the seeding of this project.

I want to also extend my thanks to my colleagues who helped me throughout my career. To Mrs. Stephanie Castro Marquez for helping me and the project with her ideas, comments, and doing the immaculate sequencing lab work. I would like to thank my friend Edmundo Torres, who helped me solve bioinformatic errors and gave many comments and feedback. I would also like to thank Raul Mojica Soto-Albors for helping me with the impeccable lab work at the earlier stages of the project. My previous instructor and friend Mr. Walter Wolfsberger who aided in the bioinformatics and gave excellent insights. Also, my friend David Repollet for helping me with useful comments, feedback, and urchin collection. All the friends, students and family that helped me with the collection, Mariana Torres Gonzales, and Victor Martinez. Thanks to my students as well for the curiosity in my projects among many other classmates and lab partners. Also, I want to thank my parents for all the support during this period.

I would like to thank the Sequencing Facility at Escuela de Medicina de Ponce who conducted sequencing as well. As thanks to the Department of Natural Resources of Puerto Rico (DRNA) for given me the permission to work with this vulnerable species. Finally, I would like to thank the University of Mayaguez of Puerto Rico and the Department of Biology for providing me with the facilities and knowledge that lead to this project and its findings.

Table of Content

Table of Figures

Introduction

The importance of Diadema antillarum

Sea urchins are a marine model that have been used extensively for scientific investigations in ecology, toxicology, aquaculture, development, molecular and cell biology, pathology, genetics, and many other fields (Agnello 2017; Bianchini et al. 2005, 2007; Bielmyer et al. 2005; Buttino et al. 2016; Defilippo et al. 2008; Zhang 2019; Varrella et al. 2016; Gambardella et al. 2018, 2015). Sea urchins appeared around half a billion years ago, before the Cambrian explosion, and they represent an important midpoint between the vertebrates and invertebrates. The apparent homology with vertebrate genomes has been used extensively in multiple comparative genomic studies: there are more than 7,000 sea urchin genes conserved in humans associated with many different illnesses (Sodergren et. al. 2006; Agnello 2017).

Sea urchins also play an important role in the ecosystem. The long-spined sea urchin *Diadema antillarum* is a keystone benthic community member that helps keep the balance of the fragile and decaying coral reef marine ecosystem by grazing on low-nutrient algae allowing for coral reef spawning (Carperter 1988; Carperter & Edmund 2006) and providing complex spaces for predator-prey dynamics with its long spines (Alvarez-Filip 2009).

Previous studies have indicated that since the 1970s, the Caribbean reef system has declined consistently and scientists have correlated this with several key events in recent history: the loss of the dominant reef-building *Acropora* corals, the mass mortality of the grazing urchin, *Diadema antillarum*, and the 1998 El Niño Southern Oscillation-induced worldwide coral bleaching event (Álvarez-Filip 2009) among with over-fishing, pollution, habitat-destruction (Precht & Aronson 2006). These events are correlated, and are partially caused by global climate change, hurricanes, and anthropogenic factors (Hughes 1994; Precht & Aronson 2006; Mumby et al. 2007). The chronic decline in the Caribbean reef system has led to a marine ecosystem phase shift from "coral- to macroalgae-dominated benthic reef community" (Precht & Aronson 2006) by a drastic reduction of branching elkhorn (*Acropora palmata*) and staghorn coral (*Acropora cervicornis*) resulting in a system with low nutritional value that hinders severely coral growth and recovery (Carpenter 1988; Edmunds & Carpenter 2001, 2006). The role of the sea urchin is essential as it physically removes this macroalgae cover and provides the substrate necessary for coral settlement (Furman & Heck 2009) however high numbers of sea urchin can also be damaging to the ecosystem (Edmunds 2001). A phase-shift in which algae is dominant has detrimental consequences for the survival of juvenile corals. One study looked at places in which *D. antillarum* has made a recovery and it was observed that the coral reef ecosystem has made a recovery by reducing macroalgae cover (Furman & Heck 2009; Chiappone et al. 2002; Pretch et al. 2010). *D. antillarum* is a keystone marine species that provides complex topographical three-dimensional space to the ecosystem that is required to maintain fish density (Hay & Taylor 1985).

History

In the early 1980's *D. antillarum* suffered a mass mortality event due to an unknown pathogen (Lessios et al. 1984; Lessios 1988, 1995, 2004, 2015), and since no other sea urchin was affected during that time, it was likely caused by a species-specific pathogen (Defilippo 2018).

This mortality appeared to spread through surface currents (Lessios 1988) and the population numbers were depleted, and more than 90% of the population failed to recover in the next two decades. Before this event, the coral reefs at places like Discovery Bay, Jamaica were characterized by having coral as much as 90% of the substratum and by 1990, the coral cover was reduced to less than 5% (Edmunds & Carpenter 2001).

While *D. antillarum* populations have recovered in some places (Pretch et al. 2010), the ecosystems in other places have shifted accordingly, resulting in less macroalgal cover and enhanced coral cover and recruitment (Mumby 2007; Blanco et al. 2010; Lessios 2016). Due to the nature of this sea urchin's reproductive strategy, ie., broadcast spawning – where individuals will release gametes into their environment, the population must be high for the species to be successful (Allele Effect, Petersen and Levitan 2001; Feehan et al. 2016). Consequently, this species has yet to recover to its historic levels because they lack the numbers to successfully reproduce (Lessios 2016; Lessios 2005, Chiappone et al. 2013). Currently in Puerto Rico, the *D. antillarum* populations appear to be stable even though there is little evidence for recovery trends back to the pre-mass mortality densities (Rodriguez-Barreras 2018; Tuohy & Weil 2020).

As continued anthropogenic global climate change will result in extinctions, reduced species diversity, drastic changes in ecosystems (Blois et al. 2013; Moritz & Agudo 2013), and an increased likelihood of disease outbreaks (Burge et al. 2014; Harvell et al. 1999), we must continue to survey population recovery across the Caribbean if we want to design appropriate conservation and management practices for this momentous creature (Quintero 2014; Ripple 2017; Stimson et al. 2007; Sharp et al. 2017). Most of the research with populations of *D. antillarum* was conducted in the wake of the massive mortality event (Lessios et al. 1984; Lessios 1979; Lessios 1981; Lessios et al. 2001) which leaves us with important questions that remain unanswered, e.g. what can be said about the genetic flow, diversity and metapopulation of the Caribbean *D. antillarum* urchin? What are the current pathogenic exposures of this species? What can be said about the microbiome of this sea urchin? What can we learn about the phylogenetic relationships of the Puerto Rican population?

Microbiome & Genetic Flow

Some of these research questions can be explored by studying the microbiome of *D. antillarum,* which are bacteria present in the gut that have important roles because act as digestive organs and have also been suggested to be a secondary endocrine organ in humans (Ahmadmehrabi 2017). These roles include increasing energy extraction from food sources and increasing energy absorption, as well as interacting with molecules that have been shown to cause disease in humans (Baohong et al. 2018; Ahmadmehrabi & Tang 2017). The functional properties of the microbiome are attributed to the numerous genes found inside the metagenome that provides the host with unique and specific biochemical pathways (Baohong et al. 2018). In humans, it has been found that healthy individuals can have variations between each other and in some cases have different functional metabolic levels between subjects considered sedentary and professional athletes (Ahmadmehrabi 2017; Barton et al. 2017). In addition, it has been speculated that the microbiome is a source of genetic flow and immunity (Baohong et al. 2018).

Sea urchins along with amny other animals have digestive compartments that contain specific environments that help the organism efficiently extract nutrients (Ceja-Navarro et al. 2019; Ishaq & Wright 2012). Recent sequencing studies have shown that three species of sea urchin, *Lytechinus variegatus Strongylocentrotus purpuratus* and *Paracentrotus lividus* have intestinal microbiomes that are uniquely compartmentalized ecosystems, which have arisen due to active selection between the host and their commensal microorganisms (Hakim et al. 2015; Hakim et al. 2016; Hakim et al. 2019; Meziti et al. 2007).

Besides monitoring their population levels over the years since the massive mortality event in the 1980s, few genetic studies (Lessios 1979, 1981; Lessios et al. 1984, 2001) have been undertaken to monitor the population gene flow and genetic diversity of *D. antillarum* following a presumed Caribbean wide population bottleneck effect. As scientists are beginning to understand the ecological, immune, and health benefits of the intestinal microbiome in a variety of organisms, it is important to study the microbiome of *D. antillarum,* as it is an essential keystone species for the Caribbean reef system (**Figure 1**). The ecological role of *D. antillarum* is simple but important, and this organism could not perform that role without its microbiome that helps it degrade low nutritional macro-algae cover into nutrients. Also, microbiomes can provide us insight into the evolutionary history of the organism in question (Moeller 2016) and even provide the context of the functional role of microbiomes and how they work.

For this experiment, we collected *Diadema* specimens along the coasts of Puerto Rico and collected its gut contents. We identified the taxonomy of the gut microbiota using NextGen Illumina MiSeq sequencing technology and bioinformatic tools including QIIME2. In addition, to understand the animal's phylogeny a *cytochrome b* amplicon was sequenced and compared. According to previous studies done with avian species (Boonseub et al. 2009) the cytochrome B region was able to place the animals into their appropriate orders as compared to other molecular clocks like cytochrome oxidase I and ND2 genes. By understanding the gene flow, genetic diversity, gut microbiome and metapopulation phylogeny of *D. antillarum*, we can understand more about their ecological role both present and past which is important information for conservation efforts if another massive mortality were to occur or be prevented.

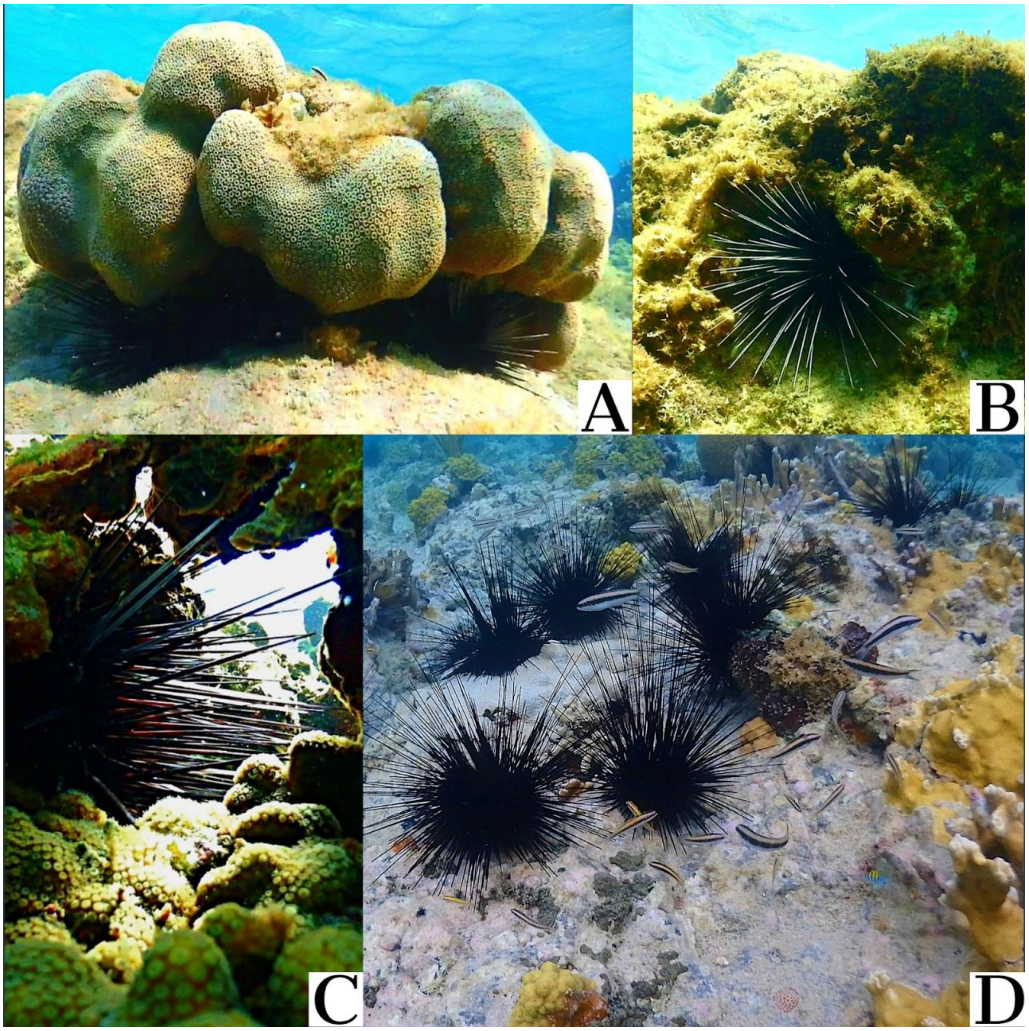

Figure 1. *The Puerto Rican subtidal reef habitat of the long-spined black sea urchin, Diadema antillarum*. Here, the sea urchins are shown hiding in different reef structures, hiding from predators, and finding food (A, B, C). The sea urchins move along the reef shelf to forage for food while other animals use their long spines to protect themselves from predators (D).

Methods & Methods

Ethical Statement

D. antillarum inhabits in fragile marine ecosystems and the procedures described here were done with extensive precaution to reduce organismal stress and environmental impact. The collection methods to work with this vulnerable species were approved by Departamento de Recursos Naturales of Puerto Rico (O-VS-PVS15AG-00047-01082018).

Animal and Demographic Collection

Sea urchins were collected across the island during December 2018. The sampled specimens were chosen independent of gender or size. To collect each animal, a diving knife was used to carefully separate *D. antillarum* from the environment by "scooping" the specimens from the place that they were found, usually in crevices and rocks across the different coral reefs. Sea urchins were collected across eight different cardinal locations from different municipalities of Puerto Rico representing: north, east, south and west. The municipalities were chosen based on accessibility and include: Ceiba, Culebra, Guánica, Guayama, Isabela, Luquillo, Ponce and Rincón. A total of 44 specimens were collected across the island (**Figure 2**).

A

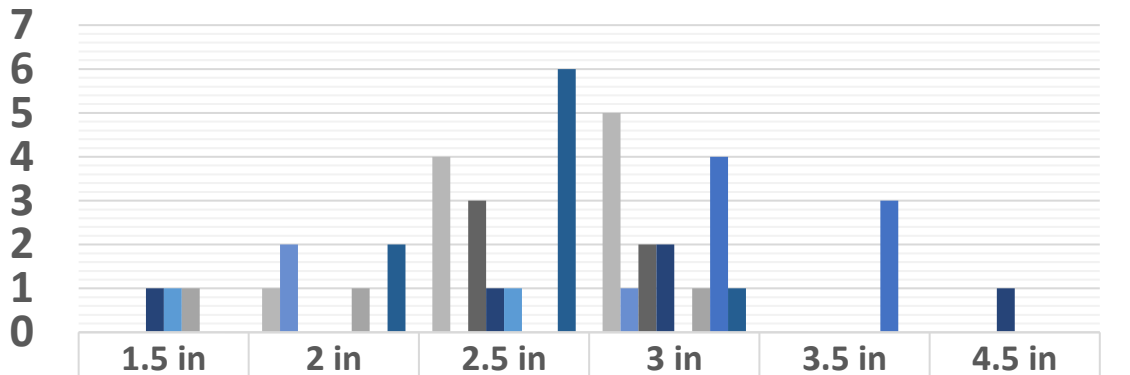

	1.5 in	2 in	2.5 in	3 in	3.5 in	4.5 in
Rincon	0	1	4	5	0	0
Ponce	0	2	0	1	0	0
Luquillo	0	0	3	2	0	0
Isabela	1	0	1	2	0	1
Guayama	1	0	1	0	0	0
Guanica	1	1	0	1	0	0
Culebra	0	0	0	4	3	0
Ceiba	0	2	6	1	0	0

B

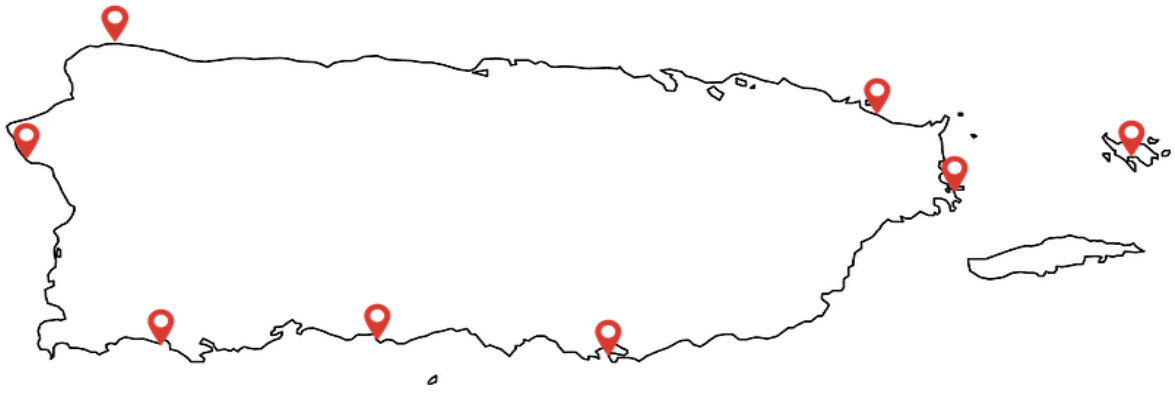

Figure 2. *Sea urchin collection distribution by location and size.* A total of 44 sea urchins were collected from the eight named municipalities in Puerto Rico (A). The number of collected animal samples, one per animal, are shown according to the size of the animal, as given by the diameter in inches (in). The locations of each collection site are indicated with a red open teardrop pin (B), which includes: Ceiba (18°13'07.8"N 65°36'15.4"W), Culebra (18°18'08.8"N 65°18'33.8"W), Guánica (17°56'05.2"N 66°57'25.6"W), Guayama (17°55'51.3"N 66°09'41.0"W; 17°55'47.3"N

66°09'32.1"W), Isabela (18°30'56.8"N 67°06'00.6"W), Luquillo (18°23'15.3"N 65°43'10.6"W), Ponce (17°57'50.5"N 66°36'35.9"W; 17°58'20.7"N 66°37'04.5"W; 17°57'54.5"N 66°36'28.1"W) and Rincón (18°20'35.2"N 67°15'36.5"W). A total of 44 samples were collected from Rincón (n=10), Guánica (n=3), Ponce(n=3), Isabela (n=5), Luquillo (n=5), Culebra (n=7), Ceiba (n=9), Guayama (n=2).

After the specimens were physically separated from the environment, they were placed in a diving bag to transport outside of the water. Once outside of the water, the specimens were placed in sea water to reduce harm until the individuals were measured and prepared for gut tissue collection (**Figure 3**).

Additional environmental was collected during animal sampling. The diameter of each animal was measured and recorded in inches. The relative surface water current was recorded as calm, medium or strong according to the cardinal sample location site, which is defined as calm in the south facing the Caribbean Sea, strong to the north facing the Atlantic Ocean and medium in the east and west, according to these positions between the Caribbean Sea and Atlantic Ocean.

Tissue Collection

Sea urchin gut samples were collected at each site to avoid overstressing the animal, potentially risk contamination, or even potentially change microbiome composition. Once the individuals were measured their spines were cut out and an incision was made in the test surrounding the peristomial membrane using ethanol sterilized scissors dissecting around the mouth (**Figure 3C**). The peristomial membrane, along with the nested mouth (Artistotle's Lantern) was lifted from the animal and the gut was collected using ethanol sterilized tweezers (**Figure 3D**). The samples were placed in a 1.5mL tube and held on ice while in immediate transition for storage in a -20 C freezer.

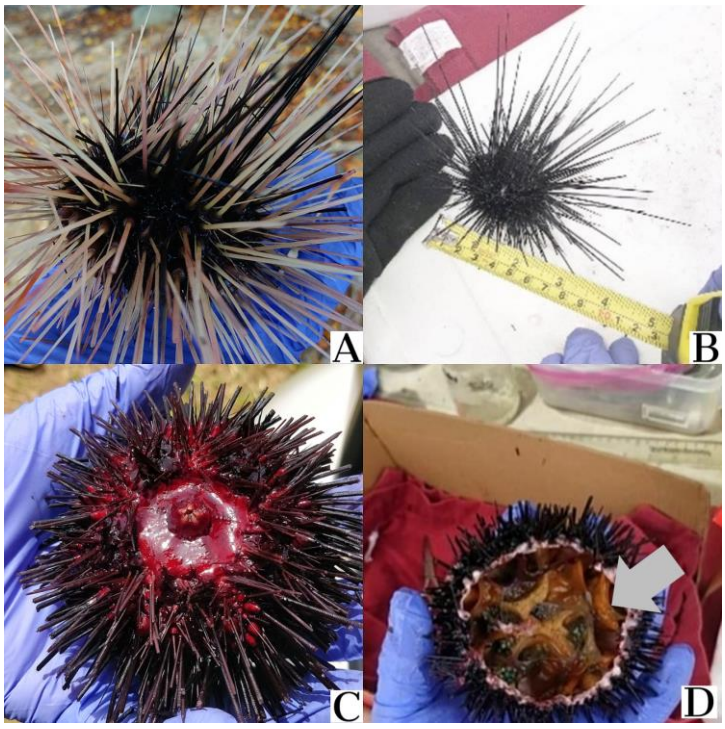

Figure 3. *Animal measurement and sample collection.* Relative specimen size is shown in (A). The diameter of the body test size was measured in inches (B). Sea urchin spines were cut prior to dissection. An incision was made through the peristomal membrane (C) to gain access to the inner wall and remove the Aristotle's lantern (mouth structure), prior to making a continuous circular incision to split the animal into two sections for sampling (D). A sample of the intestine tissue (grey arrow in D) was placed in a sterile tube and stored on ice during transit to the lab.

DNA Extraction

The Sigma-Aldrich GenElute Stool DNA Isolation Kit was used to isolate DNA from the samples according to the manufacturer's protocol. The DNA was eluted into 50 µL of the company provided buffer and immediately placed in the -20 ˚C freezer for long-term storage.

DNA Sequencing - 16S V4 Region

Samples were prepared for 16S rRNA targeted sequencing in the variable V3 and V4 region of the gene using the 16S Metagenomic Sequencing Library Preparation kit. Sequencing was performed on an Illumina MiSeq sequencing system that generated raw paired end reads. Sample preparation and sequencing were performed at the Ponce School of Medicine (Ponce, PR) core sequencing facility.

DNA Sequencing - cytochrome b Region

A subset of the 44 DNA samples (n=21) were subjected to PCR amplification targeting Cytochrome B. To construct the primers, a mitochondrial DNA sequence alignment from 27

closely related species to *D. antillarum* was used to design primers targeting Cytochrome B (Chunxia 2016; Bronstein 2019). The aligned sequences were found to be mostly conserved, at the 14,988 – 16,070 bp region in alignment. This segment of the conserved region was used to design the forward (14,968 - 14,987) and reverse (16,071-16,093) primers, which resulted in a 1,140 base pair fragment and were as follows: forward (5'-GGT|CCA|TTA|CGA|AAG|GAA|CA-3') and reverse (5'-AAT|CTT|TTT|TTC|TAG|GGT|ACA|TA-3'). Each PCR included 50 ng of template DNA, 0.5 mM of each primer, 20 mM of each deoxyribonucleotide, 25 mM MgCl2, 1x company supplied buffer, 0.025 U of Q5 High Fidelity DNA polymerase (New England Biolabs), 80% DMSO, and 25mM BSA. A total reaction volume of 25 µL was employed for each sample. The PCR program was 95 ˚C for 5 min followed by 35 cycles of 95 ˚C for 30 secs, 46˚C for 30 sec, 72 ˚C for 1:30min, with a final extension of 72 ˚C for 5 min and a hold at 4 ˚C. Amplicons were electrophoresed through 1.5% agarose 1 x TAE buffer (40 mM Tris, 20 mM Glacial Acetic Acid, 1 mM EDTA pH 8).. Amplified samples were held in the -20 ˚C freezer until transportation on ice to the OU Genomics Lab at Oakland University in Rochester, MI. PCR amplicons were purified using Ampure XP beads (Beckman Coulter) in a 0.5X dilution ratio to maximize recovery of the large amplicon size. A library of nucleotide fragments was generated per sample using the Nextera DNA Flex Library Prep Kit with a starting quantity of 100 ng, and according to the manufacturer's instructions. A unique adapter sequence was added to each sample prior to pooling. Pooled and indexed samples were diluted to a loading concentration of 200 pM prior to a final library dilution according to the iSeq100 sequencing system protocol. Samples were sequenced on an Illumina iSeq100 sequencer that generated raw paired end sequences.

Bioinformatic Analysis - Raw Data

The sample data along with commands used for this study can be found at (https://github.com/mercadocapote/diadema_ajmc2020). Two different sequencers were employed to generate the data using separate DNA aliquots from the same animal sample, that targeted the ribosomal 16S and cytochrome b genes. Additionally, there were sample metadata files generated by the researchers at the site of collection which described location, size, and habitat of each specimen. The metadata sample files are in the ". tsv" format.

Bioinformatic Analysis - QIIME2

The QIIME2 microbiome bioinformatics platform was used to perform the microbiome analysis of the 16S rRNA samples. All of the information pertaining to the installation procedures and how to use the software can be found at docs.qiime2.org. A virtual machine was installed using a Virtual Box Image previously installed with QIIME2 found in the online official documentation in QIIME2. The pipeline analysis was employed using the previously available protocols that largely followed the description given by Estaki (2020) but also according to the research described by Bolyen et al. (2019), Hall & Beiko (2018), and Hakim et al. (2016, 2015).

The data generated by Illumina's Casava software was first imported into QIIME2. Then a quality filtering process was applied based on quality scores. Quality control of sequences was then completed using a Deblur workflow with a trim length of 220 bps, which resulted in sequences that are referred to as sub-operational taxonomic units (OTUs), or more commonly called in the

QIIME2 documentation as features (Estaki 2020). This workflow included the removal of chimera and rare reads that accounted for <0.0005% of all the reads. A feature table was generated as an output of this workflow. A phylogenetic tree was then generated using the fragment-insertion tree building method described by Janseen et al. (2018) to conduct diversity analysis with Faith's phylogenetic diversity (Faith 1992) and UniFrac (Lozupone & Knight 2005). The Greengenes 16s rRNA reference database (McDonald et al. 2012) was used to identify the taxa and build a rooted phylogenetic tree. The feature table was filtered to only contain samples present in the phylogenetic tree. The sampling depth was evaluated using alpha rarefaction plots to determine if the within-sample diversity is fully reached. The sampling depth was taken from the Feature Table created in the quality filtering process and was p-max-depth 5677 which was the median frequency of features found in the samples. Using the pipeline action core-metrics-phylogenetic we rarefied the Feature Table to a p-sampling-depth of 2603 based on information on the Feature Table (Vaquez-Baeza, Pirrung, Gonzalez, & Knight 2013). This pipeline generates several alpha diversity metrics such as: Shannon's diversity index, a quantitative measure of community richness (Shannon & Weaver 1949); Observed features or OTUs; Evenness, a measure of community richness (Pielou 1966); Faith's Phylogenetic Diversity, a qualitative measure of community richness incorporating phylogenetic relationships (Faith 1992). Also this pipeline generates several beta diversity metrics such as: Jaccard distance, a qualitative measure of community dissimilarity (Jaccard 1908); Bray-Curtis distance, a quantitative measure of community dissimilarity (Sørensen 1948); unweighted UniFrac Distance, a qualitative measure of community dissimilarity with phylogenetic relationships (Lozupone & Knight 2005); weighted UniFrac distance, a quantitative measure of community dissimilarity with phylogenetic relationships (Lozupone, Hamady, Kellley, & Knight 2007). The next pipeline was to test alpha diversity and the distribution of features with boxplots and Kurskal-Wallis test (Estaki 2020). The beta diversity was tested using principal coordinate (PCoA) plots generated in the previous pipeline. The next test conducted was PERMANOVA (Anderson & Walsh 2013) per different metadata category. Finally, the data was divided into the various categories in the metadata (including municipality location, cardinal location, cardinal surface current, reef habitat, and animal size) and then the taxonomic bar plots were visualized for each category or group and all samples and transferred to Microsoft Excel files. Pearson chi-squared statistical analysis was performed on log transformed data ($\log_{10}(x+1)$) for different metadata groupings that compared the microbial profiles at the phylum level of classification.

Bioinformatic Analysis - Geneious Prime

The Geneious Prime bioinformatics platform was used to perform the cytochrome b gene analysis. All information pertaining to the use of the platform can be found at www.geneious.com. The samples were first imported and merged into paired reads using BBMerge paired Read Merger Version 38.37 (Bushnell 2017, BBDuk Geneious plugin) using the default settings and merge rate in the high setting. Paired reads were then Trimmed using BBDuk Adapter/Quality Trimming Version 38.37 (Bushnell, BBDuk Geneious plugin) using the default settings for Nextera DNA adapters with a Kmer length of 27, maximum substitutions of 1, minimum quality of 30, minimum overlap of 20 and minimum length of 100bps. Then sequences were error corrected and normalized using BBNorm error correction and read normalization version 38.37 (BBNorm, Geneious plugin)

using defaults settings. The duplicate sequences were removed using Dedupe Duplicate Read Remover version 38.37 (Geneious plugin) on default settings and Kmer seed length of 31. Chimeric reads were removed using UCHIME v4.2.40 Chimeric sequence detection using a reference database by Robert Edgar (2011) using default settings and Multiple Sea Urchin Mitochondrion Genome Alignments (Chunxia 2016; Bronstein 2019). Then, the samples were processed through a Velvet 1.2.1 de novo assembly using de Bruijn graphs to produce assembled contigs. These contigs were then edited to only contain sequence lengths that were close to our desired *cytochrome b* amplicon 1,140 bps, so anything below 900 bps and above 2,000 bps was discarded. The contigs were then aligned using Geneious Global Alignment and a cost matrix of 51% similarity (5/-3). A consensus sequence was generated using a threshold of 0% (Majority) from each of the aligned edited contigs. Finally, with the consensus sequence a phylogenetic tree was generated using Geneious Tree Builder and Global alignment using a cost matrix of 51% similarity, with a genetic distance model of Tamura-Nei and method of Neighbor-Joining tree.

Results

Raw 16S V3 and V4 Region

The total number of raw sequences generated from the Illumina MiSeq platform targeting the 16S ribosomal gene in the DNA from 44 sea urchin gut tissue samples collected from eight different locations in Puerto Rico was 1,483,248. The Deblur quality filtering pipeline produced 246,261 features in 43 samples. After removing rare-OTUs or features, the data retained 111,929 (45%) features in 43 samples at the sampling depth of 2603. One sample was removed for low quality reads. Of these, taxonomic identification was assigned to 181,713 reads, with 64,186 unidentified reads. The unidentified reads were not subjected to further statistical analysis. Rarefaction curves were reached suggesting sufficient sampling depth (data not shown).

Microbial diversity across the animal samples

Relative abundances for the sea urchin microbiome taxonomic values was determined using the RDP classifier Greengenes (v13.8) and QIIME2. The gut tissues collected showed an overabundance of organisms from the Proteobacteria phylum classification. Of the identified reads, 99.27% were identified as Proteobacteria (180,399 reads), followed by Firmicutes (1,314 reads), Bacteroidetes (344 reads) and Tenericutes (18 reads). Besides the number of reads that were classified at the phylum level of Proteobacteria (3,241 reass), at the class level, the largest represented group was Alphaproteobacteria (7,178 reads), followed by Betaproteobacteria (1,217 reads) and then Gammaproteobacteria (916 reads). Other represented groups within Proteobacteria include the class Epsilonproteobacteria (56 reads), the order Rhizobiales (42 reads), the families Alcaligenaceae (10 reads) and Bradyrhizobiaceae (21 reads), the genus Helicobacteraceae (42 reads) and species *Rhizobium daejeonense* (12 reads; represented in n=4 individuals). The largest represented group within the Firmicutes was the class Clostridiales (1,253 reads). Within the Firmicutes there were also unspecified reads (952 reads) and other represented groups within this phylum include the families Lachnospiraceae (34 reads) and Ruminococcaceae (13 reads). For the phylum Tenericutes, only the species *Candidatus hepatoplasma* (18 reads) was represented.

The type of bacteria found in the samples differ by sample locations and only bacteria from the phyla Proteobacteria and Bacteroidetes were represented in samples from all eight collection sites (**Figure 4**). Within Proteobacteria, bacteria from the classes Alpha-, Beta-, and Gammaproteobacteria were also represented in gut tissue samples from all collection sites. Within Alphaproteobacteria, the order Rhizobiales and the family Bradyrhizobiaceae were represented in most sample location sites, with a few exceptions, e.g., samples classified in the order Rhizobiales were not found in samples collected from Guayama and Guánica, and samples classified in the family Bradyrhizobiaceae were not found in samples collected from Culebra and Guánica. The Gram-negative nitrogen fixing bacteria *Rhizobium daejeonense*, from the order Rhizobiales were identified in four different animal samples collected from three sites, including Rincón, Luquillo (n=2) and Culebra. The family Alcaligenaceae from the phylum Betaproteobacteria were represented in five animal samples collected from Rincón, Isabela, Culebra (n=2) and Ceiba. Bacteria from the phylum Gammaproteobacteria found in samples representing all collection sites were not further classified into more specific taxonomic groups. Bacteria from the class

Epsilonproteobacteria as well as those classified further into the genus Helicobacteraceae were found in multiple animals but were restricted to the animal samples collected in Ceiba (n=4). Within the phylum Firmicutes, bacteria were classified at different taxonomic levels, and at various locations. For example, one animal sample from Guánica was harboring bacteria classified as Firmicutes, whereas the class Clostridiales was found in different animal samples collected at all municipalities. Within Clostridiales, the families Lachnospiraceae and Ruminococcaceae were represented in samples from Rincón, Luquillo, and Ceiba.

Within the phylum Tenericutes, no bacteria was classified at the higher taxonomic levels, but the species, *Candidatus hepatoplasma*, within the class Mollicutes was found in multiple animal samples at most of the municipality collection sites, except for Ponce, Isabela, and Guayama.

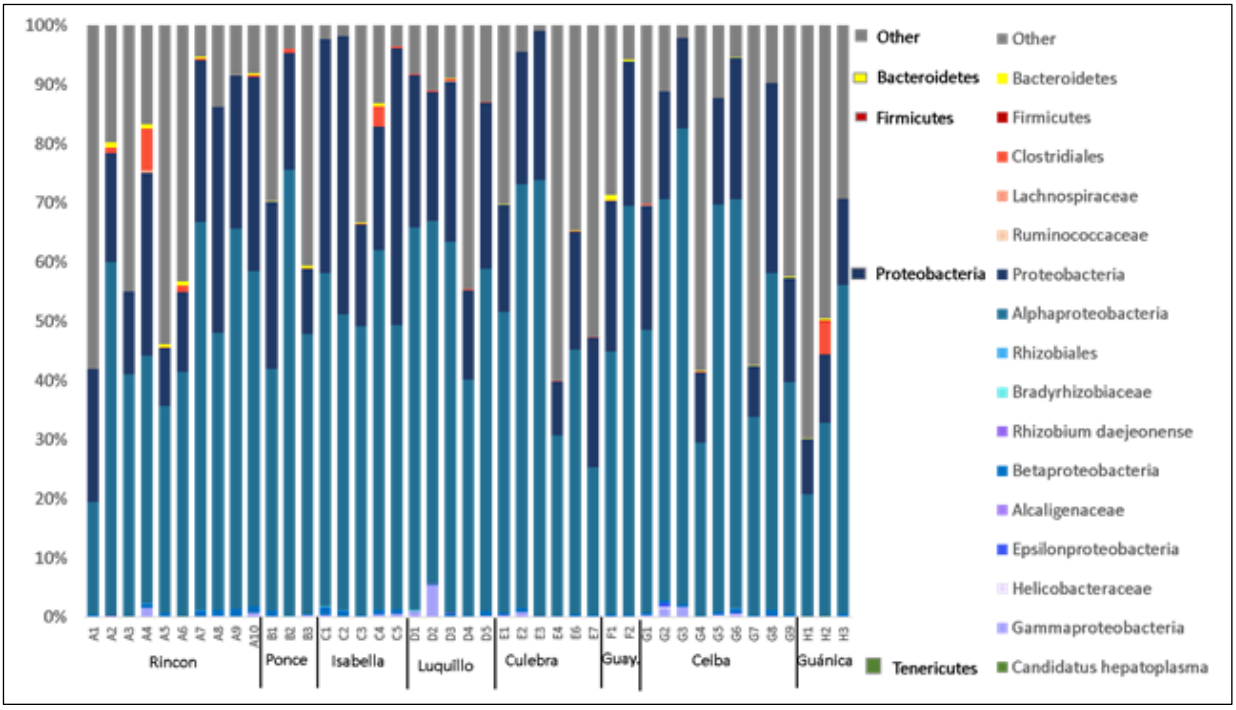

Figure 4. *Taxonomic classification of urchin intestine*. Intestinal microbiome of *D. antillarum* (n=44) collected in the coastal waters of eight different municipalities across Puerto Rico. Microbiome data was generated using 16S metagenomic sequencing. Bars indicate the percentage of microbiota present in each animal sample, in which "Other" refers to the unidentified feature data or OTUs. Samples were labeled as A – H according to the different municipality locations and the order of collection, e.g., 10 different animal samples were collected in Rincón (A1 – A10).

Statistical Analysis of Log Transformed data

Overall chi-squared statistical analysis performed on the log transformed data comparing the microbial profiles contained within the phyla (Bacteriodetes, Proteobacteria, Firmicutes and Tenericutes) to animal samples grouped by municipality, cardinal location, cardinal surface current, and animal size resulted in no significant differences between these groupings (results not

shown). Pairwise comparisons resulted in significant differences between taxa and groupings pertaining to municipalities, cardinal location, cardinal surface current, and size. For example, bacteria represented in the samples from Guayama were statistically different from all other municipalities (**Figure 5**).

A

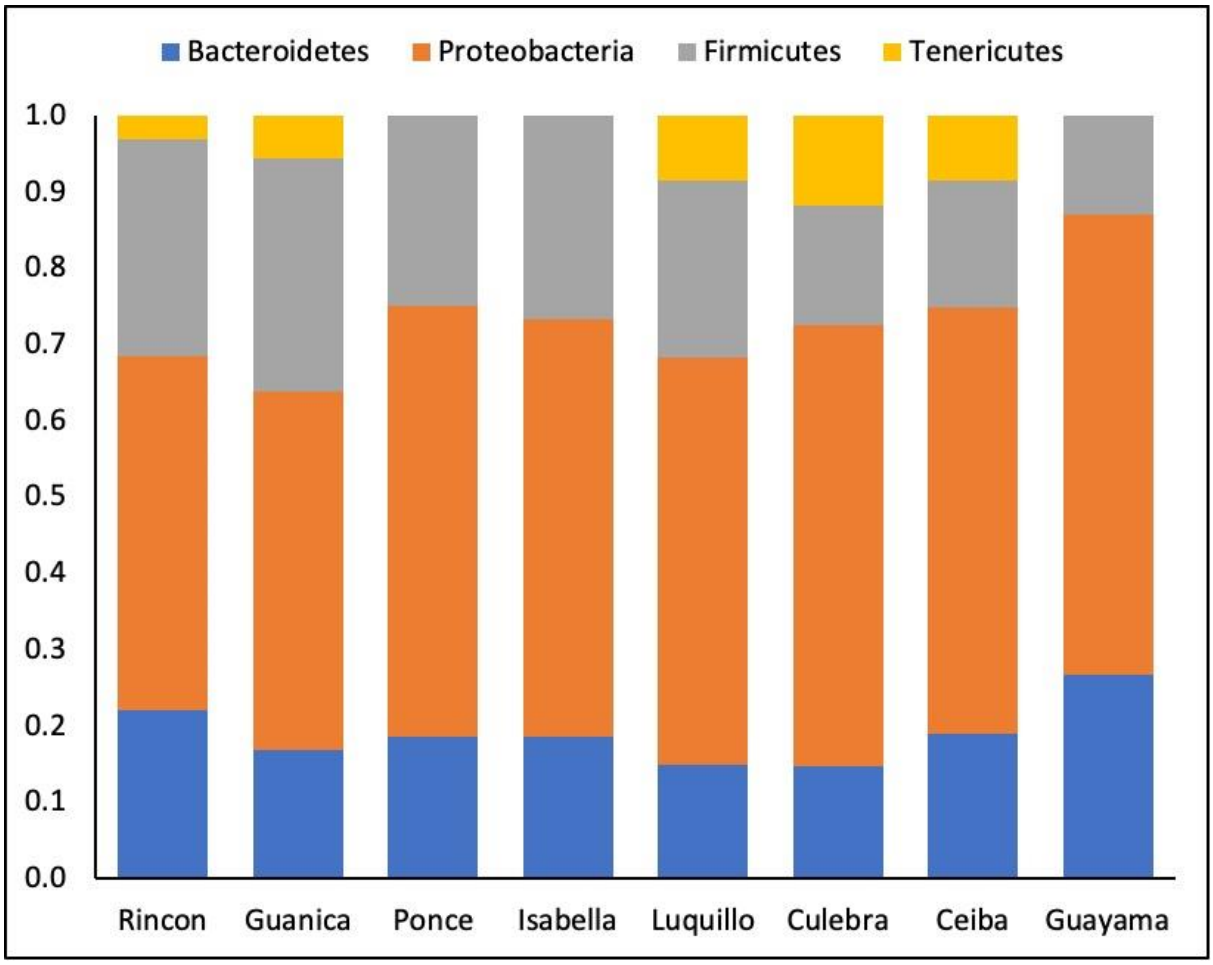

B

	Rincón	Guánica	Ponce	Isabela	Luquillo	Culebra	Ceiba	Guayama
Rincón	-	0.4360	**0.0068**	**0.0098**	**0.0385**	**0.0001**	**0.0042**	**1.24E-06**
Guánica		-	**0.0487**	**0.0802**	0.2671	**0.0013**	**0.0256**	**2.94E-05**
Ponce			-	0.9845	**0.0325**	**0.0006**	**0.0089**	**0.0055**
Isabela				-	**0.03**	**0.0002**	**0.0038**	**0.0011**
Luquillo					-	0.1829	0.3265	**2.34E-18**
Culebra						-	0.5091	**1.1E-31**

Figure 5. *Gut microbiome of D. antillarum by municipalities of Puerto Rico.* Relative taxonomic values are represented in the bar graph (A) by location municipalities. A total of 44 samples were collected from Rincón (n=10), Guánica (n=3), Ponce(n=3), Isabela (n=5), Luquillo (n=5), Culebra

(n=7), Ceiba (n=9), and Guayama (n=2). Bars indicate the relative proportions of microbiota found in each specimen. Pairwise Pearson chi-square analyses was used to test differences between the microbiota profiles according to municipality. P-values are shown in (B) and bolded text indicates significant differences.

There was a greater proportion of bacteria in the phyla Bacteriodetes and Proteobacteria, and no bacteria from the phylum Tenericutes in the samples from Guayama. Similarly, samples from Ponce and Isabela did not include bacteria from the phylum Tenericutes, yet other proportions making up the microbiota profile for these locations were different from Guayama. In addition, the microbiota profile for Luquillo, Culebra and Ceiba were similar to each other, as were the profiles for Rincón and Guánica, however, these two data sets were mostly different from each other in the pairwise comparisions, with the exception of the profiles between Luquillo and Guánica.

When municipalities were grouped by cardinal location, the microbiota profile of the East (Ceiba and Culebra) was significantly different from that of the West (Rincón), as well as the South (Guánica, Ponce and Guayama), in which East and West had the highest level of significance (**Figure 6**; p-value 3.1278E-05). There were no differences in the microbial profiles between other pairwise comparisons including West vs. South, West vs. North, North vs. South and North vs. East.

A

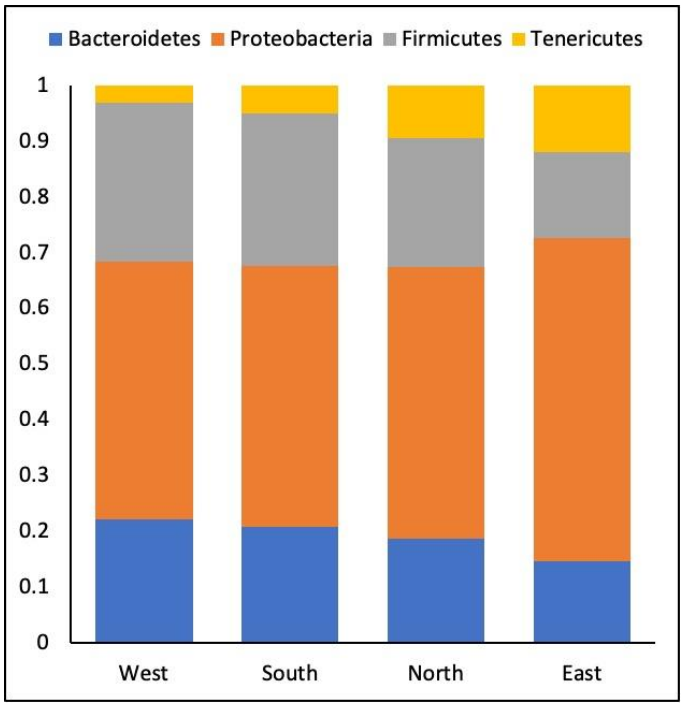

B

	South	North	East
West	0.8391	0.1049	**3.1278E-05**
South		0.3701	**0.0005**
North			0.0692

Figure 6. *Gut microbiome of D. antillarum by cardinal location in Puerto Rico.* Bars indicate the percentage of microbiota that was present in each sample organized by the respective cardinal grouping (A). The bars were generated by QIIME2 analysis which were then log transformed and graphed without unknown taxa. Cardinal groupings included west (n=10), south (n=8), north (18) and east (n=7). Collection sites are categorized into West (Rincón), South (Guánica, Ponce, Guayama), North (Luquillo, Isabela) and East (Ceiba, Culebra). A pairwise for the Pearson chi-square test was conducted to test differences in taxonomic grouping and collection site by cardinal location (B). The p-values are outlined in the bottom table and bolded text indicates significant differences.

When the animal samples were grouped according to cardinal surface current at the collection site, there were no significant differences between the profiles of microbiota and the groupings into calm, medium, and strong (**Figure 7**).

A

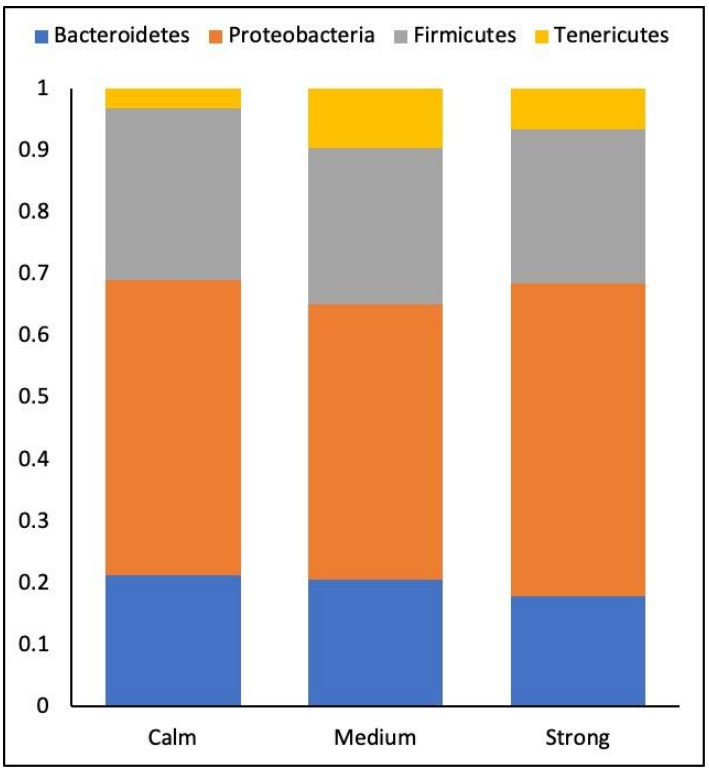

B

	Medium	Strong
Calm	0.18	0.42
Medium		0.47

Figure 7. *Gut microbiome of D. antillarum by surface water currents.* Surface water currents were categorized by calm in the south facing the Caribbean Sea, strong to the north facing the Atlantic Ocean and medium strength in the east and west being in between both bodies of water. The bars in the graph (A) indicate the relative percentage of microbiota present in each sample based on the current classification that was generated using QIIME2, log transforming data and then graphed without unknown taxa. The corresponding animal sample numbers are calm (n=8), medium (n=26) and strong (n=10). A pairwise statistical analysis was performed using Pearson Chi-square analysis (B). The p-values are shown in the bottom table.

When the animals were grouped by size and relative proportion, there were differences between the profiles of microbiota and these data groupings (**Figure 8A, C**). For example, while the microbial profiles for the sea urchins measured at 2.5 in. and 3 in. were similar, these were significantly different from all other profiles of sea urchins in the other size categories, including 1.5 in., 2 in., 3.5 in. and 4.5 in. Apart from this, all other microbial profiles were significantly different from each other (**Figure 8C**). When the animal sample taxonomic data were grouped into relative proportion, including Small (1.5 - 2 in.), Medium (2.5 - 3 in) and Large (3.5 - 4.5 in.), the microbiota profile of the Medium animals was significantly different from that of the Small, as well as the Large animals (**Figure 8B, D**). For these comparisons, the largest significant difference was between the Medium and Large animals (**Figure 8D**; p-value 1.552E-25).

A

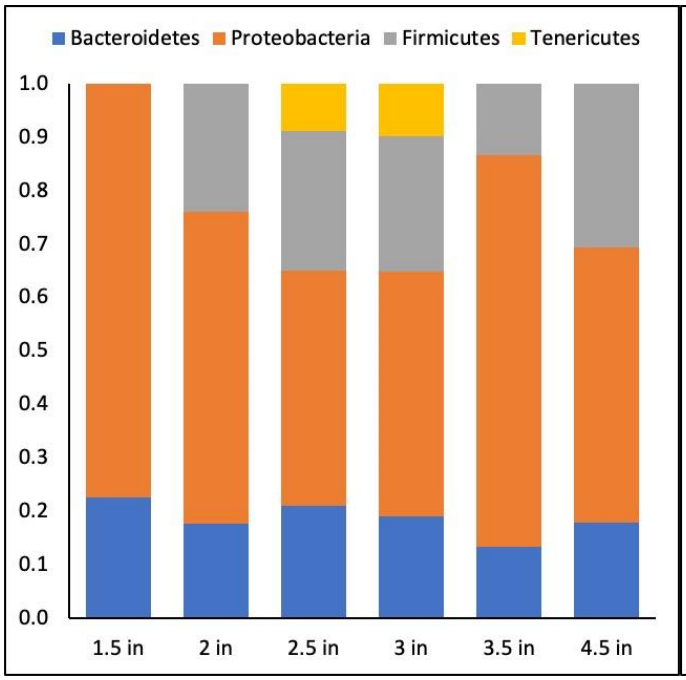

B

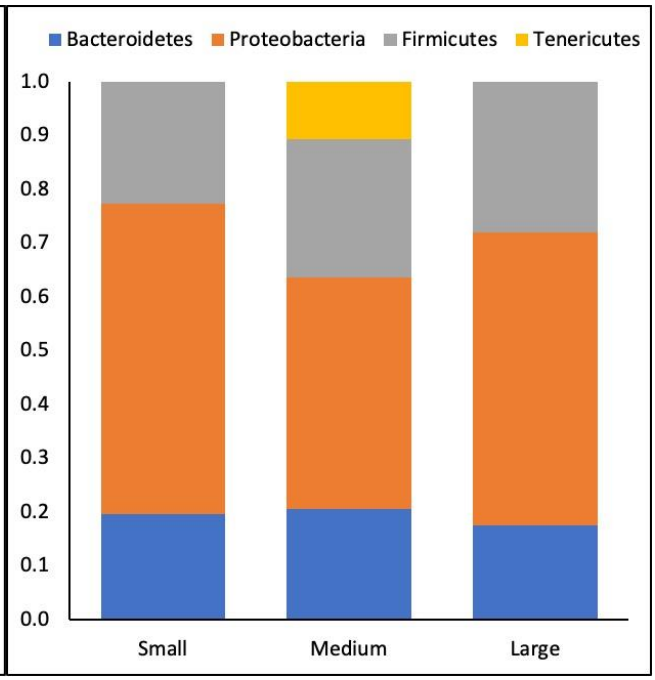

C

	Two	Two Point Five	Three	Three Point Five	Four Point Five
One Point Five	0.0000	0.0000	0.0000	0.0003	0.0000
Two		0.0044	0.0059	0.0077	0.5073
Two Point Five			0.9419	0.0000	0.0000
Three				0.0000	0.0000
Three Point Five					0.0002

D

	Medium	Large
small	0.0017	0.7097
medium		0.0000

Figure 8. *Gut microbiota of D. antillarum based on size and relative proportion.* Relative taxonomic values for the different sizes in inches (A). Animal body diameters were measured and placed in the following categories one point five (n=3), two (n=6), two point five (n=15), three (n=16), three point five (n=3), four point five (n=1). Animals in the proportion category were placed into categories relative to their size, namely small (1.5 - 2 in.), medium (2.5 - 3 in.), and large (3.5 - 4.5 in.). The animal sample numbers include small (n=9), medium (n=31), and large (n=4). A pairwise statistical analysis was performed using Pearson Chi-squared analysis for the size (C) and the relative proportion (D).

An additional chi-square analysis was performed by grouping the taxonomic microbial data into groups based on island surface current, which is known to sweep across the island from the east towards the west, with a stronger current sweeping across the north of the island (**Figure 9**). The previous analysis of grouping the taxonomic microbial data samples into the collection sites according to North, South, East and West indicated that there was no difference in the microbial profiles for samples from the North vs. South, but there was a highly significant difference between microbial profiles for samples from the East vs. West. Thus, we grouped taxonomic microbial data samples according to East (Luquillo, Ceiba and Culebra), West (Rincón and Isabela) and South (Guánica, Ponce, and Guayama). Pairwise chi-square analyses indicated that there was a significant difference between the microbial profiles in the samples representing the East vs. West. Although not significant, there was a trend indicating that the microbial profiles between samples representing East vs. South were also different.

A

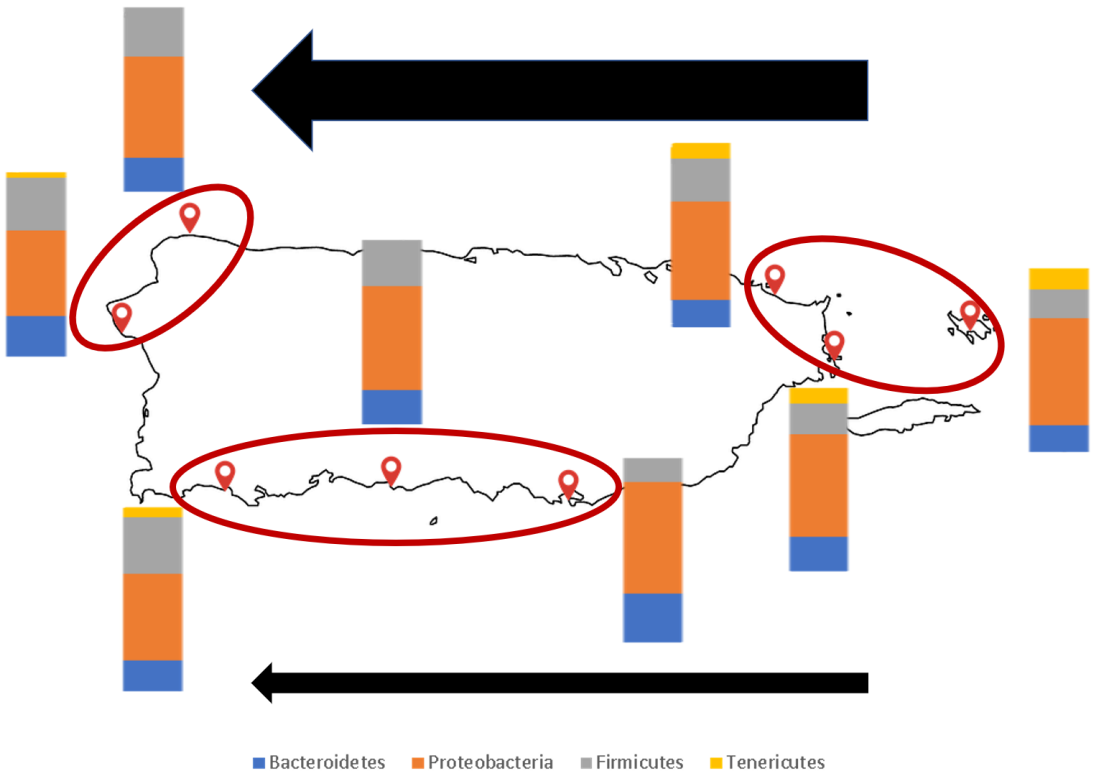

B

West-South	0.79821168
West-East	0.00819983
South-East	0.05602085

Figure 9. *Gut microbiome of D. antillarum by sampling location and island wide currents.* The bars in the map represent the relative taxonomic profile of each municipality (A). Animal samples were collected from Rincón (n=10), Guánica (n=3), Ponce (n=3), Isabela (n=5), Luquillo (n=5), Culebra (n=7), Ceiba (n=9), and Guayama (n=2). Samples were grouped into island wide currents (red circles) East (n=21), South (n=8), and West (n=15). Surface water current strength and direction is indicated using the thickness of the arrows and direction of the arrow, respectively. In the top arrow the current corresponds to the north Atlantic Ocean water currents which are stronger than the bottom calmer waters of the Caribbean Sea. P-values are shown at the bottom table (B).

A heatmap was generated to visualize the overall results of the different metadata groupings by municipalities, cardinal location, cardinal surface current, size, and reef habitat (**Figure 10**) in comparison to the taxonomic microbial data by phyla. As represented in **Figure 10**, there is no clustering of the taxonomic data among the samples pertaining to Proteobacteria and Bacteroidetes, which is similar to the data shown in **Figure 4**. In addition, Firmicutes are also largely dispersed across the different samples; however, this refers to reads that were classified at the class level Clostridiales. Within Clostridiales, the family Lachnospiraceae was represented in

the sample labeled as A4 collected in Rincón, and the family Ruminococcaceae was represented in samples labeled as A9 (Rincón), D3 (Luquillo), and G1 (Ceiba). Finally, taxonomic data pertaining to the phyla Tenericutes was clustered for several samples which refer to the six samples (A1, D4, E4, E6, G7, and H2) that contained bacteria of the species *Candidatus hepatoplasma*.

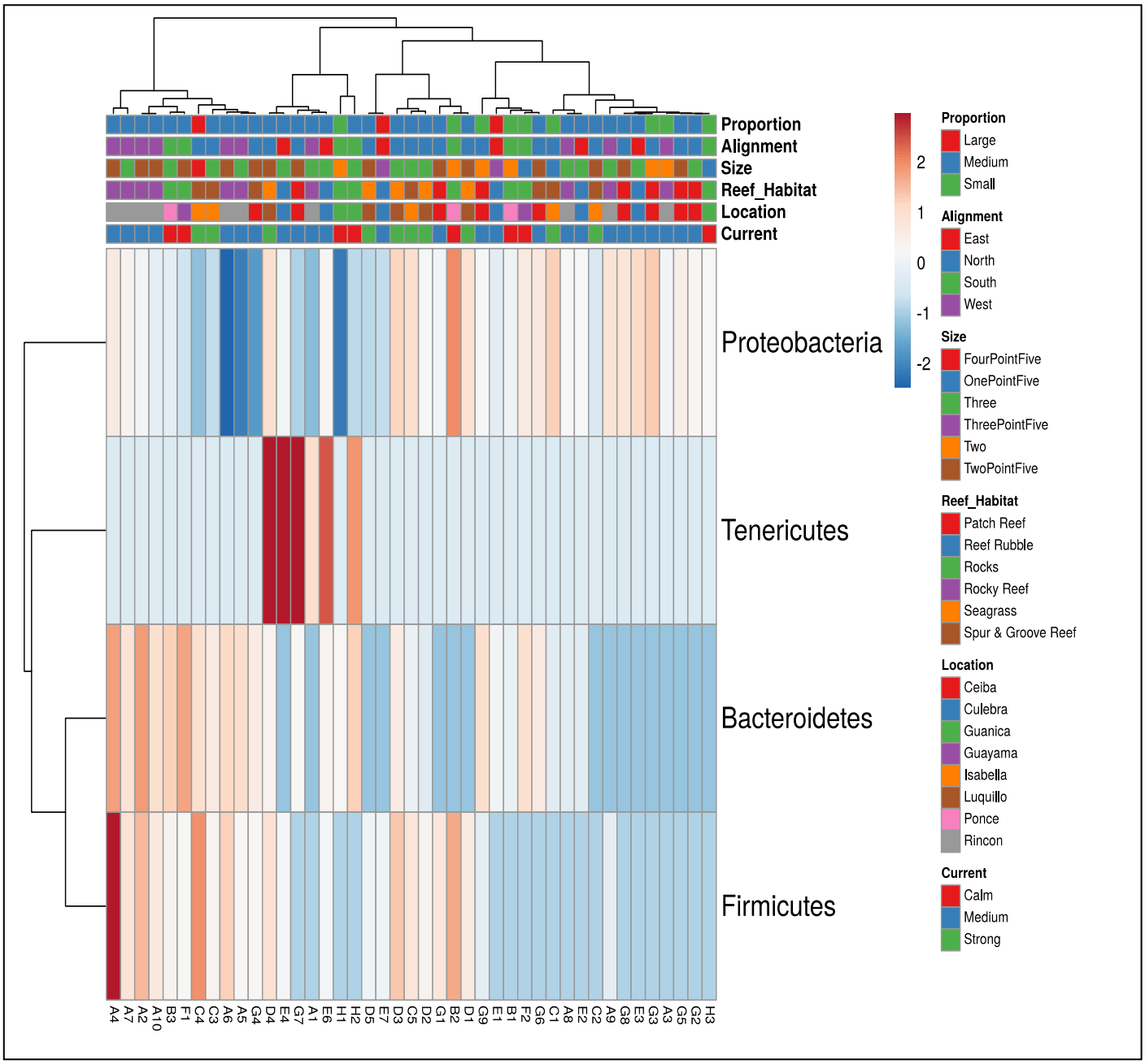

Figure 10. *Heatmap generated using ClustVis*. This image shows a heatmap generated using multiviance analysis that includes the metadata and relative taxonomic representation of each sample (Mersalu & Vilo 2015). The top rows represent the different metadata categories for each sample which are the columns represented by the identifiers at the bottom. In the following rows the taxonomic groups are represented. The relative presence in each sample is indicated by the intensity of the color. To the left and at the top appears a hierarchical category of the groups.

Population genetic diversity across the animal samples

Analysis of population genetic diversity in *D. antillarum* from eight municipalities across Puerto Rico according to *cytochrome b* indicate there is substantial gene flow between animals at the different cardinal location sites (**Figure 11**). According to the phylogenetic tree shown in **Figure 11** (left), there is no formation of clades restricted to locations pertaining to animal samples characterized as North (Luquillo and Isabela), South (Guánica, Ponce and Guayama) East (Ceiba and Culebra) and West (Rincón). Rather, clades have formed between animals at various cardinal locations (including animals collected at sites labeled as West and North, South and North, South and West, West and East, and East and North) with no clear animal migration pattern between these locations. The phylogenetic tree is also paired with the *16S* sequencing results by taxonomic classification **Figure 11** (right) according to the animal sample shown in the tree. To test for patterns of *16S* taxonomic diversity between the four major clades in the phylogenetic tree (**Figure 11** left; see asterisks), Simpson and Shannon diversity indices were calculated to test differences between these clades. Results from these analyses indicated there were no significant differences between the species represented in the samples between clades and the abundance of these species between the clades (results not shown).

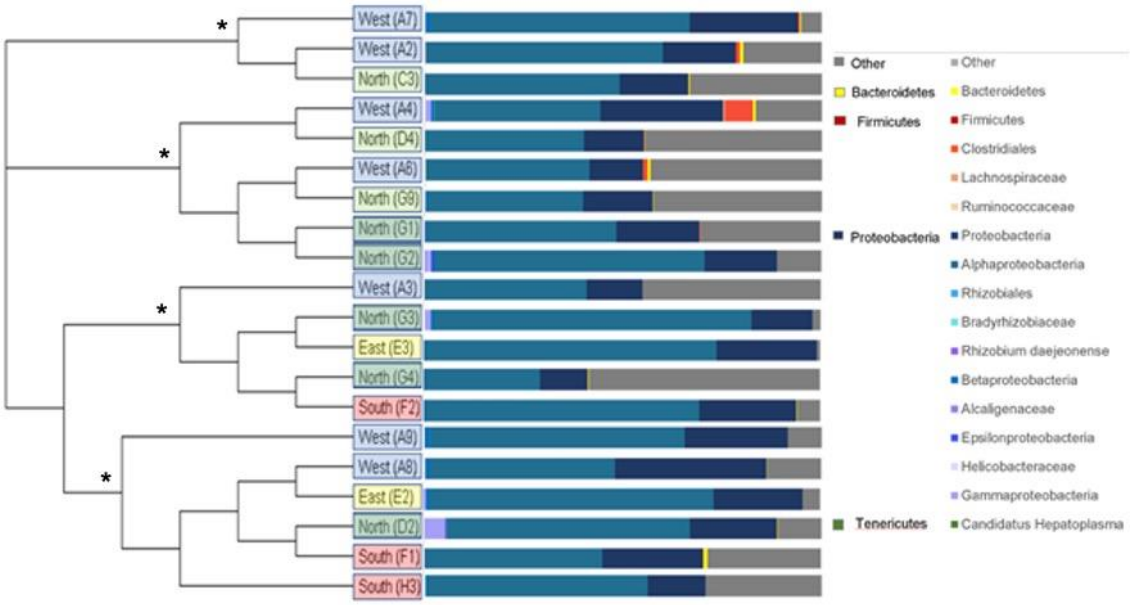

Figure 11. *Phylogenetic tree of cytochrome b (left) with 16S sequence results (right) by individual animals.* Animals are labeled at tree nodes according to cardinal location site of collection and animal identification (**Figure 4**). A Tamura-Nei Neighbor-Joining phylogenetic tree was generated using Geneious Prime software and the taxonomic classification was generated in QIIME2. There are four major clades represented in the tree, each marked with an asterisk.

Discussion

It is well documented that the coral reef ecosystem has been in decline for decades and that this has disastrous consequences for the biodiversity that inhabits this ecosystem. The great *D. antillarum* die off in the 1980's had serious consequences that also contributed to this ecosystem decay. We know very little of what caused the great die off, but it is believed that a water borne pathogen was responsible for the event (Lessios et al. 1984). In 1987, an experiment conducted by Bauer found bacterial isolates from *D. antillarum's* digestive tract and gonad tissues which were confirmed to be strains of *Clostridia perfringes* and *Clostridia sordellii*. It is well documented that *Clostridia* strains are commonly associated with polluted estuarine water (Daily et al. 1981; Watkins & Cabelli 1985). In this experiment (Bauer 1987), Clostridium bacteria were found to be highly infectious especially at a higher temperature.

The correlation between temperature and pathogenicity has been studied in recent investigations involving the sea urchin *Lytechinus variegatus* (Brothers et al. 2018) and it has been proposed that perhaps at higher temperature sea urchins experience a destabilization of the microbiome (also known as dysbiosis) which has disastrous consequences for the overall health of the organism. In this same study also, there is some evidence of an increase of virulence of opportunistic organisms inside the microbiome of the *L. variegatus* as it has been reported that some bacteria respond by activating pathogenic genes with increasing temperature. In another sea urchin *Heliocidaris erythrogramma*, elevated temperatures have been observed to cause a degradation of the coelomocyte concentrations which impact overall immunity (Brothers et al. 2016). Sea urchins do not have an adaptive immune system and fight off pathogens with specialized cells called coelomocytes, located in their coelomic fluid, that can mount a proper immune response (Deflippo 2018). Innate immunity involves various components and mounts a rapid nonspecific response to pathogens mediated by coelomocytes (Bochud et al. 2007; Lin et al. 2001; Medzhitov & Janeway 2002; Deflippo 2018). More importantly sea urchin gut microbiomes play a role in sea urchin host health and this has been demonstrated in *S. droebaciensis* in which microbial suppression through antibiotics showed an impaired capacity for production of amino acids (Fong et al. 1980).

Another important factor affecting immune responses is high ocean acidity. In a study, it was found that the adult sea star *Asteria rubens'* coelomic fluid had an impaired immune response in a high pH environment (Hernroth et al. 2011). Based on a study done by DeFlippo 2018, *Diadema antillarum* is "no less capable" of mounting a proper innate immunity response even though there is prior evidence of a diminished humoral response (Beck et al. 2014). The authors in DeFlippo (2018) suggest that maybe the humoral arm of the immune system is impaired, that the recovering population has a stronger immune system than the population that died, or an over-activity of the humoral defenses created a selection for a weak humoral response. In this case some of these scenarios are difficult to prove because of lack of immunological studies during the die-off. In the case of our study, it is probable that *Clostridium* is the number one suspect of the great *D. antillarum* die off. This bacterium reproduces by spores and can travel large distances with this apparatus (Bauer 1987). Perhaps these added synergistic effects of elevated sea temperatures, an

ocean with an increasing pH values, an impaired immune response and a highly virulent strain of *Clostridium* could present a challenge for the survival of *D. antillarum* in the wild.

Previous studies done on the sea urchin digestive tissue have found distinct bacteria not found in outer environment or ingested feed (Guerinot & Patriquin 1981; Hakim et al. 2015) which suggest host selection. Bacteroidetes and Proteobacteria have been found in the guts of the mussel *Mytolus galloprovincialis* (Li et al. 2019), a small abalone *Haliotisdiversicolor* (Zhao et al. 2018), a crab *Callinectes sapidus* (Givens et al. 2013), a sea cucumber *Holothuria glaberrima* (Pagan-Jimenez 2019), and more importantly other sea urchins such as *Lytechinus variegatus* (Hakim et al. 2015), *Strongylocentrotus purpuratus* (Hakim et al. 2019), *Diadema setosum, Stomopneustes variolaris, Echinothrix calamaris, Diadema savignyi,* and *Tripneustes gratilla* (Qiucui et al. 2019). Proteobacteria, including Alphaproteobacteria and Gammaproteobacteria have been also found the species of corals *P. aestreoides* and *M. faveolate* while betaproteobacteria and firmicutes have been found in *P. astreoides* (Morrow et al., 2012).

This suggests that the Bacteroidetes and Proteobacteria found in *D. antillarum* may not be antagonistic to the host. This is because there is a near-dominant and consistent presence of these bacteria that can support a host-selection mechanism and there is evidence for a non-detrimental association for other orders of bacterium in sea urchins along with bioinformatical predictions of the role of this bacterium that show it might be related to symbiont-host energy metabolism (Hakim et al. 2015). In the sea urchin *Strongylocentrotu*s an extremely low abundance of Tenericutes was also found (Hakim et al. 2019). Bacteroides have been found in polluted waters as well (Daily et al. 1981). However, they do seem to be also associated with marine microbiomes (Li et al. 2019). Bacteroides are considered to be specialists de grading proteins and carbohydrates (Thomas et al. 2011; Qiucui et al. 2019).

Bactereoidetes, Proteobacteria and a small percentage of Firmicutes have been found in sea water columns in the Hadopelagic region of the Puerto Rican Trench (Eloe et al. 2011) suggesting that the sea is the normal habitat for these microorganisms. In Anones (Dávila-Santiago et al. 2018) Proteobacteria, Bacteroidetes and Firmicutes was found at the Anones beach in Puerto Rico. In this study the human impacted Condado lagoon in Puerto Rico the phylum's Bacteroidetes, Firmicutes, and Proteobacteria were found. The authors (Dávila-Santiago et al. 2018) conducted an analysis to test if these phylum of the Condado lagoon reflected human-gut bacteria and found evidence suggesting that these bacteria are environmentally adapted and do not emerge from the human-gut.

An important result was not finding *Campylobacteraceae* or *Vibrio* which are both bacterium that have been found in various sea urchins (Guerinot et al.1982; Hakim et al. 2015). In the sea urchin *Strongylocentrotus* the most abundant bacteria found were *Epsilonproteobacteria* that were from the order *Campulobacterales*. *Campylobacteraceae* and *Vibrio* was also represented in the gut (Hakim et al. 2015). *Vibrio* isolated from the gut of *Strongylocentrotus nudus* has produced amylase and other byproducts that suggest a role in the host's digestion (Beleneva & Kukhlevskii, 2010). This could suggest that either these bacteria do not play an important role in the microbiome of *D. antillarum* or the organism is experiencing a form of dysbiosis which negatively affects the relationships between the symbiont and host. However, this has not been the first time that *Clostridia* have been found in a sea urchin as it has been found in *D. setosum*

(Tanrattanapitak 2018). It could be very well that *Diadema* needs *Clostridium* to process food and this changes the microbiome of the sea urchin. In the study done by Qiucui et al. (2019) found that gut digesta analysis reveals the urchin *T.gratilla* feeds on macroalgae while *D. setosum, D. savignyi, E. calamaris,* and *S. variolaris,* feed on coral, filamentous, turf algae, and other animals. This result is also shown in the dissimilarity of the microbiome of *T.gratilla* compared to the other urchins. Diet has been one of the key factors that mold the microbiome of organisms (Miyake et al. 2015) but we do not have a clue about the influence of other factors such as size or location.

The pairwise comparison between the different categorical findings paints a clearer picture about the life of the Puerto Rican *D. antillarum* population. The size and proportion grouping categories show significance with potentially small and medium specimens. This suggests that there might be a maturation of the microbiome, however more research is needed for this. Also, who is responsible for the adaptation the microbiome or the sea urchin? In 2014 a survey was conducted in PR to assess the recovery *D. antillarum* and found relatively low abundances of small size *D. antillarum* individuals (Rodriguez-Barreras et al. 2014) suggesting the reason why the population has not recovered yet: low recruitment of small individuals. It could be the case that these individuals have a hard time regulating the microbiome and do not survive into adulthood.

Other findings in the location-based and current-based categories paint a different picture. Guayama is inherently different from the rest of the other municipalities possibly due to the high level of anthropogenic activity. In the cardinal categories east seems to be most different from the rest of the cardinal points, this might be due perhaps to the currents in the island originate from the eastern region and drag across the island. However, we did not find any statistical significance between the current categories based on strength. Based on this we grouped together the locations into three to form the island wide current category and we had a statistical significance between East and West. This finding suggests that the drag of the current across the island makes the west population different from the east population. Could this suggest that the specimens found in the east are healthier than the other sides that were bombarded with island debris. Also, the South and East categories were almost statistically significant that perhaps can be addressed in future bioinformatic studies. The problem with this data is that there is a small sample size for some categories like Guayama and ‘small’. For this reason, the experiment must be replicated in a different place to see if the same taxa relationships are reported and if these categories are observed and are significant.

Understanding more about the microbiome of *D. antillarum* requires a recreation of this experiment in a different location to see if the same taxa groups can be found and if there is any significant difference between the small and large individuals. We suggest as well to seek the diversity of algae and diet found in these locations and compare the diversity in diet with diversity in microbiome. Another study worth doing is understanding more about the pathogenicity of Clostridia and the microbiome of *D. antillarum*. It could be the case that inhibiting the microbiome of a healthy adult sea urchin could create a space in which allows Clostridia to infect it.

Having accurate information about the genetic diversity, gene flow, and microbiome of key species of this environment is essential information to conserve the species if another disastrous mortality event were to occur. In this study, we unlocked the mysteries of one of the

most important microbiomes of the coral reef ecosystem helping us understand the ecosystem a little bit further. In summary, the results of this study reveal the genetic diversity of the sea urchin *D. antillarum* via the sequencing of its microbiome. The sea urchin has a highly compartmentalized gastrointestinal tract along with unique microbial profiles for each compartment that can indicate a specific functional profile for that bacteria, as shown in previous studies (Hakim et al. 2016). The bacteria of the gastrointestinal tract play a huge role in the digestion of complex sugars and cellulose especially considering both the physiological limitations of the sea urchin gut and the low nutritional value of seagrass (Arafa et al. 2012). Further studies can reveal the functional genome of some of these bacteria which can then reveal more about the function in the sea urchin and can be a source of antibiotics or synthetic functions via genetic engineering. Also, it is important to note that anthropocentric induced climate change along with the prevalence of disease in coral and other important benthic coral reef community members hinders the positive effect of keystone animals such as *D. antillarum* on the coral reef ecosystem (Burge et al. 2014; Carperter & Edmund 2006) thus taking care of that ecosystem is our priority.

References

Agnello, M. 2017. Introductory Chapter: Sea Urchin - Knowledge and Perspectives. Sea Urchin - From Environment to Aquaculture and Biomedicine. doi:10.5772/intechopen.70415

Ahmadmehrabi, S., & Tang, W. W. (2017). Gut microbiome and its role in cardiovascular diseases. *Current Opinion in Cardiology,32*(6), 761-766. doi:10.1097/hco.0000000000000445

Alvarez-Filip, L., Dulvy, N. K., Gill, J. A., Côté, I. M., & Watkinson, A. R. 2009. Flattening of Caribbean coral reefs: Region-wide declines in architectural complexity. Proceedings of the Royal Society B: Biological Sciences,276(1669), 3019-3025. doi:10.1098/rspb.2009.0339

Anderson, M. J., & Walsh, D. C. I. (2013). PERMANOVA, ANOSIM, and the mantel test in the face of heterogeneous dispersions: What null hypothesis are you testing? Ecological Monographs, 83(4), 557–574. doi: 10.1890/12-2010.1.

Arafa S Chouaibi M Sadok S et al... 2012. The influence of season on the gonad index and biochemical composition of the sea urchin Paracentrotus lividus from the Golf of Tunis Sci World J

Baohong, W., Mingfei, Y., Longxian, L., Zongxin, L., & Lanjuan, L. 2018. Human Microbiota in Health and Disease. Microecology—Review. doi:10.1016/c2017-0-01893-1

Barton, W., Penney, N. C., Cronin, O., Garcia-Perez, I., Molloy, M. G., Holmes, E., . . . Osullivan, O. (2017). The microbiome of professional athletes differs from that of more sedentary subjects in composition and particularly at the functional metabolic level. Gut. doi:10.1136/gutjnl-2016-313627

Bauer, J.C., Agerter, C.J., 1987. Isolation of bacteria pathogenic for the sea urchin Diadema antillarum (Echinodermata: Echinoidea). B. Mar. Sci. 401, 161e165.

Beck, G., Miller, R., Ebersole, J., 2014. Mass mortality and slow recovery of Diadema antillarum: could compromised immunity be a factor? Mar. Biol. 161, 1001e1013. http://dx.doi.org/10.1007/s00227-013-2382-6.

Beleneva, I. A., and Kukhlevskii, A. D. (2010). Characterization of Vibrio gigantis and isolated from invertebrates of peter the great bay, Sea of Japan. Microbiology 79, 402–407. doi: 10.1134/S0026261710030173

Bianchini, A., Playle, R. C., Wood, C. M., & Walsh, P. J. (2005). Mechanism of acute silver toxicity in marine invertebrates. Aquatic Toxicology,72(1-2), 67-82. doi:10.1016/j.aquatox.2004.11.012

Bianchini, A., Playle, R. C., Wood, C. M., & Walsh, P. J. (2007). Short-term silver accumulation in tissues of three marine invertebrates: Shrimp Penaeus duorarum, sea hare Aplysia californica, and sea urchin Diadema antillarum. Aquatic Toxicology,84(2), 182-189. doi:10.1016/j.aquatox.2007.02.021

Bielmyer, G., Brix, K., Capo, T., & Grosell, M. (2005). The effects of metals on embryo-larval and adult life stages of the sea urchin, Diadema antillarum. Aquatic Toxicology,74(3), 254-263. doi:10.1016/j.aquatox.2005.05.016

Blanco, F. M., Alonso, L. C., Sansón, G. G., & Amargós, F. P. 2010. Influence of Diadema antillarum populations (Echinodermata: Diadematidae) on algal community structure in Jardines de la Reina, Cuba. Revista De Biología Tropical,0(0). doi:10.15517/rbt.v0i0.3387

Blois, J. L., Zarnetske, P. L., Fitzpatrick, M. C., & Finnegan, S. 2013. Climate Change and the Past, Present, and Future of Biotic Interactions. Science, 341(6145), 499–504. doi: 10.1126/science.1237184

Bochud, P., Bochud, M., Telenti, A., & Calandra, T. (2007). Innate immunogenetics: A tool for exploring new frontiers of host defence. The Lancet Infectious Diseases, 7(8), 531-542. doi:10.1016/s1473-3099(07)70185-8

Bolyen, Evan, et al... "Reproducible, Interactive, Scalable and Extensible Microbiome Data Science Using QIIME 2." Nature Biotechnology, vol. 37, no. 8, 2019, pp. 852–857., doi:10.1038/s41587-019-0209-9.

Boonseub, S., Linacre, A., & Tobe, S. (2009). The use of mitochondrial DNA genes to identify closely related avian species. Forensic Science International: Genetics Supplement Series, 2(1). doi:https://doi.org/10.1016/j.fsigss.2009.08.050

Brothers, C. J., Pol, W. J., Morrow, C. D., Hakim, J. A., Koo, H., & Mcclintock, J. B. (2018). Ocean warming alters predicted microbiome functionality in a common sea urchin. Proceedings of the Royal Society B: Biological Sciences, 285(1881), 20180340. doi:10.1098/rspb.2018.0340

Brothers, C. J., Harianto, J., Mcclintock, J. B., & Byrne, M. (2016). Sea urchins in a high-CO 2 world: The influence of acclimation on the immune response to ocean warming and acidification. Proceedings of the Royal Society B: Biological Sciences, 283(1837), 20161501. doi:10.1098/rspb.2016.1501

Bronstein, O., & Kroh, A. (2019). The first mitochondrial genome of the model echinoid Lytechinus variegatus and insights into Odontophoran phylogenetics. Genomics,111(4), 710-718. doi:10.1016/j.ygeno.2018.04.008

Burge, C. A., Eakin, C. M., Friedman, C. S., Froelich, B., Hershberger, P. K., Hofmann, E. E., … Harvell, C. D. (2014). Climate Change Influences on Marine Infectious Diseases: Implications for Management and Society. Annual Review of Marine Science, 6(1), 249–277. doi: 10.1146/annurev-marine-010213-135029

Bushnell, B., Rood, J., & Singer, E. (2017). BBMerge – Accurate paired shotgun read merging via overlap. Plos One, 12(10). doi:10.1371/journal.pone.0185056

Buttino, I., Hwang, J., Romano, G., Sun, C., Liu, T., Pellegrini, D., . . . Sartori, D. (2016). Detection of malformations in sea urchin plutei exposed to mercuric chloride using different fluorescent

techniques. *Ecotoxicology and Environmental Safety,123*, 72-80. doi:10.1016/j.ecoenv.2015.07.027

Carpenter, R. C. 1988. Mass mortality of a Caribbean sea urchin: Immediate effects on community metabolism and other herbivores. Proceedings of the National Academy of Sciences,85(2), 511-514. doi:10.1073/pnas.85.2.511

Carpenter, R. C., & Edmunds, P. J. (2006). Local and regional scale recovery of Diadema promotes recruitment of scleractinian corals. Ecology Letters,9(3), 271-280. doi:10.1111/j.1461-0248.2005.00866.x

Ceja-Navarro, J. A., Karaoz, U., Bill, M., Hao, Z., White, R. A., Arellano, A., … Brodie, E. L. (2019). Gut anatomical properties and microbial functional assembly promote lignocellulose deconstruction and colony subsistence of a wood-feeding beetle. Nature Microbiology, 4(5), 864–875. doi: 10.1038/s41564-019-0384-y

Chiappone, .M., Swanson, .D., Miller, .S. et al... Large-scale surveys on the Florida Reef Tract indicate poor recovery of the long-spined sea urchin Diadema antillarum. Coral Reefs 21, 155–159 (2002). https://doi.org/10.1007/s00338-002-0232-y

Chunxia Li, Guyuan Wu, Wanying Fu & Xiaoqi Zeng (2016) The complete mitochondrial genome of Diadema setosum (Aulodonta: diadematidae), Mitochondrial DNA Part B, 1:1, 873-874, DOI: 10.1080/23802359.2016.1253039

Daily, O. P., Joseph, S. W., Gillmore, J. D., Colwell, R. R., & Seidler, R. J. (1981). Identification, distribution, and toxigenicity of obligate anaerobes in polluted waters. Applied and Environmental Microbiology, 41(4), 1074-1077. doi:10.1128/aem.41.4.1074-1077.1981

Dávila-Santiago, L., Deleón-Rodriguez, N., Lasanta-Pagán, K., Hatt, J. K., Kurt, Z., Massol-Deyá, A., & Konstantinidis, K. T. (2018). Microbial Diversity in a Military Impacted Lagoon (Vieques, Puerto Rico) as Revealed by Metagenomics. BioRxiv. doi:10.1101/389379

Defilippo, J., Ebersole, J., & Beck, G. 2018. Comparison of phagocytosis in three Caribbean Sea urchins. Developmental & Comparative Immunology,78, 14-25. doi:10.1016/j.dci.2017.09.007

Edgar, R. C., Haas, B. J., Clemente, J. C., Quince, C., & Knight, R. (2011). UCHIME improves sensitivity and speed of chimera detection. Bioinformatics, 27(16), 2194-2200. doi:10.1093/bioinformatics/btr381

Edmunds, P. J., & Carpenter, R. C. (2001). Recovery of Diadema antillarum reduces macroalgal cover and increases abundance of juvenile corals on a Caribbean reef. Proceedings of the National Academy of Sciences,98(9), 5067-5071. doi:10.1073/pnas.071524598

Eloe, E. A., Fadrosh, D. W., Novotny, M., Allen, L. Z., Kim, M., Lombardo, M., . . . Bartlett, D. H. (2011). Going Deeper: Metagenome of a Hadopelagic Microbial Community. PLoS ONE, 6(5). doi:10.1371/journal.pone.0020388

Estaki, Mehrbod, et al... “QIIME 2 Enables Comprehensive End-to-End Analysis of Diverse Microbiome Data and Comparative Studies with Publicly Available Data.” Current Protocols in Bioinformatics, vol. 70, no. 1, 2020, doi:10.1002/cpbi.100.

Faith, D. P. (1992). Conservation evaluation and phylogenetic diversity. Biological Conservation, 61(1), 1–10. doi: 10.1016/0006-3207(92) 91201-3.

Feehan, Colette J., et al... “Fertilization Limitation OfDiadema Antillarumon Coral Reefs in the Florida Keys.” *Ecology*, vol. 97, no. 8, 2016, pp. 1897–1904., doi:10.1002/ecy.1461.

Furman, B., & Heck, K. (2009). Differential Impacts of Echinoid Grazers on Coral Recruitment. Bulletin of Marine Science, 85(2), 121–132.

Gambardella, C., Ferrando, S., Gatti, A. M., Cataldi, E., Ramoino, P., Aluigi, M. G., . . . Falugi, C. (2015). Review: Morphofunctional and biochemical markers of stress in sea urchin life stages exposed to engineered nanoparticles. *Environmental Toxicology*,*31*(11), 1552-1562. doi:10.1002/tox.22159

Gambardella, Chiara, et al... “Ecotoxicological Effects of Polystyrene Microbeads in a Battery of Marine Organisms Belonging to Different Trophic Levels.” *Marine Environmental Research*, vol. 141, 2018, pp. 313–321., doi:10.1016/j.marenvres.2018.09.023.

Givens, C. E., Burnett, K. G., Burnett, L. E., & Hollibaugh, J. T. (2013). Microbial communities of the carapace, gut, and hemolymph of the Atlantic blue crab, Callinectes sapidus. Marine Biology, 160(11), 2841-2851. doi:10.1007/s00227-013-2275-8

Guerinot, M., and Patriquin, D. 1981. N2-fixing vibrios isolated from the gastrointestinal tract of sea urchins. Can. J. Microbiol. 27, 311–317. doi: 10.1139/m81-048

Hakim JA, Koo H, Dennis LN, Kumar R, Ptacek T, Morrow CD, Lefkowitz EJ, Powell ML, Bej AK and Watts SA (2015) An abundance of Epsilonproteobacteria revealed in the gut microbiome of the laboratory cultured sea urchin, Lytechinus variegatus. Front. Microbiol. 6:1047. doi: 10.3389/fmicb.2015.01047

Hakim, J. A., Koo, H., Kumar, R., Lefkowitz, E. J., Morrow, C. D., Powell, M. L., … Bej, A. K. (2016). The gut microbiome of the sea urchin,Lytechinus variegatus, from its natural habitat demonstrates selective attributes of microbial taxa and predictive metabolic profiles. FEMS Microbiology Ecology, 92(9). doi: 10.1093/femsec/fiw146

Hakim, J., Schram, J., Galloway, A., Morrow, C., Crowley, M., Watts, S., & Bej, A. (2019). The Purple Sea Urchin Strongylocentrotus purpuratus Demonstrates a Compartmentalization of Gut Bacterial Microbiota, Predictive Functional Attributes, and Taxonomic Co-Occurrence. Microorganisms, 7(2), 35. doi:10.3390/microorganisms7020035

Hall, Michael, and Robert G. Beiko. “16S RRNA Gene Analysis with QIIME2.” Methods in Molecular Biology Microbiome Analysis, 2018, pp. 113–129., doi:10.1007/978-1-4939-8728-3_8.

Harvell, C. D. 1999. Emerging Marine Diseases--Climate Links and Anthropogenic Factors. Science, 285(5433), 1505–1510. doi: 10.1126/science.285.5433.1505

Hay, Mark E., and Phillip R. Taylor. “Competition between Herbivourous Fishes and Urchins on Caribbean Reefs.” Oecologia, vol. 65, no. 4, 1985, pp. 591–598., doi:10.1007/bf00379678.

Hernroth, B., Bade, S., Thorndyke, M., & Dupont, S. (2011). Immune suppression of the echinoderm Asterias rubens (L.) following long-term ocean acidification. Aquatic Toxicology, 103, 222-224.

Hughes, T.P. 1994. Catastrophes, phase shifts and large-scale degradation of a Caribbean coral reef. Science 265: 1547-1551

Ishaq, S. L., & Wright, A. G. (2012). Insight into the bacterial gut microbiome of the North American moose (Alces alces). *BMC Microbiology*,*12*(1), 212. doi:10.1186/1471-2180-12-212

Jaccard, P. (1908). Nouvelles researches sur la distribution florale. Bulletin de la Société Vaudense des Sciences Naturelles, 44, 223−270.

Janssen, S., Mcdonald, D., Gonzalez, A., Navas-Molina, J. A., Jiang, L., Xu, Z. Z., . . . Knight, R. (2018). Phylogenetic Placement of Exact Amplicon Sequences Improves Associations with Clinical Information. MSystems, 3(3). doi:10.1128/msystems.00021-18

Lessios, H. A. 2004. Diadema antillarum populations in Panama twenty years following mass mortality. Coral Reefs, 24(1), 125–127. doi: 10.1007/s00338-004-0443-5

Lessions, H. A. 1995. Diadema antillarum 10 years after mass mortality: still rare, despite help from a competitor. Proceedings of the Royal Society of London. Series B: Biological Sciences, 259(1356), 331–337. doi: 10.1098/rspb.1995.0049

Lessios, H. 1988. Mass Mortality Of Diadema-Antillarum In The Caribbean: What Have We Learned. Annual Review of Ecology and Systematics, 19(1), 371–393. doi: 10.1146/annurev.ecolsys.19.1.371

Lessios, H. A., Cubit, J. D., Robertson, D. R., Shulman, M. J., Parker, M. R., Garrity, S. D., & Levings, S. C. 1984. Mass mortality of Diadema antillarum on the Caribbean coast of Panama. Coral Reefs, 3(4), 173–182. doi: 10.1007/bf00288252

Lessios, H.A., 2016. The great Diadema antillarum die-off: 30 Years later. Annu. Rev. Mar. Sci. 8, 267e283. http://dx.doi.org/10.1146/annurev-marine-122414- 033857

Lessios, H. A. (1979). Use of Panamanian sea urchins to test the molecular clock. Nature, 280(5723), 599–601. doi: 10.1038/280599a0

Lessios, H. A., Robertson, D. R., & Cubit, J. D. (1984). Spread of Diadema Mass Mortality Through the Caribbean. Science,226(4672), 335-337. doi:10.1126/science.226.4672.335

Lessios, H. A., Garrido, M. J., & Kessing, B. D. (2001). Demographic history of Diadema antillarum , a keystone herbivore on Caribbean reefs. Proceedings of the Royal Society of London. Series B: Biological Sciences,268(1483), 2347-2353. doi:10.1098/rspb.2001.1806

Levitan, D. R., & Petersen, C. (1995). Sperm limitation in the sea. Trends in Ecology & Evolution, 10(6), 228-231. doi:10.1016/s0169-5347(00)89071-0

Lin, W., Zhang, H., & Beck, G. (2001). Phylogeny of natural cytotoxicity: Cytotoxic activity of coelomocytes of the purple sea urchin,Arbacia punctulata. Journal of Experimental Zoology, 290(7), 741-750. doi:10.1002/jez.1124

Li, Y., Xu, J., Chen, Y., Ding, W., Shao, A., Liang, X., . . . Yang, J. (2019). Characterization of Gut Microbiome in the Mussel Mytilus galloprovincialis in Response to Thermal Stress. Frontiers in Physiology, 10. doi:10.3389/fphys.2019.01086

Lozupone, C. A., Hamady, M., Kelley, S. T., & Knight, R. (2007). Quantitative and qualitative beta diversity measures lead to different insights into factors that structure microbial communities. Applied and Environmental Microbiology, 73(5), 1576–1585. doi: 10.1128/AEM. 01996-06.

Lozupone, C.,&Knight, R. (2005).UniFrac:A new phylogenetic method for comparing microbial communities. Applied and Environmental Microbiology, 71(12), 8228–8235. doi: 10.1128/AEM.71.12.8228-8235.2005

McDonald, D., Price, M. N., Goodrich, J., Nawrocki, E. P., DeSantis, T. Z., Probst, A., … Hugenholtz, P. (2012). An improved Greengenes taxonomy with explicit ranks for ecological and evolutionary analyses of bacteria and archaea. The ISME Journal, 6(3), 610–618. doi: 10.1038/ismej.2011.139.

Medzhitov, R., & Janeway, C., Jr. (2002). Decoding the Patterns of Self and Nonself by the Innate ... Retrieved December 10, 2020, from https://science.sciencemag.org/content/296/5566/298.full

Meziti, A., Kormas, K. A., Pancucci-Papadopoulou, M.-A., and Thessalou-Legaki, M. (2007). Bacterial phylotypes associated with the digestive tract of the sea urchin Paracentrotus lividus and the ascidian Microcosmus sp. Russ. J. Mar. Biol. 33, 84–91. doi: 10.1134/S1063074007020022

Metsalu, Tauno and Vilo, Jaak. Clustvis: a web tool for visualizing clustering of multivariate data using Principal Component Analysis and heatmap. Nucleic Acids Research, 43(W1):W566–W570, 2015. doi: 10.1093/nar/gkv468.

Miyake, S., Ngugi, D. K., and Stingl, U. (2015). Diet strongly influences the gut microbiota of surgeonfishes. Mol. Ecol. 24, 656–672. doi: 10.1111/mec.13050

Moeller, A. H., Caro-Quitero, A., Mjungu, D., Georgiev, A. V., Lonsdorf, E. V., Mueller, M. N., . . . Ochman, H. 2016. Cospeciation of gut microbiota with hominids. Science, 353(6297), 380-382. doi:10.1126/science.aaf3951

Moritz, C., & Agudo, R. 2013. The Future of Species Under Climate Change: Resilience or Decline? Science, 341(6145), 504–508. doi: 10.1126/science.1237190

Mumby, P. J. et al... 2007 Trophic cascade facilitates coral recruitment in a marine reserve. Proc. Natl Acad. Sci. 104, 8362–8367. (doi:10.1073/pnas.0702602104)

Pagán-Jiménez, M., Ruiz-Calderón, J. F., Dominguez-Bello, M. G., & García-Arrarás, J. E. (2019). Characterization of the intestinal microbiota of the sea cucumber Holothuria glaberrima. Plos One, 14(1). doi:10.1371/journal.pone.0208011

Pielou, E. C. (1966). The measurement of diversity in different types of biological collections. Journal of Theoretical Biology, 13, 131–144. doi: 10.1016/0022-5193(66)90013-0.

Precht, W. F. & Aronson, R. B. 2006. Death and resurrection of Caribbean coral reefs: a paleoecological perspective. In Coral reef conservation (eds I. M. Coˆte´ & D. J. Reynolds), pp. 40–77. Cambridge, UK: Cambridge University Press

Precht, W. F., Aronson, R. B., Moody, R. M., & Kaufman, L. (2010). Changing Patterns of Microhabitat Utilization by the Threespot Damselfish, Stegastes planifrons, on Caribbean Reefs. PLoS ONE, 5(5). doi:10.1371/journal.pone.0010835

Ripple, K. J. 2017. Tandem Restoration of Diadema antillarum and Acropora cervicornis for Enhanced Reef Recovery. Retrieved from https://ufdc.ufl.edu/UFE0051142/00001

Rodríguez-Barreras, R., Montañez-Acuña, A., Otaño-Cruz, A., & Ling, S. D. 2018. Apparent stability of a low-density Diadema antillarum regime for Puerto Rican coral reefs. ICES Journal of Marine Science, 75(6), 2193–2201. doi: 10.1093/icesjms/fsy093

Rodriguez-Barreras, R., Perez, M., Mercado-Molina, A. E., Williams, S., & Sabat, A. (2014). Higher population densities of the sea urchin Diadema antillarum linked to wave sheltered areas in north Puerto Rico Archipelago. Journal of the Marine Biological Association of the United Kindom, 94(8). doi:10.1017/S0025315414000666

Shannon, C. E., & Weaver, W. (1949). The mathematical theory of communication. Retrieved from https://pure.mpg.de/rest/items/item_2383164/component/file_2383163/content.

Sharp, W. C., Delgado, G. A., Hart, J. E., and Hunt, J. H. (2017). Comparing the behavior and morphology of wild-collected and hatchery-propagated long-spined urchins (Diadema antillarum): implications for coral reef ecosystem restoration. Bull. Mar. Sci. 94, 103–122. doi: 10.5343/bms.2017.1068

Sodergren E, Weinstock GM, Davidson EH et al... 2006 The genome of the sea urchin Strongylocentrotus purpuratus. Science; 314:941-952

Sørensen, T. (1948). A method of establishing groups of equal amplitude in plant sociology based on similarity of species content and its application to analyses of the vegetation on Danish commons. København: I kommission hos E. Munksgaard. Retrieved from https://www.worldcat.org/title/method-of-establishing-groups-of-equal-amplitude-in-plant-sociology-based-on-similarity-of-species-content-and-its-application-to-analyses-of-the-vegetation-on-danish-commons/oclc/4713331.

Stimson, J., Cunha, T., & Philippoff, J. (2007). Food preferences and related behavior of the browsing sea urchin Tripneustes gratilla (Linnaeus) and its potential for use as a biological control agent. Marine Biology, 151, 1761-1772.

Tanrattanapitak, N., & Pairohakul, S. (2018). Bacterial Community in Gut Contents of the Sea Urchin Diadema setosum (Leske, 1778) and the Ambient Sediments from Sichang Island using Metagenomics Approaches. International Journal of Science, 15(1).

Thomas, F., Hehemann, J. H., Rebuffet, E., Czjzek, M., and Michel, G. (2011). Environmental and gut bacteroidetes: the food connection. Front. Microbiol. 2:93. doi: 10.3389/fmicb.2011.00093

Tuohy, E., Wade, C., & Weil, E. (2020). Lack of recovery of the long-spined sea urchin Diadema antillarum Philippi in Puerto Rico 33 years after the Caribbean-wide mass mortality. PeerJ, 8. doi:10.7717/peerj.8428

Qiucui, Y., Kefu, Y., Jiayuan, L., Yinghui, W., Xueyong, H., Biao, C., & Zhenjun, Q. (2019). The Composition, Diversity and Predictive Metabolic Profiles of Bacteria Associated With the Gut Digesta of Five Sea Urchins in Luhuitou Fringing Reef (Northern South China Sea). Frontiers in Microbiology, 10, 1168. doi:10.3389/fmicb.2019.01168

Quintero, B. 2014, April 9. Restoring Diadema. Retrieved from https://isercaribe.org/blog/2014/4/9/restoring-diadema.

Varrella, S., Romano, G., Costantini, S., Ruocco, N., Ianora, A., Bentley, M. G., & Costantini, M. (2016). Toxic Diatom Aldehydes Affect Defence Gene Networks in Sea Urchins. *Plos One,11*(2). doi:10.1371/journal.pone.0149734

Vázquez-Baeza, Y., Pirrung, M., Gonzalez, A., & Knight, R. (2013). EMPeror: A tool for visualizing high-throughput microbial community data. GigaScience, 2(1), 16. doi: 10.1186/2047-217X-2-16.

Watkins, W. D., & Cabelli, V. J. (1985). Effect of fecal pollution on Vibrio parahaemolyticus densities in an estuarine environment. Applied and Environmental Microbiology, 49(5), 1307-1313. doi:10.1128/aem.49.5.1307-1313.1985

Zhang, W., Lv, Z., Li, C., Sun, Y., Jiang, H., Zhao, M., . . . Chang, Y. (2019). Transcriptome profiling reveals key roles of phagosome and NOD-like receptor pathway in spotting diseased Strongylocentrotus intermedius. *Fish & Shellfish Immunology,84*, 521-531. doi:10.1016/j.fsi.2018.10.042

Zhao, J., Ling, Y., Zhang, R., Ke, C., & Hong, G. (2018). Effects of dietary supplementation of probiotics on growth, immune responses, and gut microbiome of the abalone Haliotis diversicolor. Aquaculture, 493, 289-295. doi:10.1016/j.aquaculture.2018.05.011

Appendix

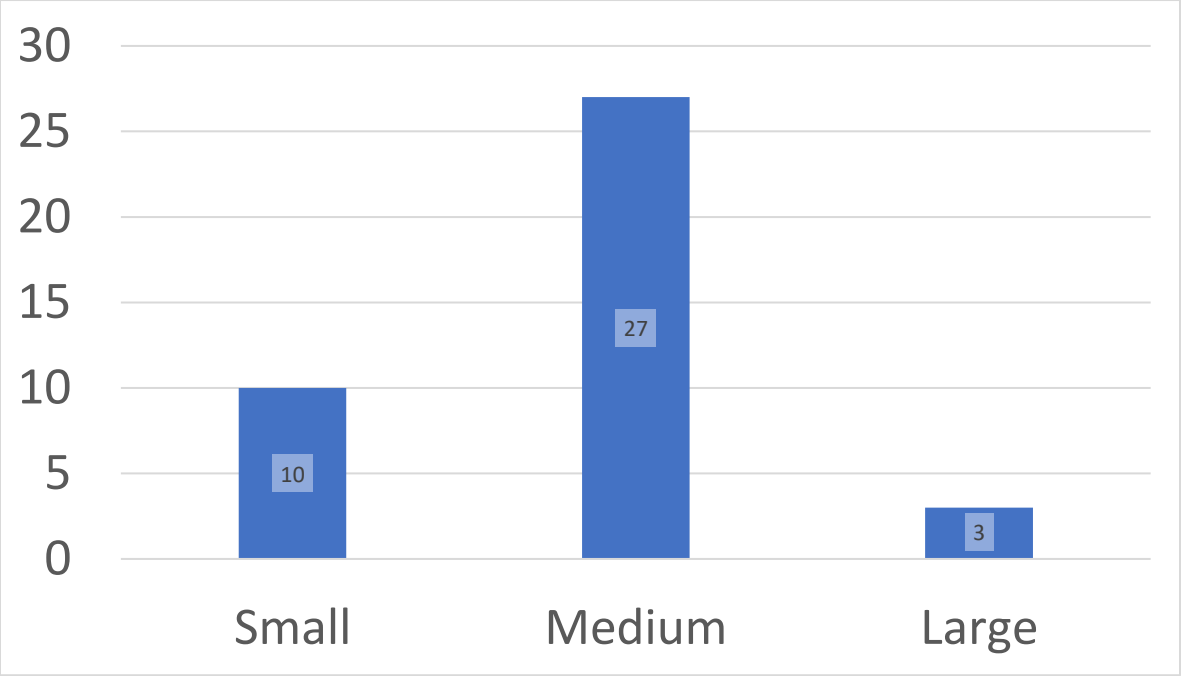

Figure 11. *Histogram distribution of graphs*. This table shows the amount of sea urchins collected in each proportion category. Animal body diameter size was categorized by small (1.5 - 2 in), medium (2.5 - 3 in) and large (3.5 - 4.5 in). The amount of sea urchins per category were 10 small, 27 medium, and 3 large.

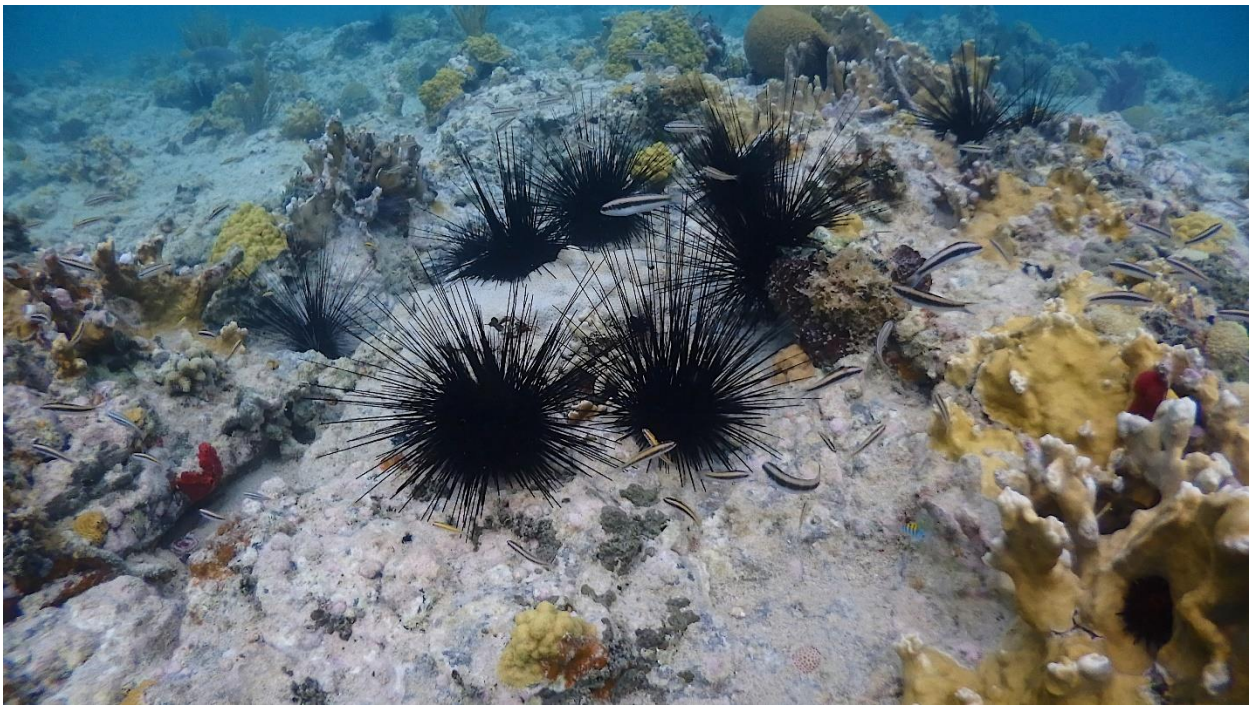

Figure 12. *Diadema antillarum at Playa Tamarindo in Culebras, Puerto Rico.* The Puerto Rico habitat of *Diadema antillarum* in Playa Tamarindo in Culebras Puerto Rico. This photo shows Playa Tamarindo in Culebra, Puerto Rico where a natural reserve is located. Underwater photography taken by Alejandro J Mercado Capote.

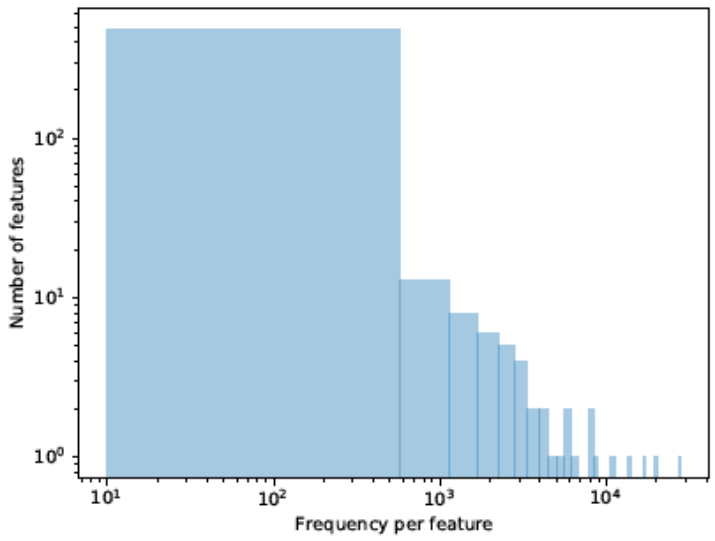

Figure 13. *Number of Features and frequency per feature.* The number of features found in the samples and the frequency per feature found. There was a total of 43 samples with 534 number of features that had a total frequency of 246,261. The minimum frequency was 2,603. The median frequency was 5,677. The maximum frequency was 10,427. The mean frequency was 5,727.

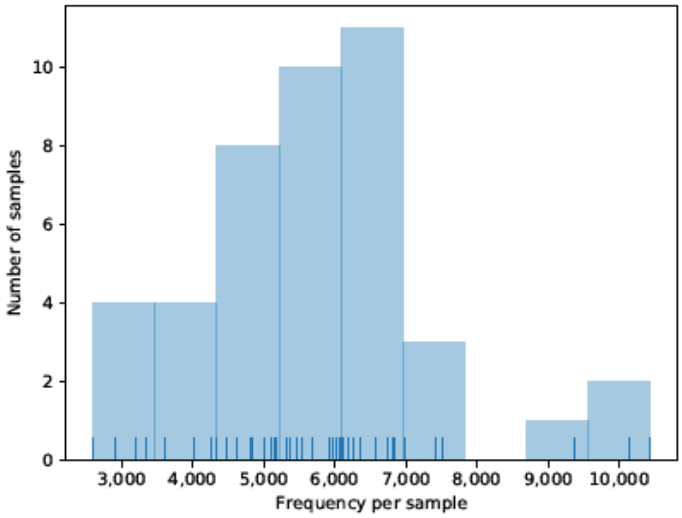

Figure 14. *Frequency of sample per sample*. This figure shows the number of samples and the frequency per sample. There was a total of 43 samples with 534 number of features that had a total frequency of 246,261. The minimum frequency was 10. The median frequency was 27. The mean frequency was 461.1629213483146.

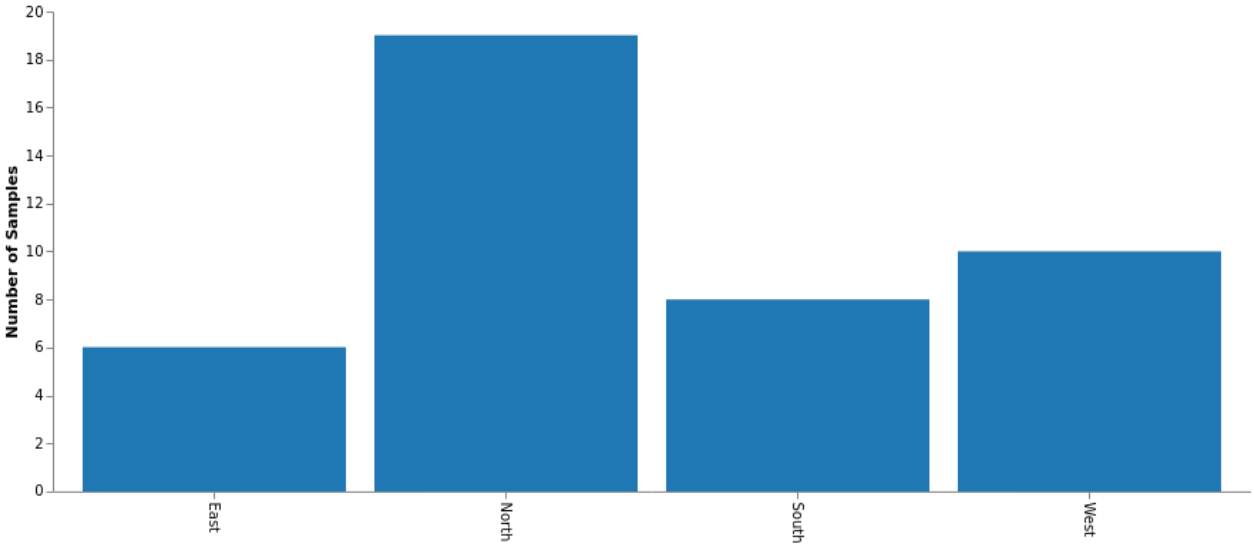

Figure 15. *Distribution of samples per cardinal point.* This table shows the number of samples per alignment category which includes sea urchins divided into cardinal grouping based on municipality location west (n=10), south (n=8), north (18) and east (n=7). A total of 43 samples were collected.

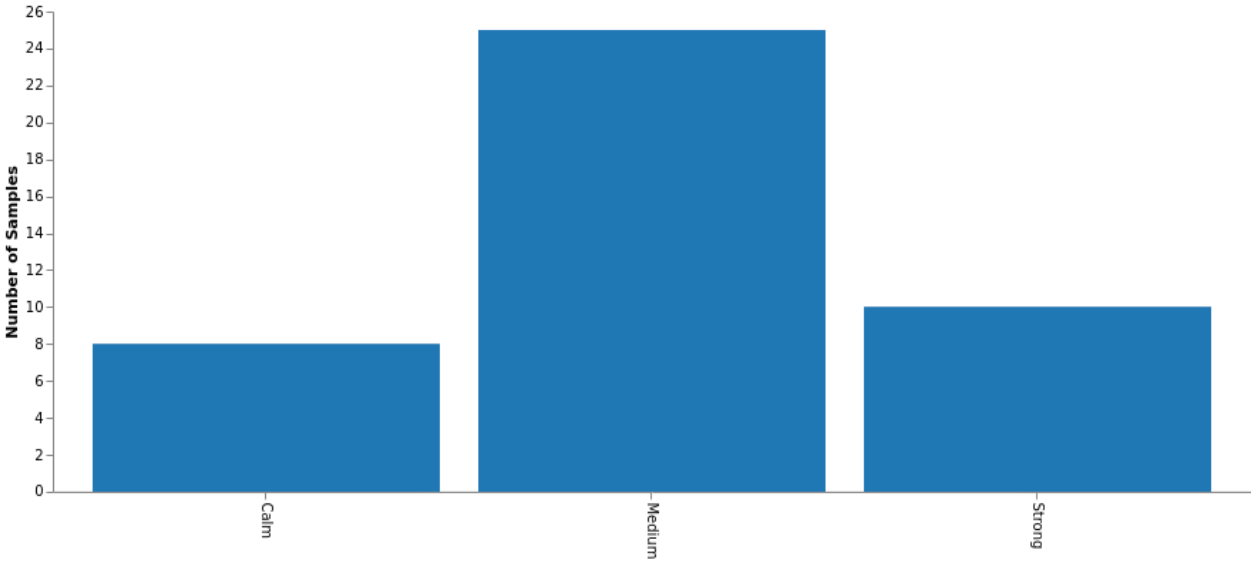

Figure 16. *Distribution of samples per current.* This table shows the number of samples per current category. Surface water is categorized by calm waters in the south to the Caribbean Sea, strong waters to the north Atlantic Ocean and medium waters in the east and west side being in between both bodies of water. The corresponding animal sample amounts are calm (n=8), medium (n=26) and strong (n=10).

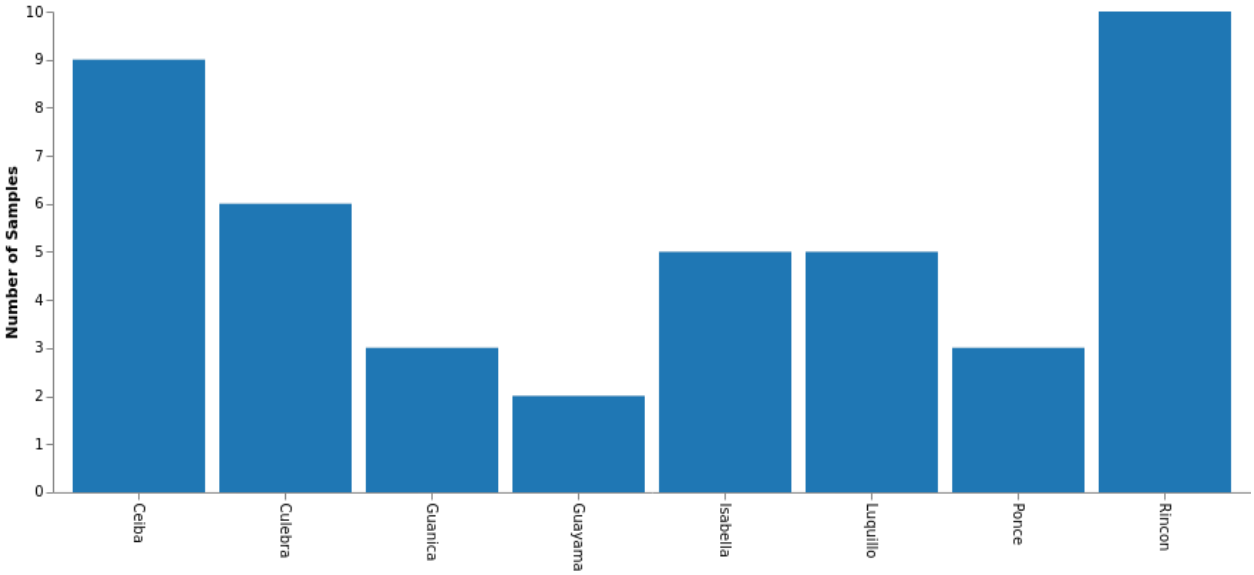

Figure 17. *Distribution of samples per location.* This table shows the number of samples per location. A total of 44 samples were collected from Ceiba (n=9), Culebra (n=7), Guayama (n=2), Guánica (n=3), Isabela (n=5), Luquillo (n=5), Ponce(n=3), Rincón (n=10).

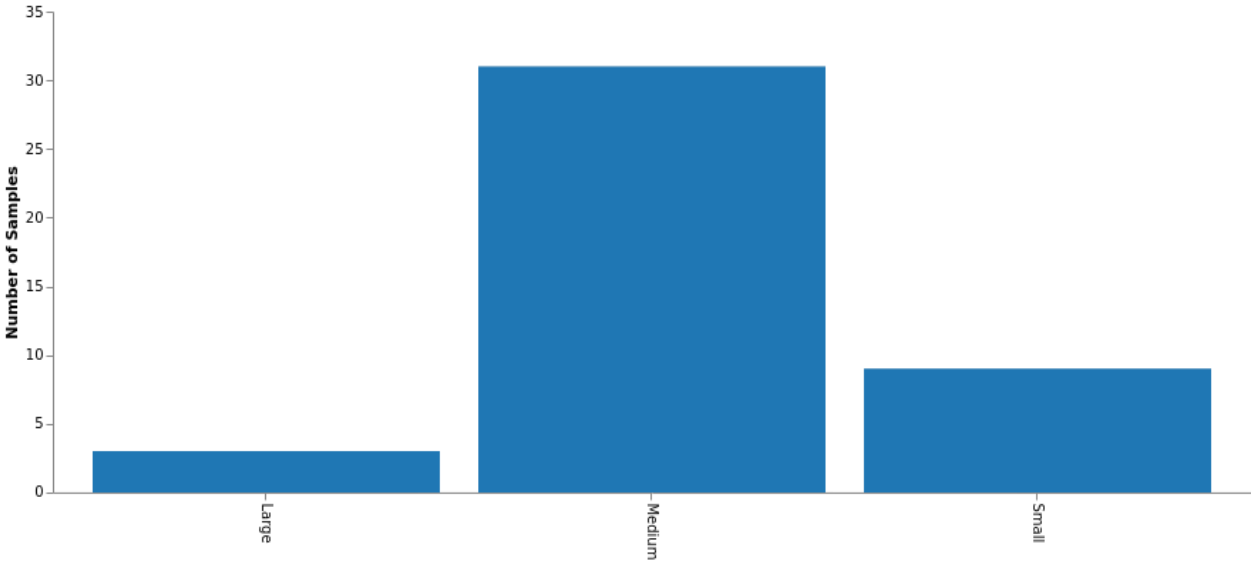

Figure 18. *Distribution of samples per proportion.* Number of samples per proportion category. Sea urchins were measured in inches and categorized by small (1.5 - 2 in, n=8), medium (2.5 - 3 in, n=31) and large (3.5 - 4.5 in, n=4).

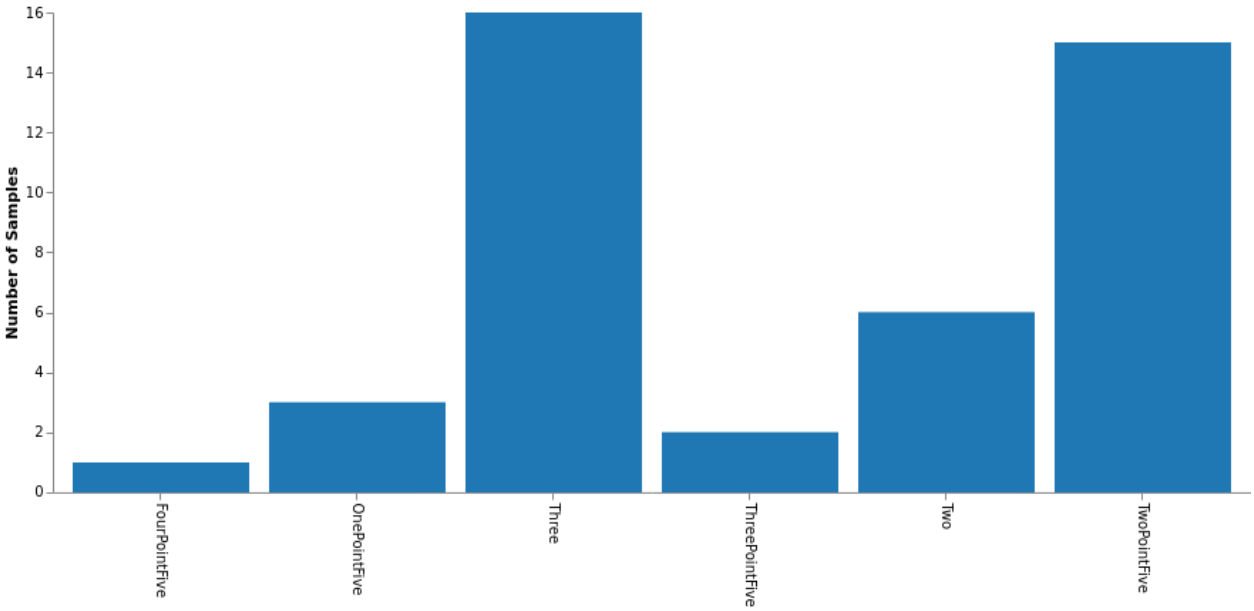

Figure 19. *Distribution of samples per size in inches.* Number of samples per size category in inches. Animal body diameters were measured and placed in the following categories one point five (n=3), two (n=6), two point five (n=15), three (n=16), three point five (n=3), four point five (n=1). Animals in the proportion category were placed into categories relative to their size, namely small (1.5 - 2 in), medium (2.5 - 3 in) and large (3.5 - 4.5 in).

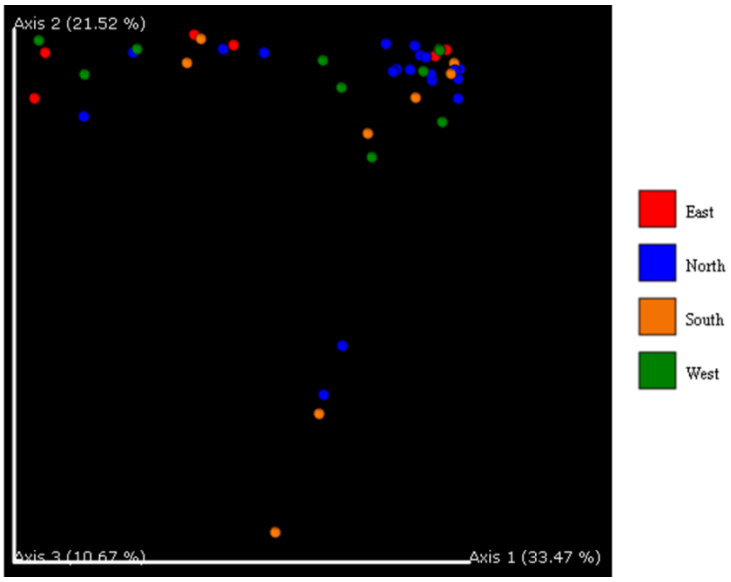

Figure 20. *Bray Curtis Dissimilarity Emperor Plot for the cardinal alignment category*. This graph shows a beta diversity analysis of the Bray-Curtis dissimilarity. This is used to quantify the differences in species populations between the different categories.

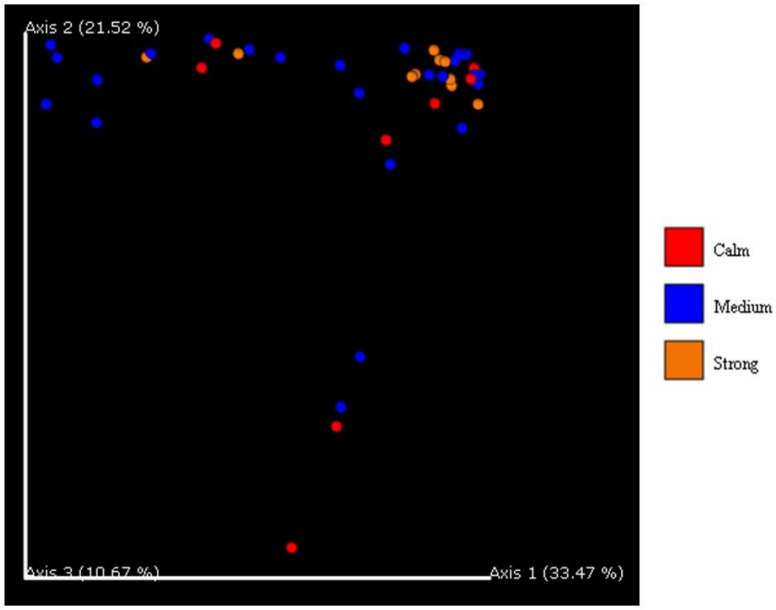

Figure 21. *Bray Curtis Dissimilarity Emperor Plot for the current category.* This graph shows a beta diversity analysis of the Bray-Curtis dissimilarity. This is used to quantify the differences in species populations between the different categories.

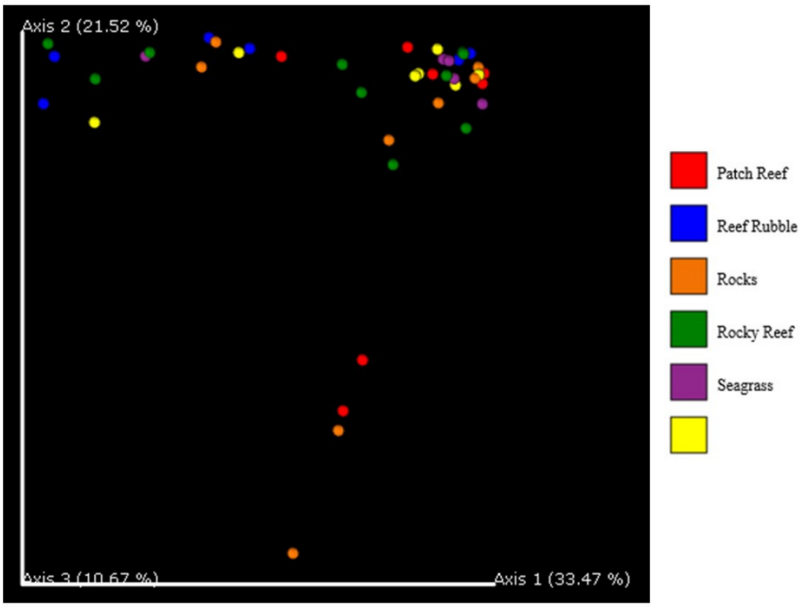

Figure 22. *Bray Curtis Dissimilarity Emperor Plot for the habitat category*. This graph shows a beta diversity analysis of the Bray-Curtis dissimilarity. This is used to quantify the differences in species populations between the different categories.

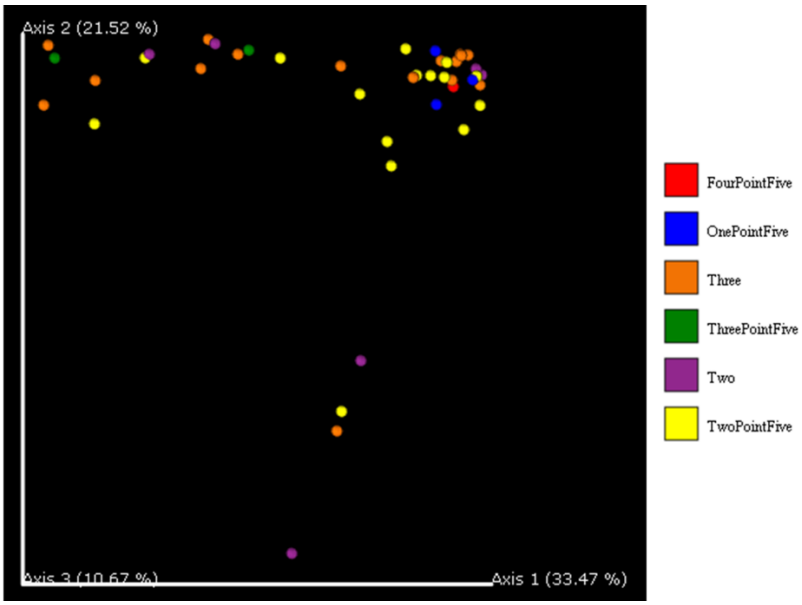

Figure 23. *Bray Curtis Dissimilarity Emperor Plot for the size category*. This graph shows a beta diversity analysis of the Bray-Curtis dissimilarity. This is used to quantify the differences in species populations between the different categories.

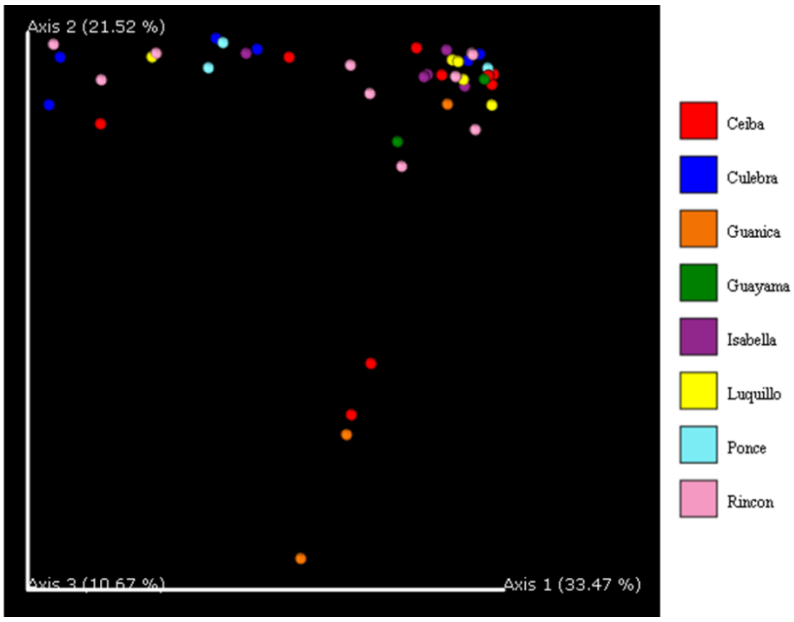

Figure 24. *Bray Curtis Dissimilarity Emperor Plot for the location category*. This graph shows a beta diversity analysis of the Bray-Curtis dissimilarity. This is used to quantify the differences in species populations between the different categories.

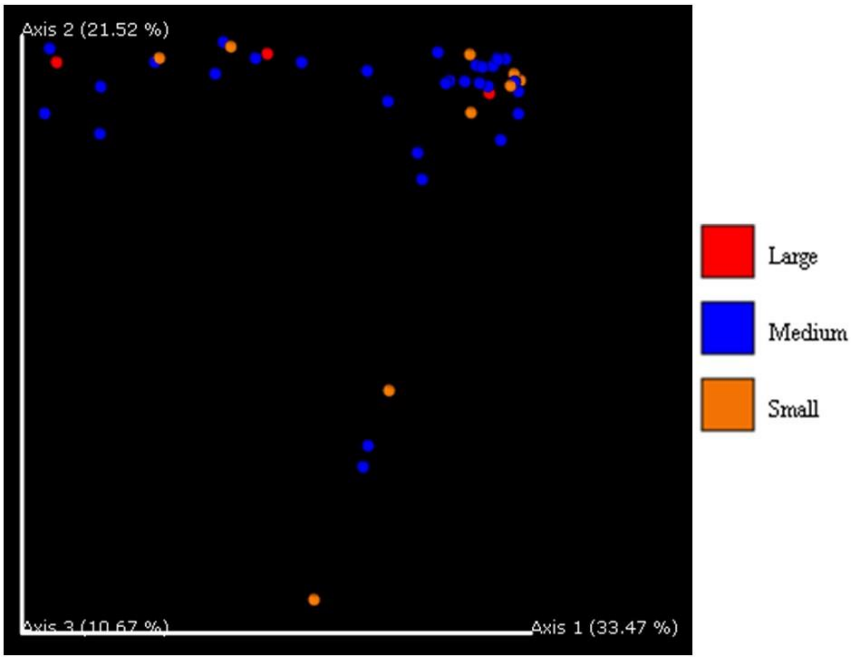

Figure 25. *Bray Curtis Dissimilarity Emperor Plot for the proportion category.* This graph shows a beta diversity analysis of the Bray-Curtis dissimilarity. This is used to quantify the differences in species populations between the different categories.

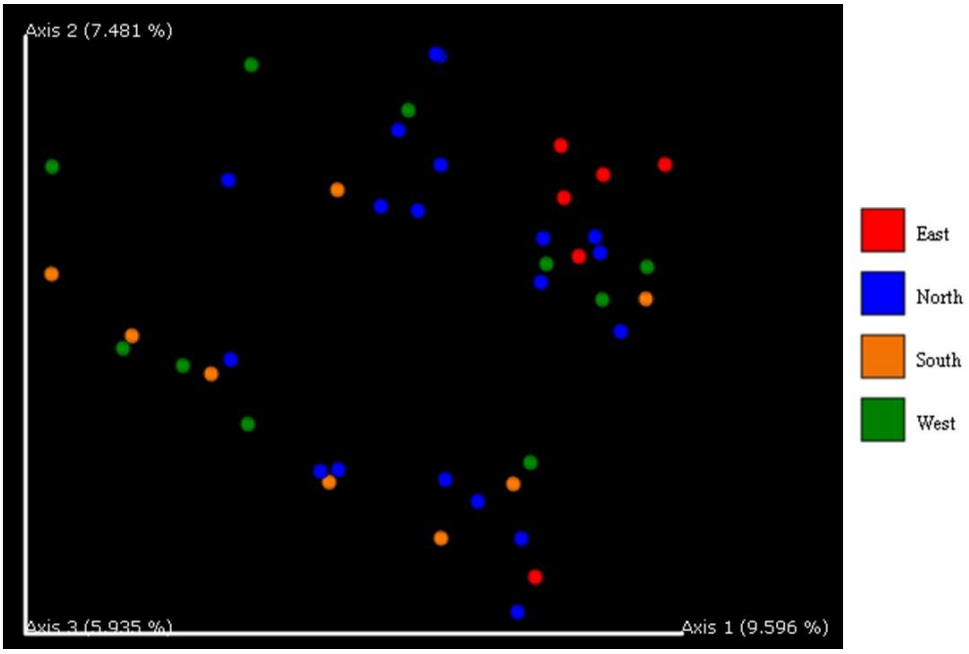

Figure 26. *Jaccard distance emperor plot for the cardinal location category*. This graph shows a beta diversity analysis of the Jaccard dissimilarity. This is a qualitative measure of the microbial community dissimilarity.

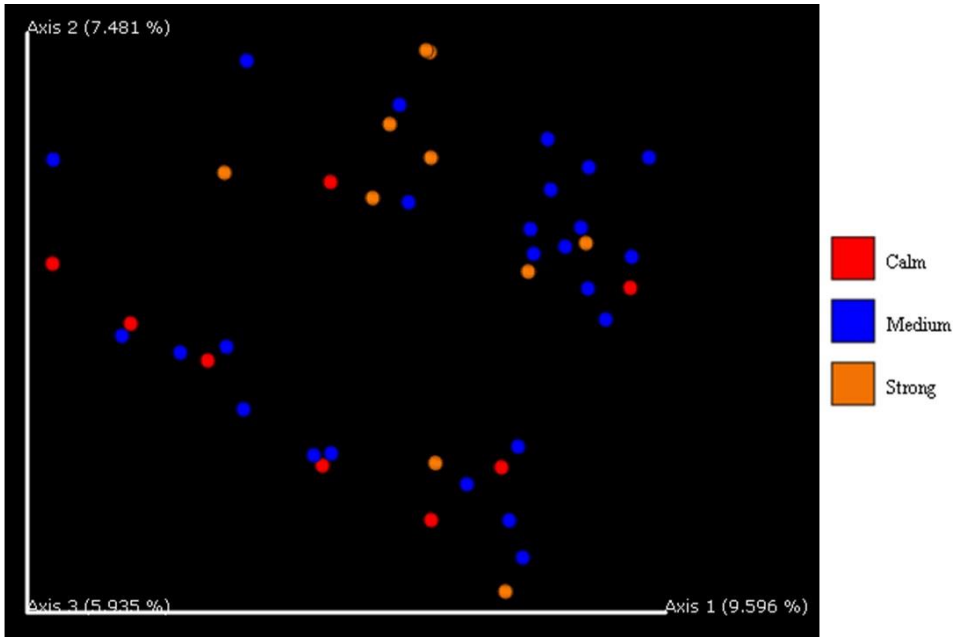

Figure 27. *Jaccard distance emperor plot for the current strength category.* This graph shows a beta diversity analysis of the Jaccard dissimilarity. This is a qualitative measure of the microbial community dissimilarity.

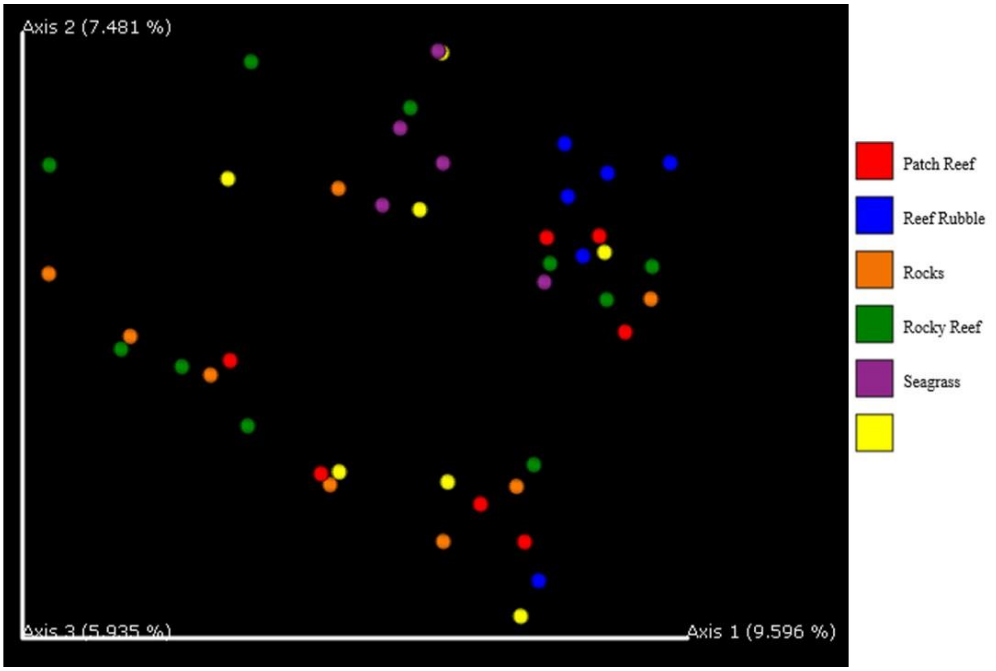

Figure 28. *Jaccard distance emperor plot for the habitat category.* This graph shows a beta diversity analysis of the Jaccard dissimilarity. This is a qualitative measure of the microbial community dissimilarity.

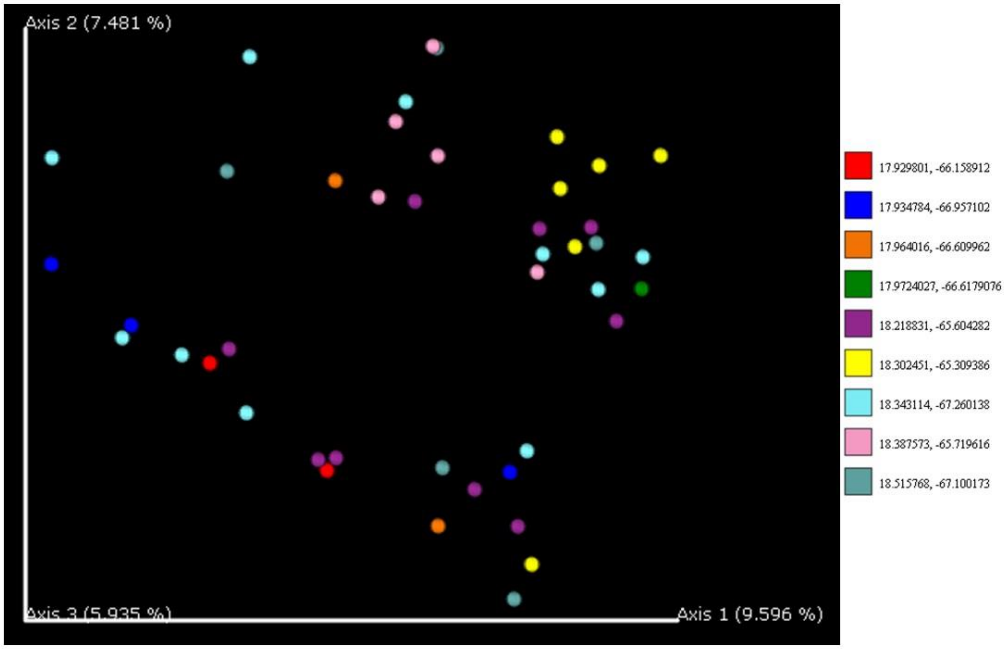

Figure 29. *Jaccard distance emperor plot for the latitude longitude category.* This graph shows a beta diversity analysis of the Jaccard dissimilarity. This is a qualitative measure of the microbial community dissimilarity

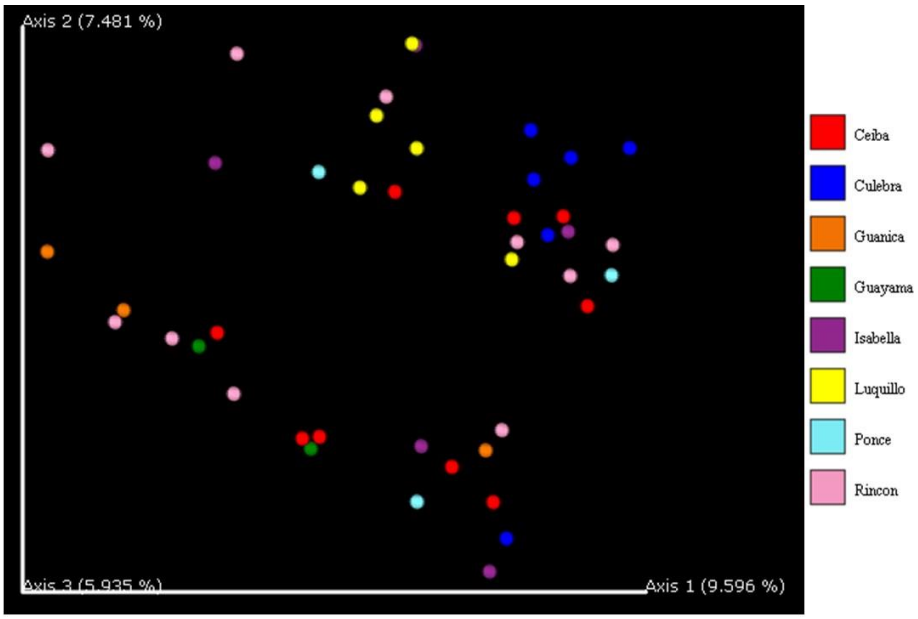

Figure 30. *Jaccard distance emperor plot for the location category*. This graph shows a beta diversity analysis of the Jaccard dissimilarity. This is a qualitative measure of the microbial community dissimilarity.

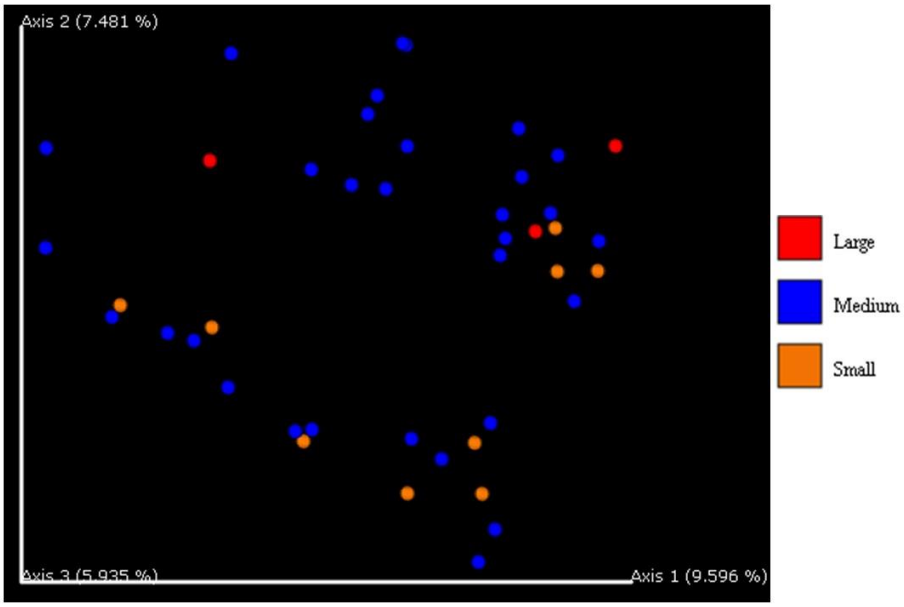

Figure 31. *Jaccard distance emperor plot for the proportion category.* This graph shows a beta diversity analysis of the Jaccard dissimilarity. This is a qualitative measure of the microbial community dissimilarity.

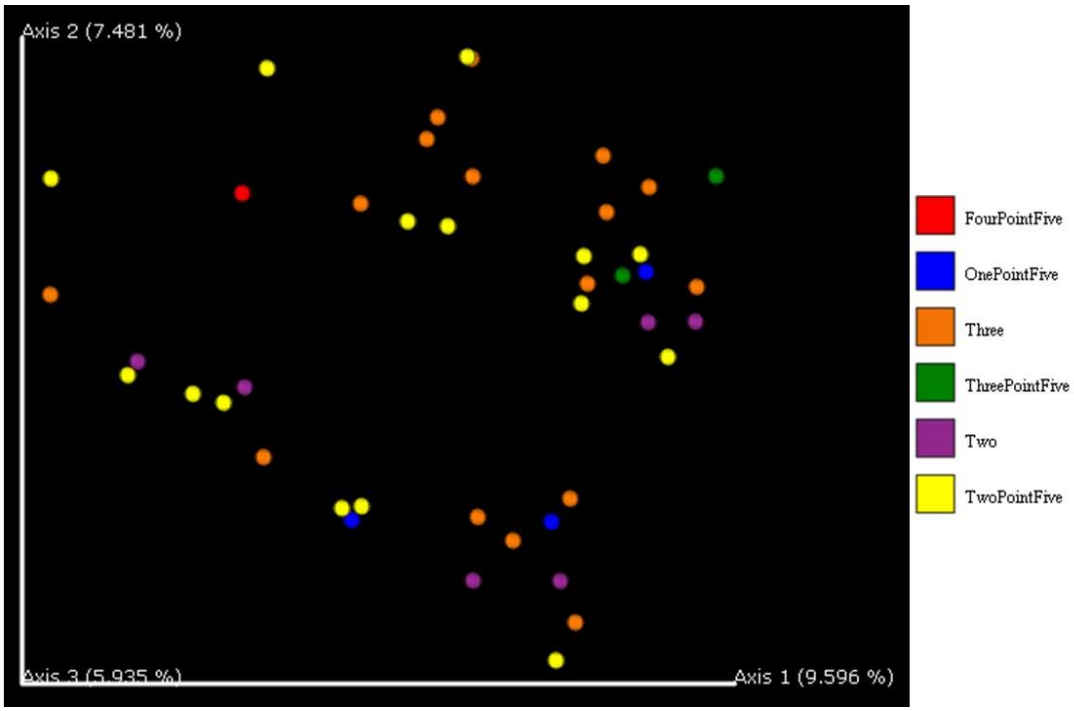

Figure 32. *Jaccard distance emperor plot for the size category.* This graph shows a beta diversity analysis of the Jaccard dissimilarity. This is a qualitative measure of the microbial community dissimilarity.

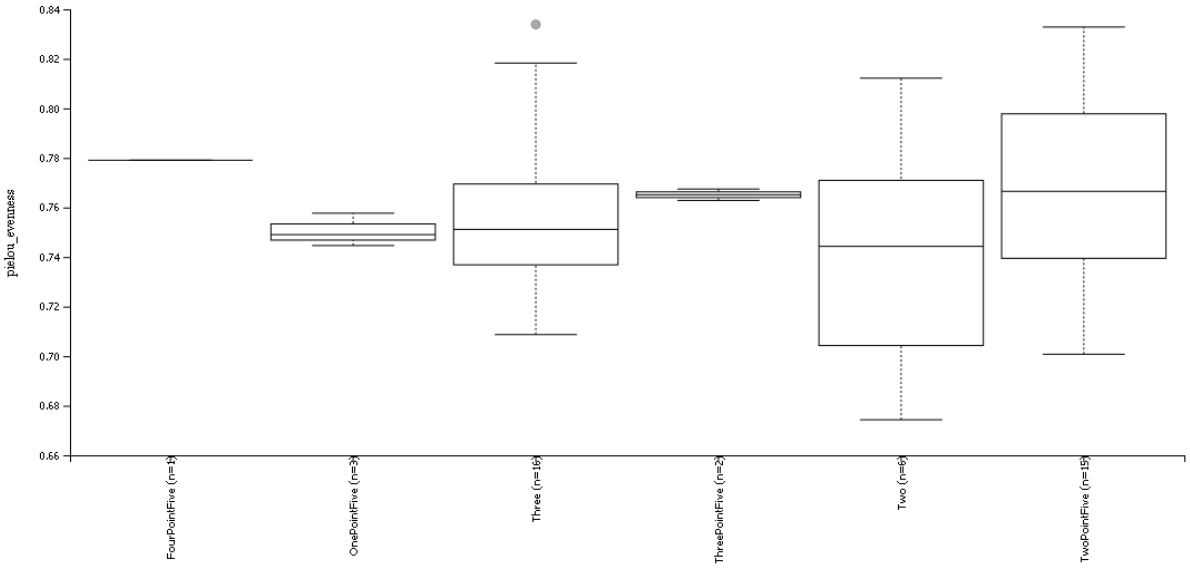

Figure 33. *Pielou's Evenness boxplots for the size category.* This graph shows the alpha diversity that represents a measure of a community relative evenness of species richness.

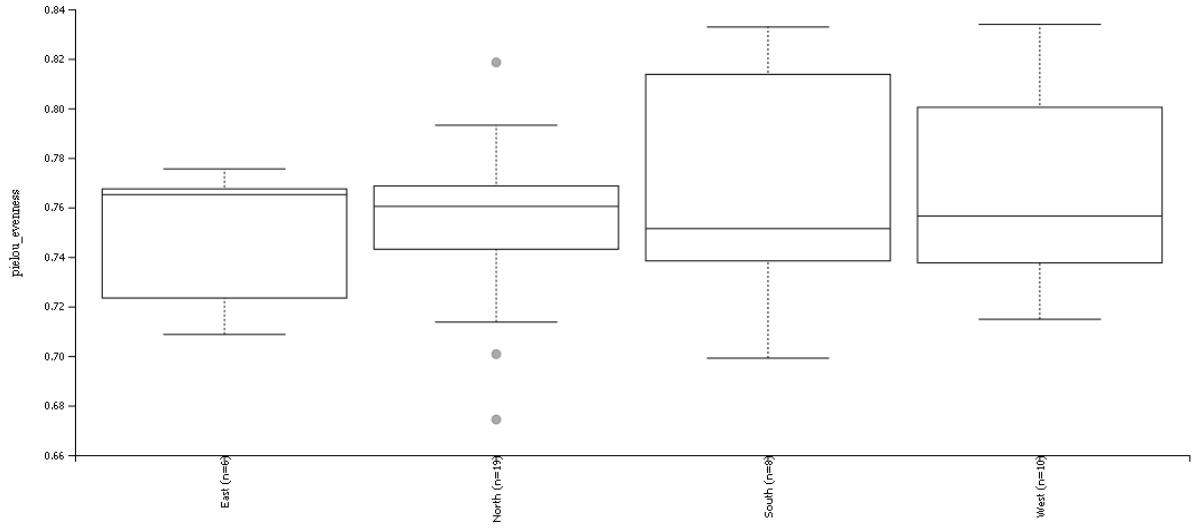

Figure 34. *Pielou's Evenness boxplots for the alignment category*. This graph shows the alpha diversity that represents a measure of a community relative evenness of species richness.

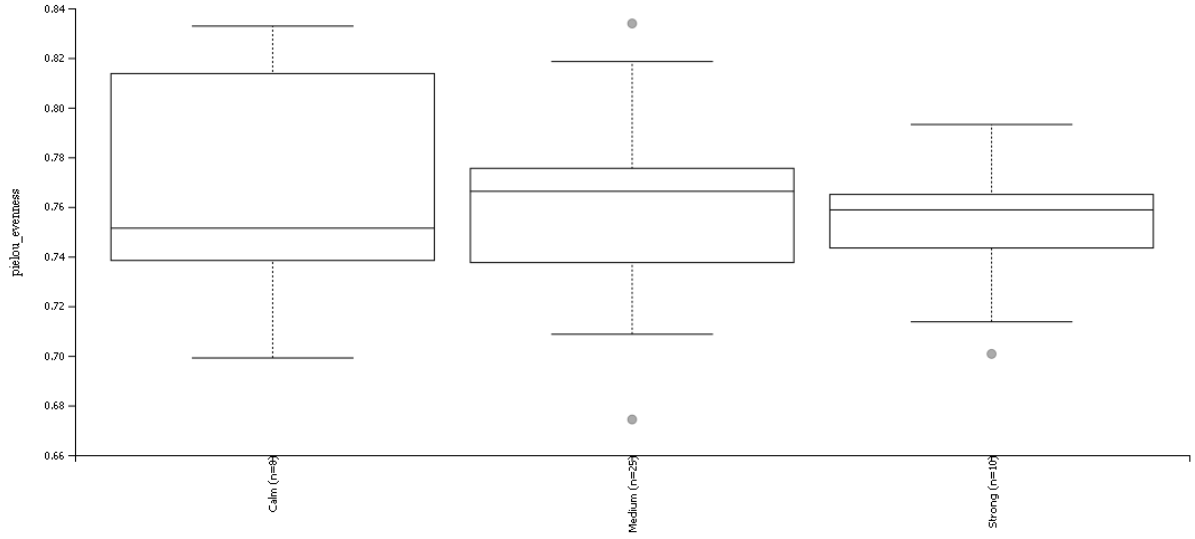

Figure 35. *Pielou's Evenness boxplots for the current strength category*. This graph shows the alpha diversity that represents a measure of a community relative evenness of species richness.

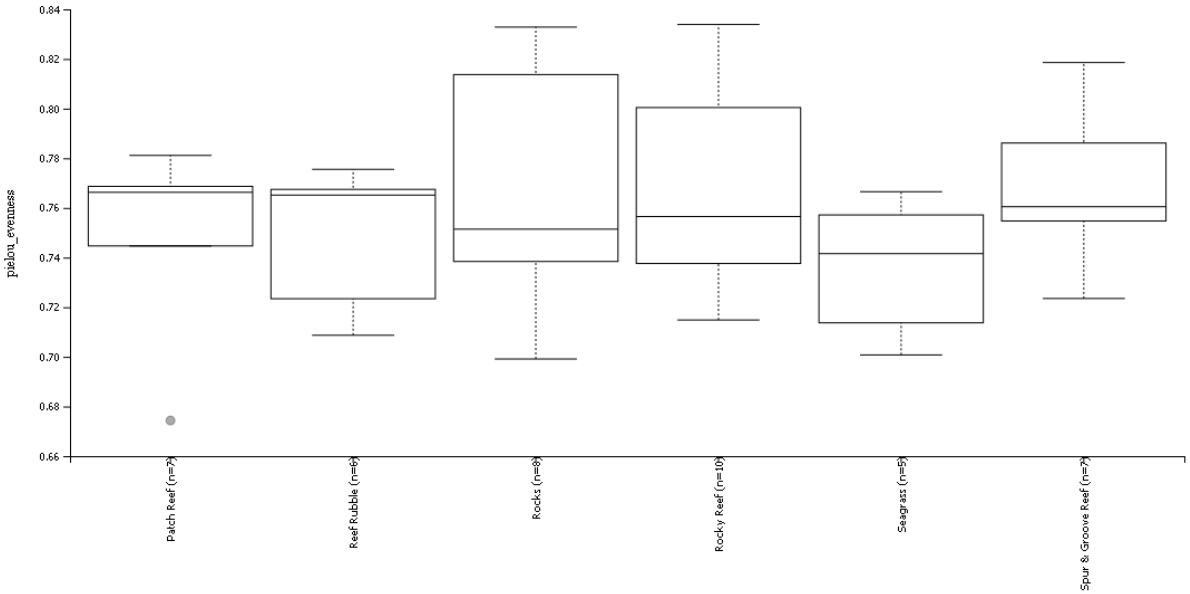

Figure 36. *Pielou's Evenness boxplots for the current habitat category.* This graph shows the alpha diversity that represents a measure of a community relative evenness of species richness.

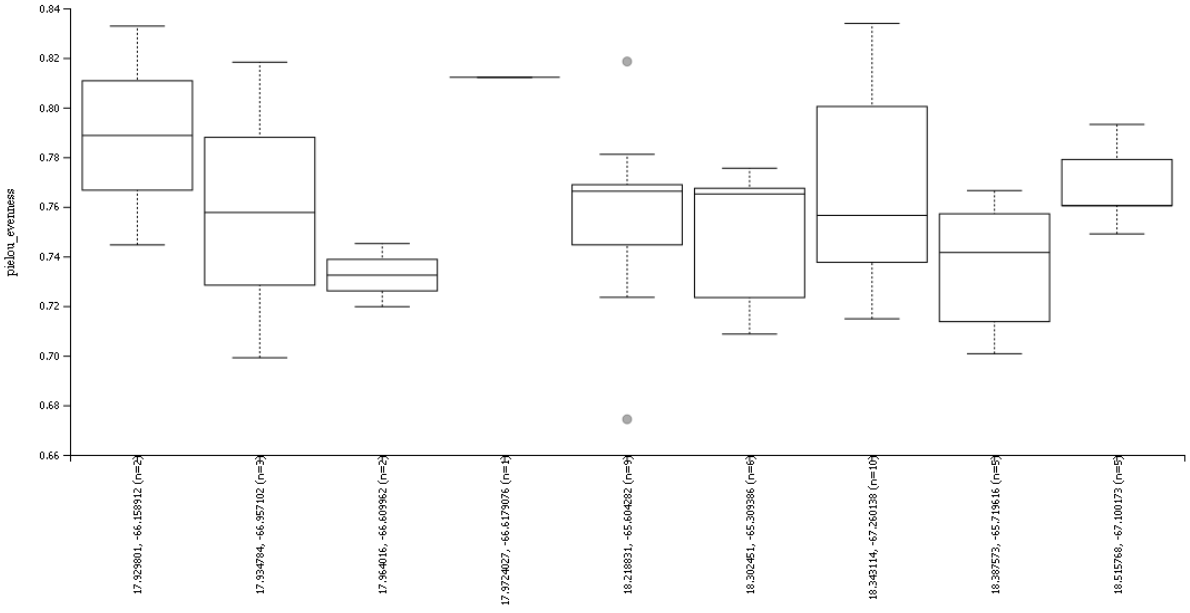

Figure 37. *Pielou's Evenness boxplots for the latitude and longitude category.* This graph shows the alpha diversity that represents a measure of a community relative evenness of species richness.

i

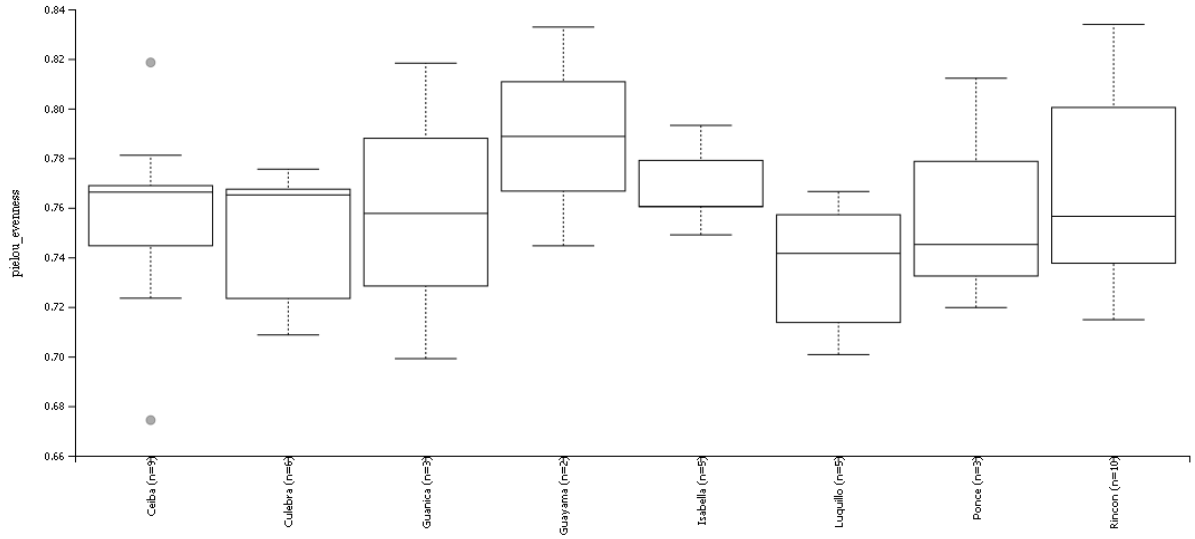

Figure 38. *Pielou's Evenness boxplots for the location category.* This graph shows the alpha diversity that represents a measure of a community relative evenness of species richness.

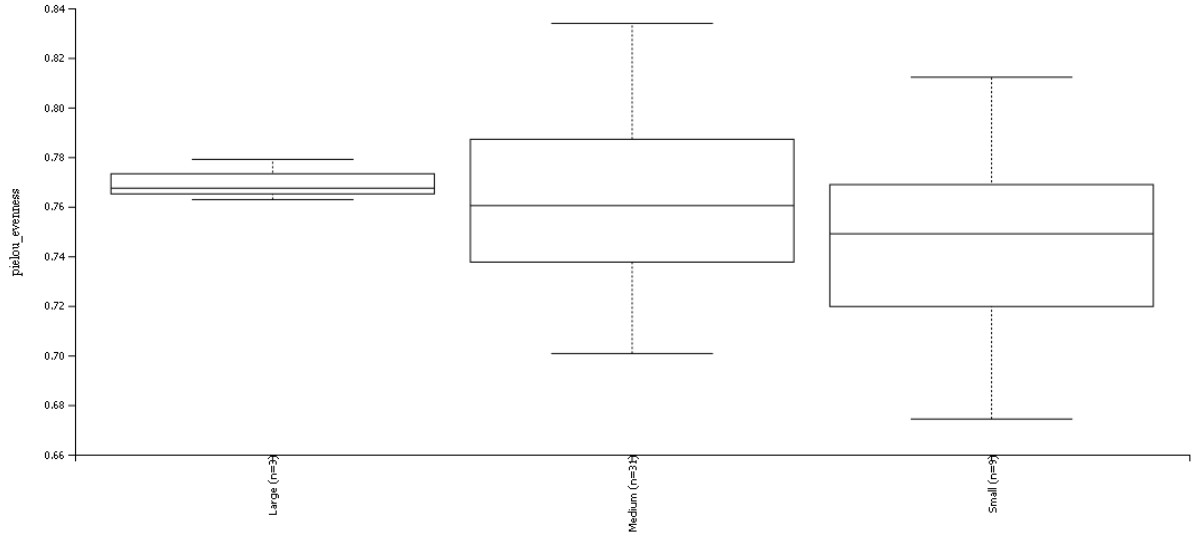

Figure 39. *Pielou's Evenness boxplots for the proportion category.* This graph shows the alpha diversity that represents a measure of a community relative evenness of species richness.

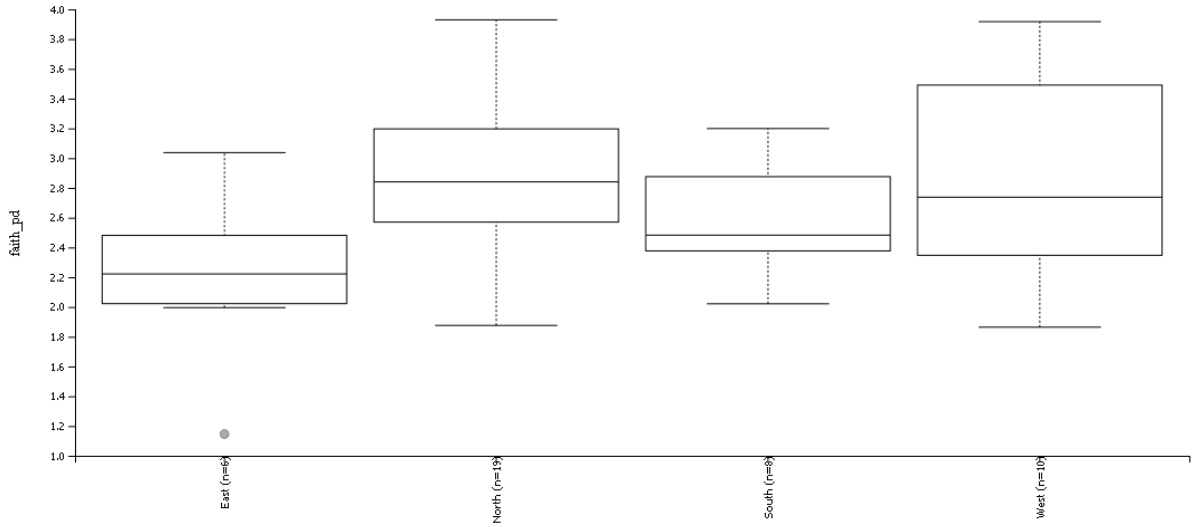

Figure 40. *Faith Phylogenetic diversity boxplots for the cardinal alignment category.* This graph shows the alpha diversity that represents a measure of a community richness that incorporates phylogenetic relationships between the features.

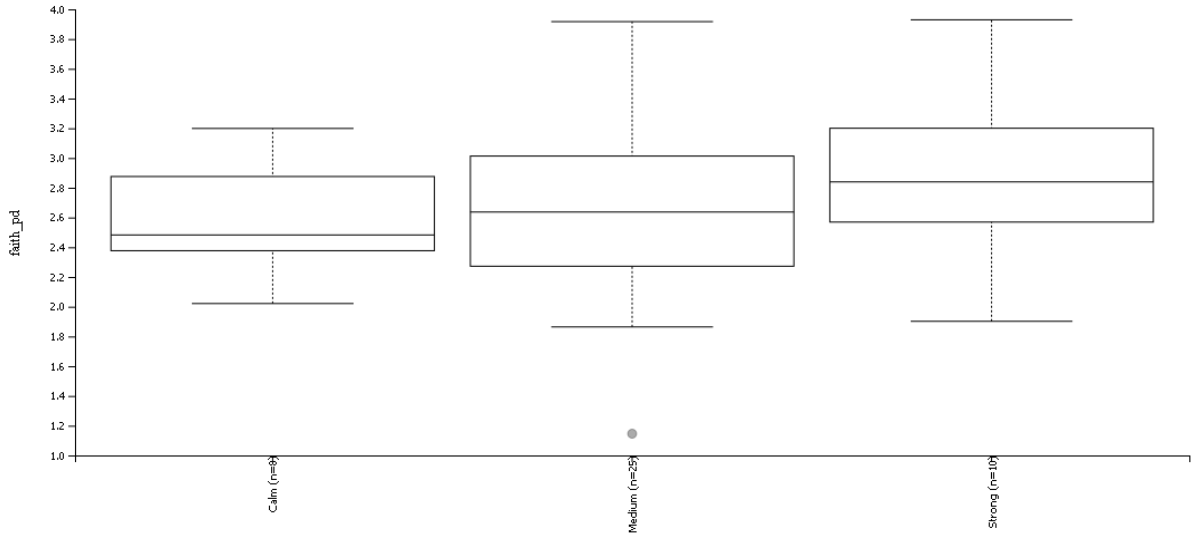

Figure 41. *Faith Phylogenetic diversity boxplots for the current category.* This graph shows the alpha diversity that represents a measure of a community richness that incorporates phylogenetic relationships between the features.

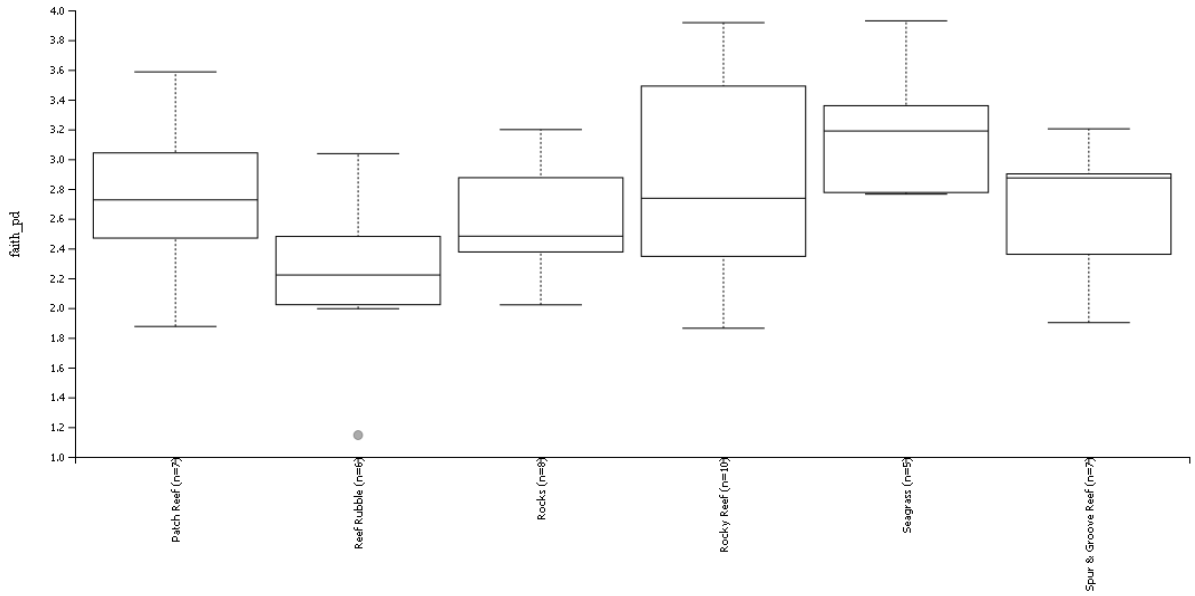

Figure 42. *Faith Phylogenetic diversity boxplots for the habitat category*. This graph shows the alpha diversity that represents a measure of a community richness that incorporates phylogenetic relationships between the features.

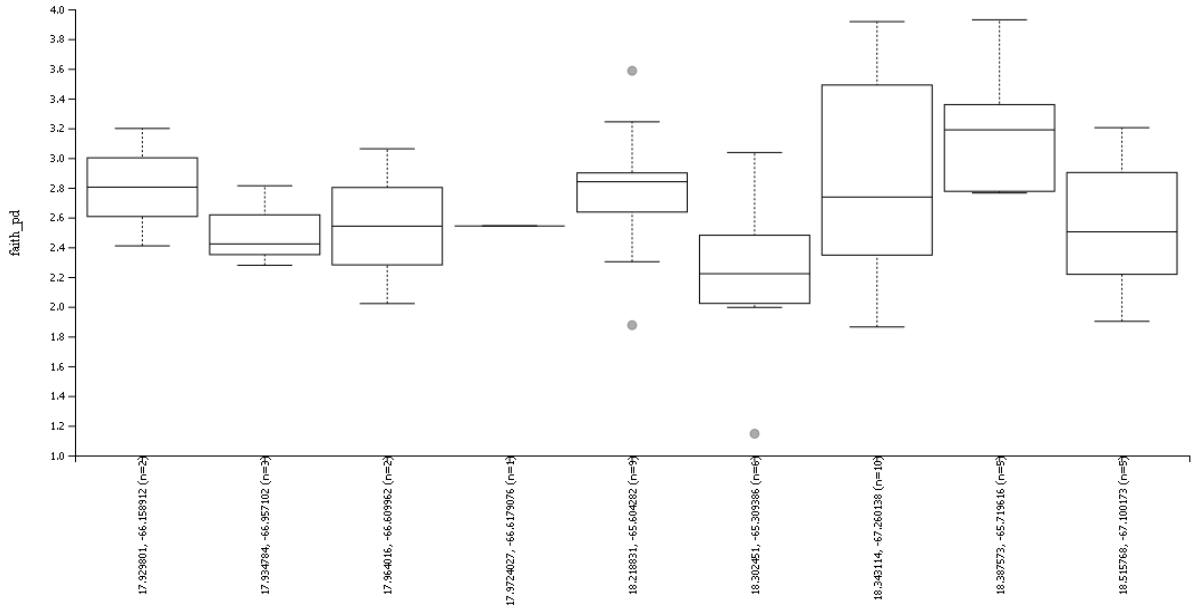

Figure 43. *Faith Phylogenetic diversity boxplots for the latitude and longitude category. This* graph shows the alpha diversity that represents a measure of a community richness that incorporates phylogenetic relationships between the features.

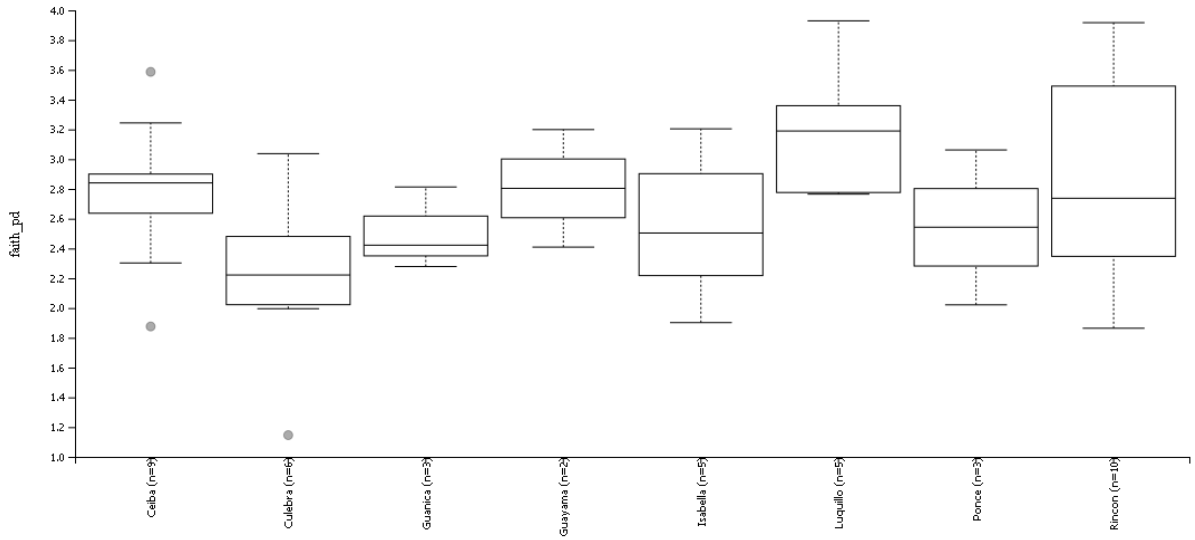

Figure 44. *Faith Phylogenetic diversity boxplots for the location category.* This graph shows the alpha diversity that represents a measure of a community richness that incorporates phylogenetic relationships between the features.

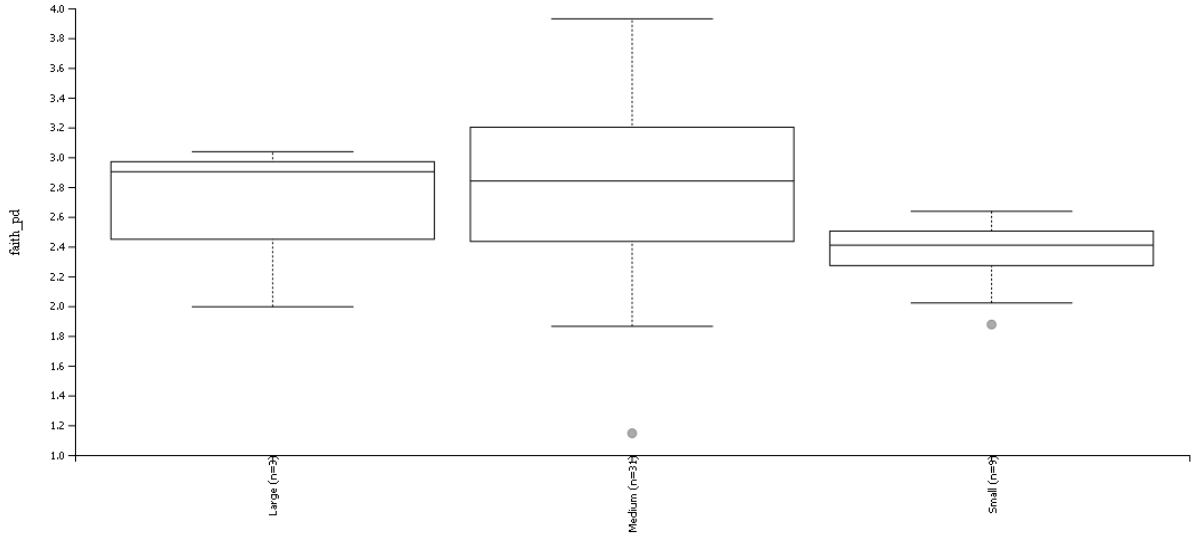

Figure 45. *Faith Phylogenetic diversity boxplots for the proportion category.* This graph shows the alpha diversity that represents a measure of a community richness that incorporates phylogenetic relationships between the features.

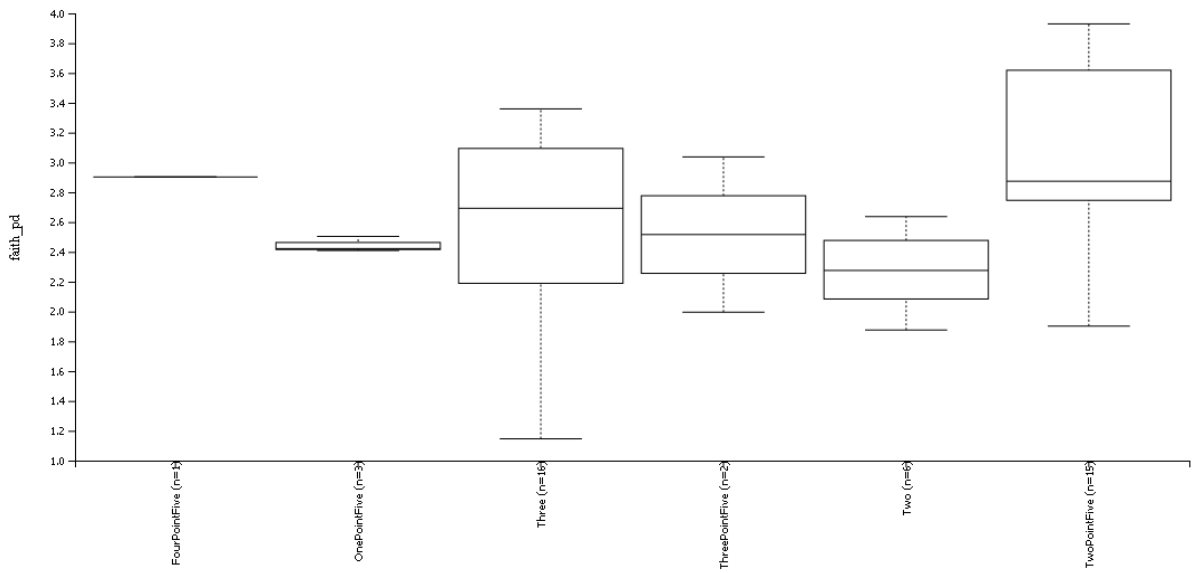

Figure 46. *Faith Phylogenetic diversity boxplots for the size category. This* graph shows the alpha diversity that represents a measure of a community richness that incorporates phylogenetic relationships between the features.

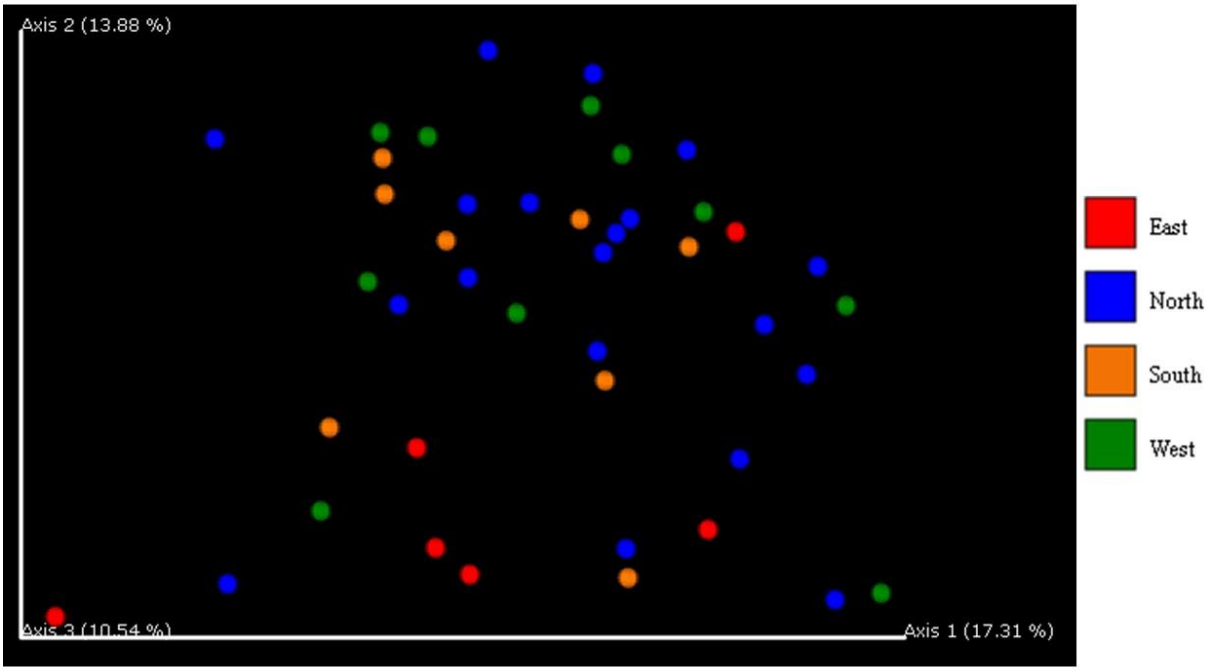

Figure 47. *Beta diversity significance boxplots unweighted UniFrac distance by cardinal location.* This graph shows a qualitative measure of community dissimilarity that incorporates phylogenetic relationships between the features in the samples and groups.

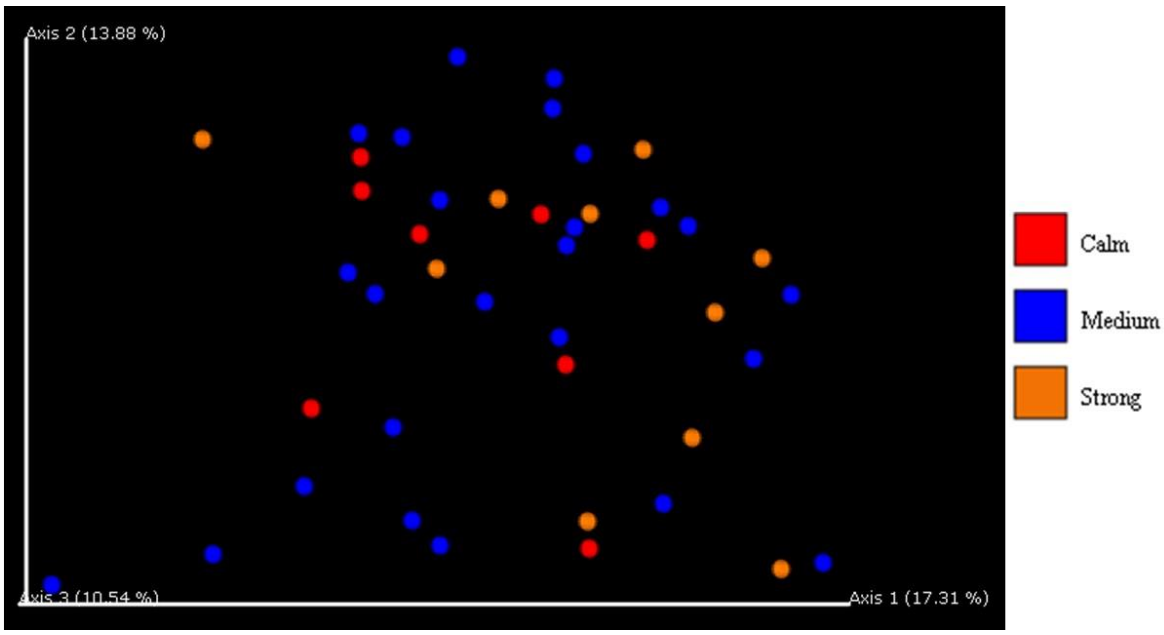

Figure 48. *Beta diversity significance unweighted UniFrac distance by current strength.* This graph shows a qualitative measure of community dissimilarity that incorporates phylogenetic relationships between the features in the samples and groups.

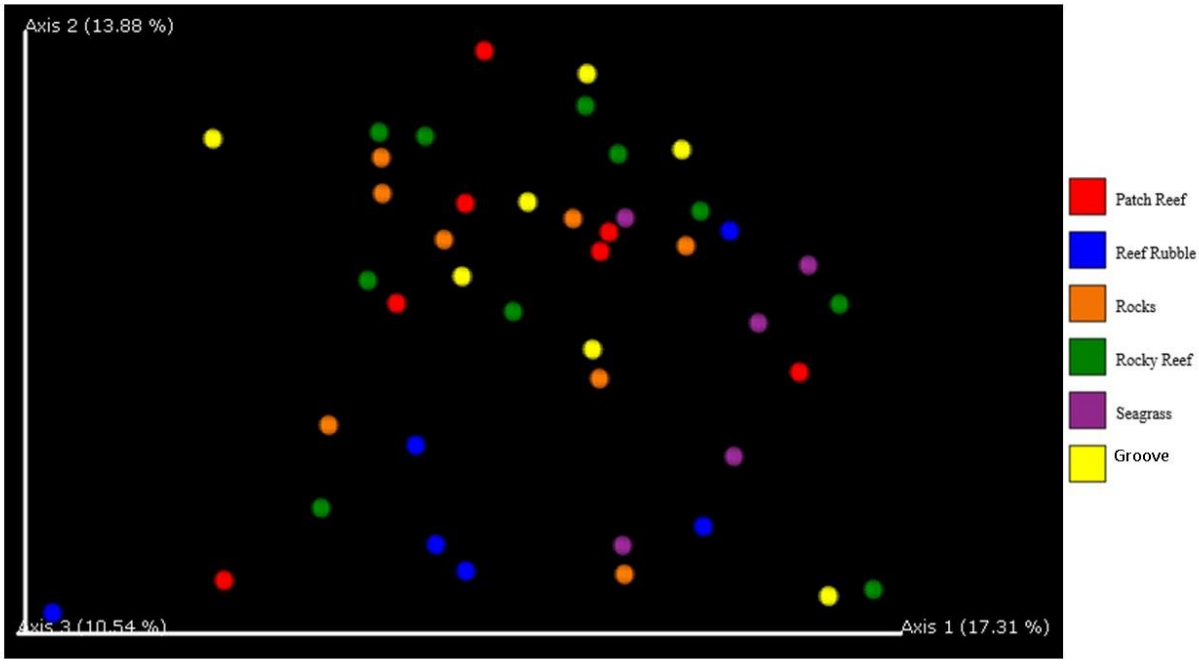

Figure 49. *Beta diversity significance unweighted UniFrac distance by habitat.* This graph shows a qualitative measure of community dissimilarity that incorporates phylogenetic relationships between the features in the samples and groups.

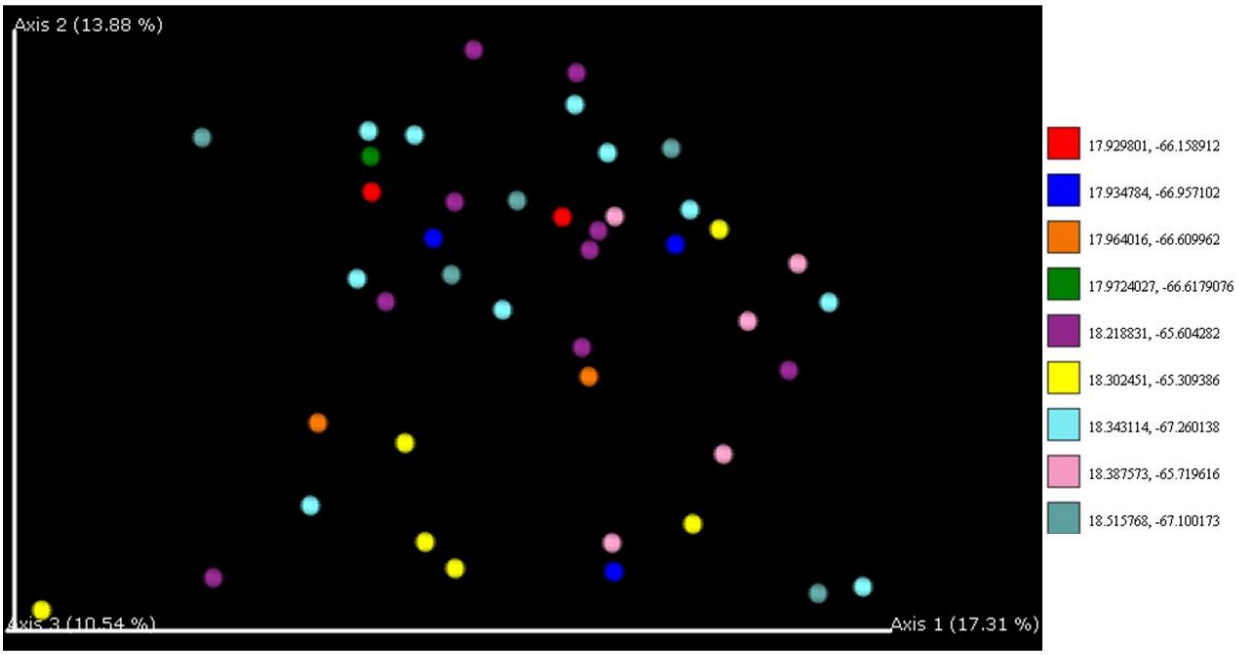

Figure 50. *Beta diversity significance unweighted UniFrac distance by latitude longitude*. This graph shows a qualitative measure of community dissimilarity that incorporates phylogenetic relationships between the features in the samples and groups.

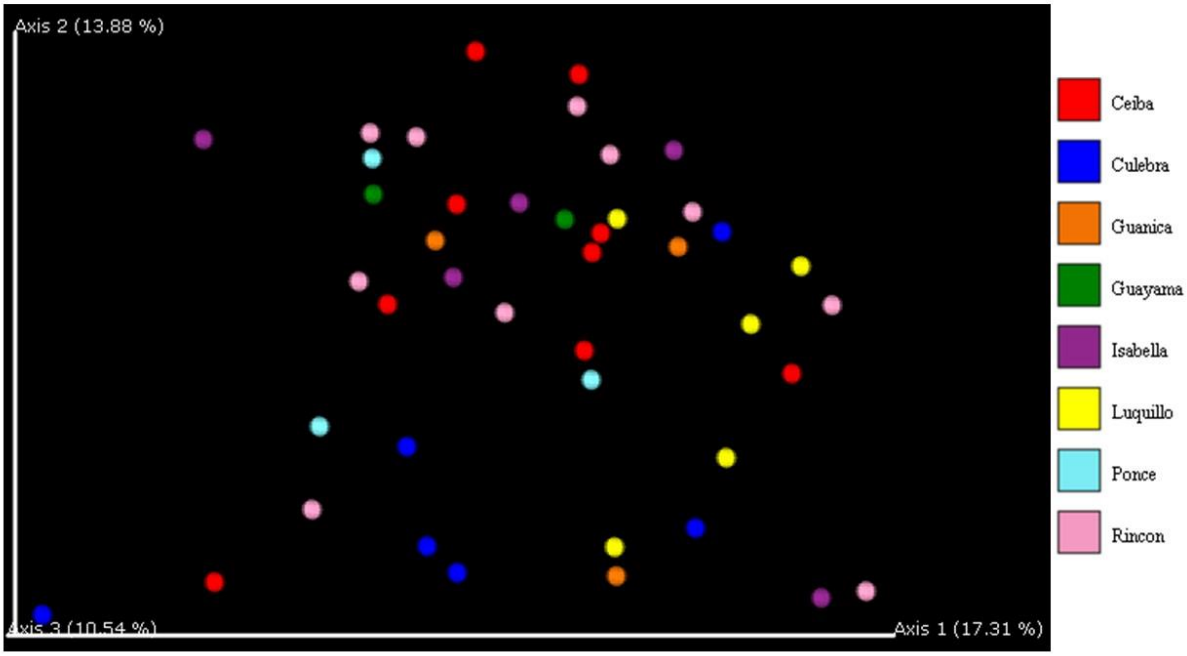

Figure 51. *Beta diversity significance unweighted UniFrac distance by location.* This graph shows a qualitative measure of community dissimilarity that incorporates phylogenetic relationships between the features in the samples and groups.

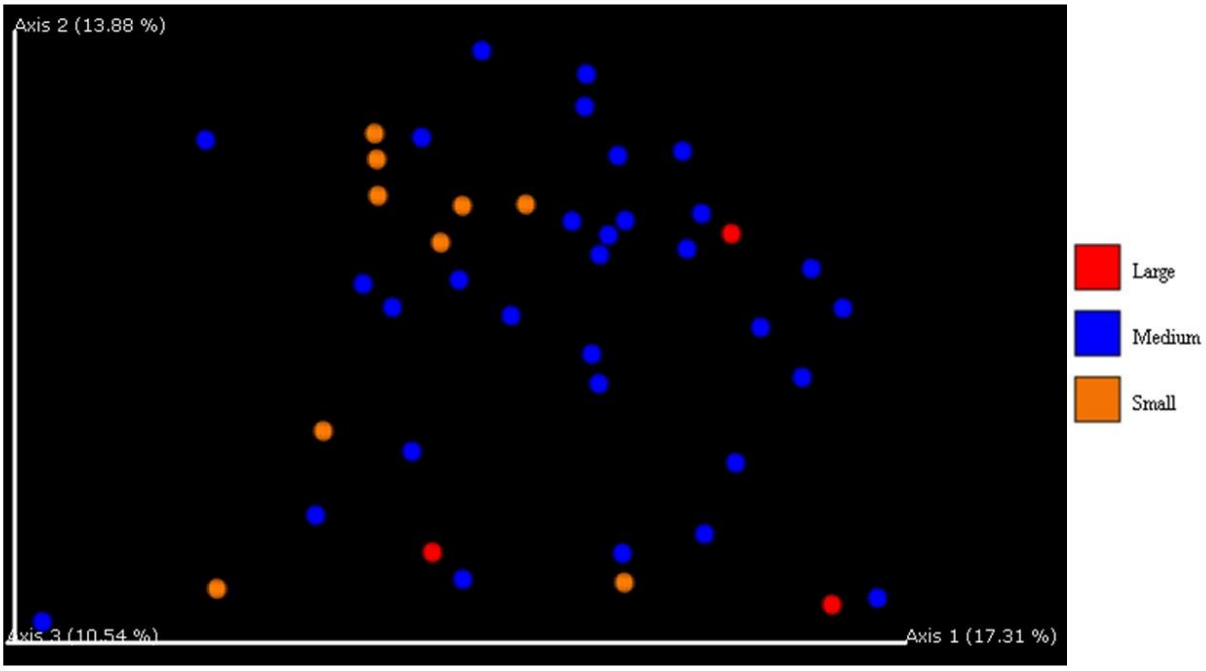

Figure 52. *Beta diversity significance unweighted UniFrac distance by proportion.* This graph shows a qualitative measure of community dissimilarity that incorporates phylogenetic relationships between the features in the samples and groups.

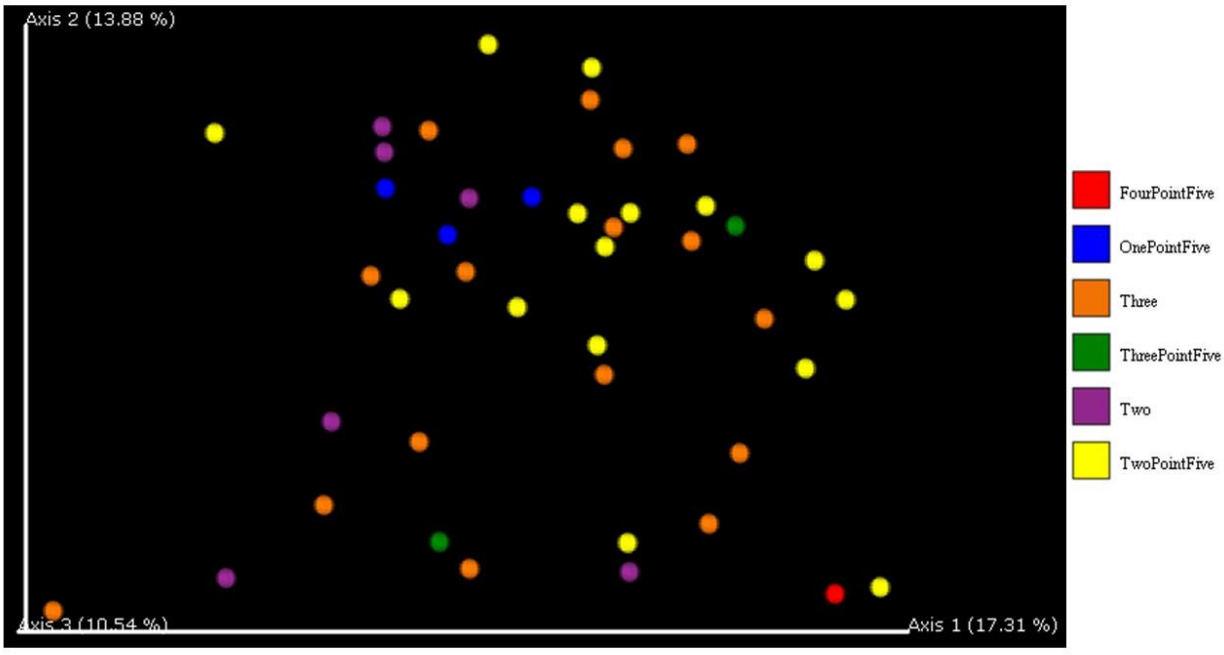

Figure 53. *Beta diversity significance unweighted UniFrac distance by size (in inches). This* graph shows a qualitative measure of community dissimilarity that incorporates phylogenetic relationships between the features in the samples and groups.

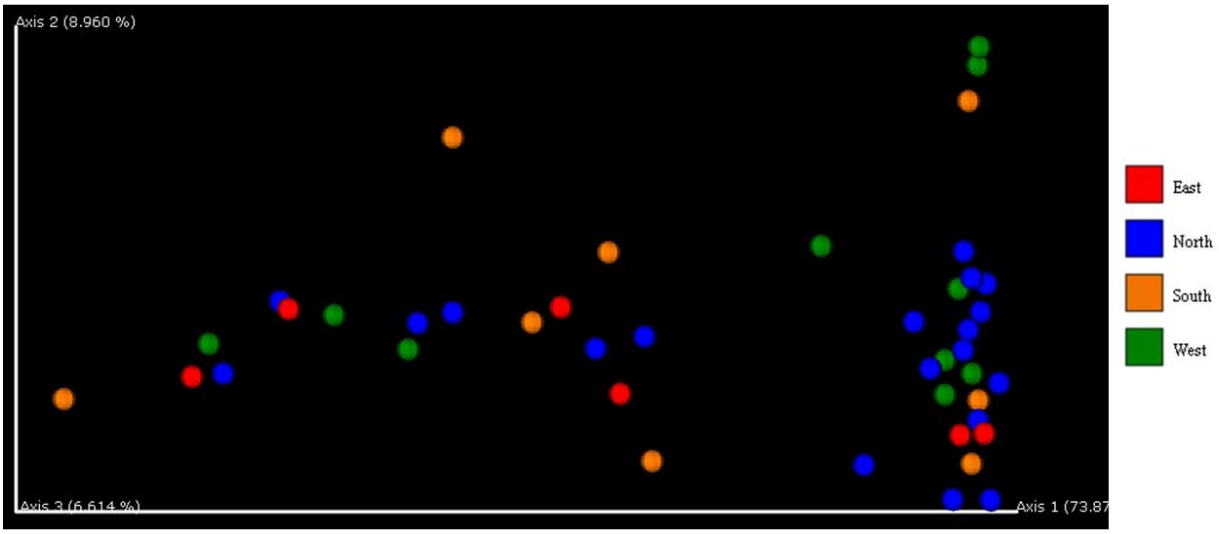

Figure 54. *Beta diversity significance weighted UniFrac distance by cardinal location.* This graph shows a quantitative measure of community dissimilarity that incorporates phylogenetic relationships between the features in the samples and groups.

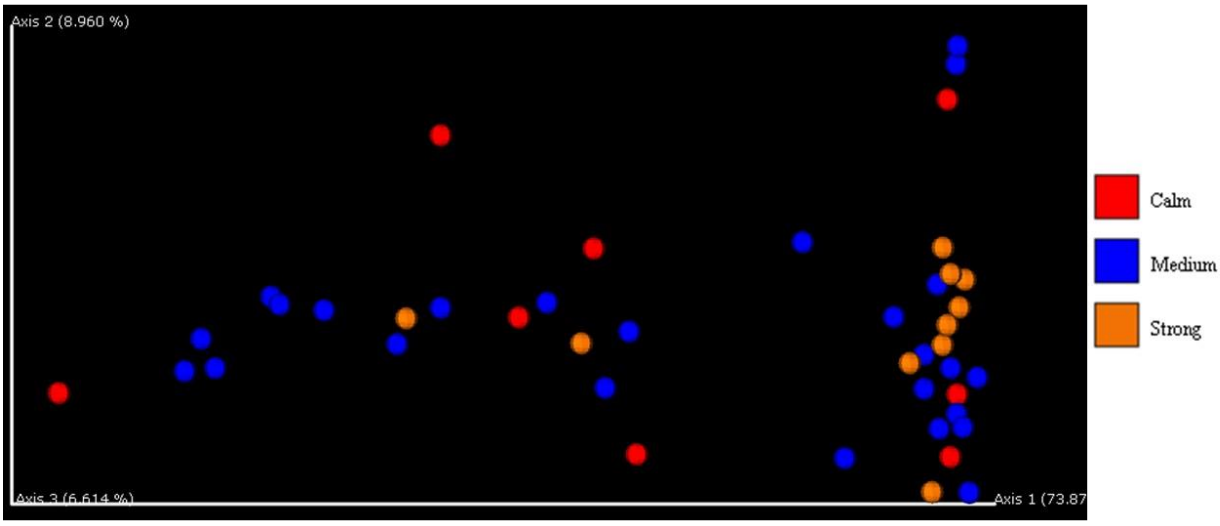

Figure 55. *Beta diversity significance weighted UniFrac distance by current strength.* This graph shows a quantitative measure of community dissimilarity that incorporates phylogenetic relationships between the features in the samples and groups.

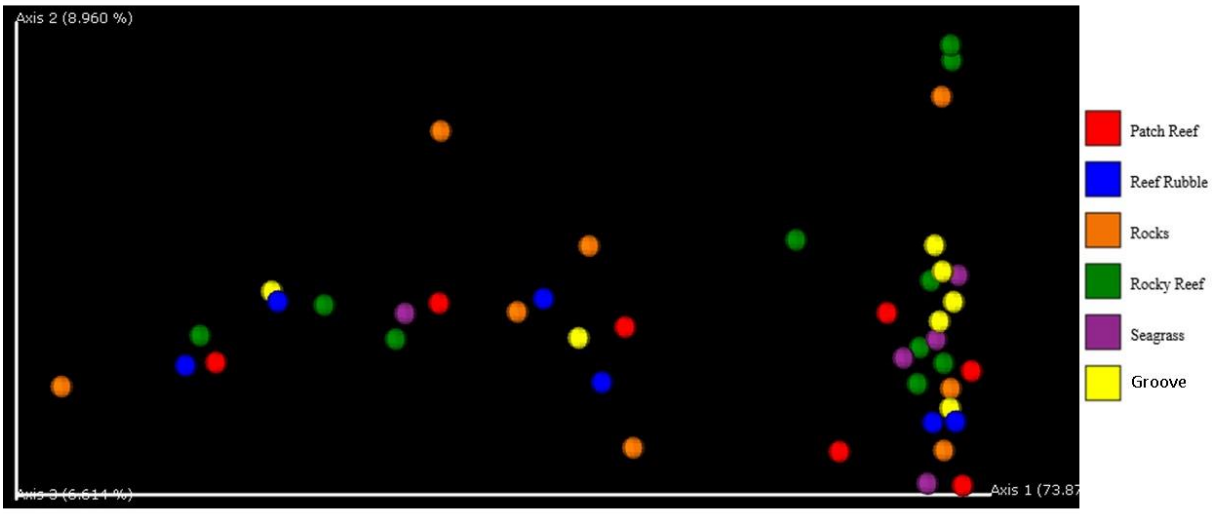

Figure 56. *Beta diversity significance weighted UniFrac distance by habitat.* This graph shows a quantitative measure of community dissimilarity that incorporates phylogenetic relationships between the features in the samples and groups.

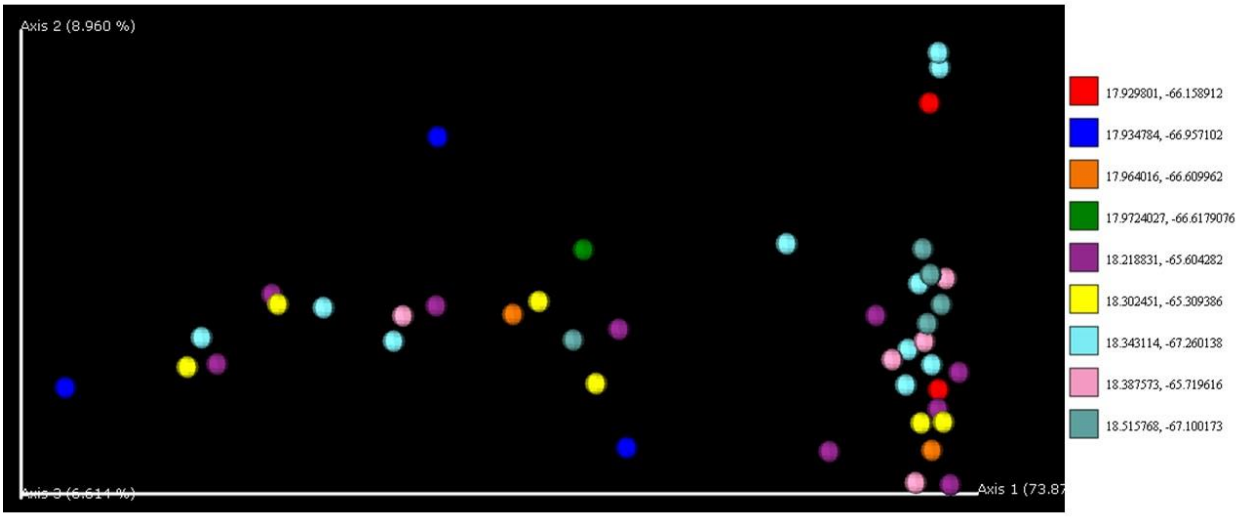

Figure 57. *Beta diversity significance weighted UniFrac distance by latitude and longitude*. This graph shows a quantitative measure of community dissimilarity that incorporates phylogenetic relationships between the features in the samples and groups.

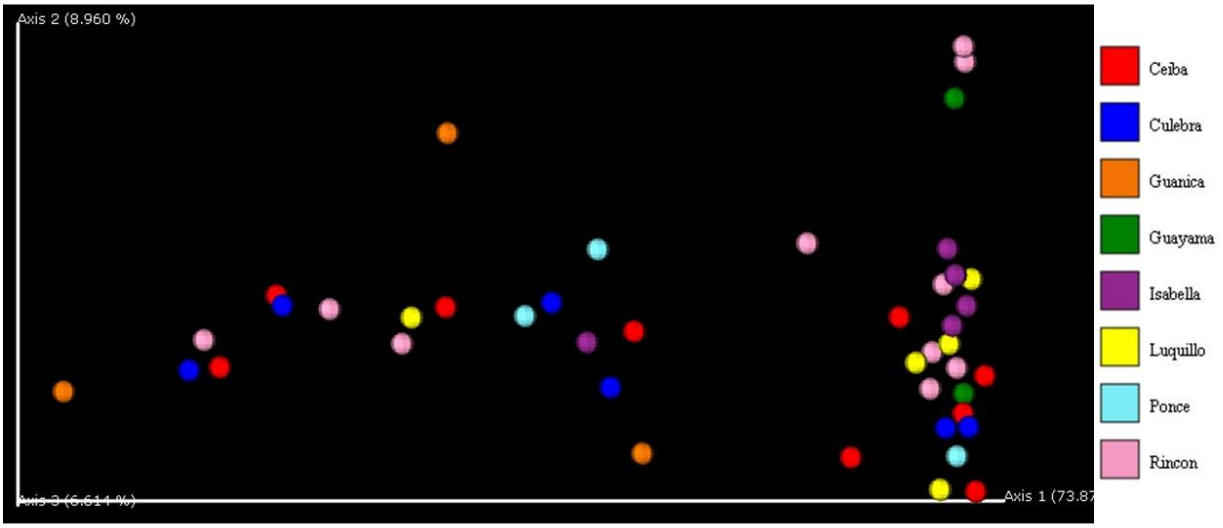

Figure 58. *Beta diversity significance weighted UniFrac distance by location.* This graph shows a quantitative measure of community dissimilarity that incorporates phylogenetic relationships between the features in the samples and groups.

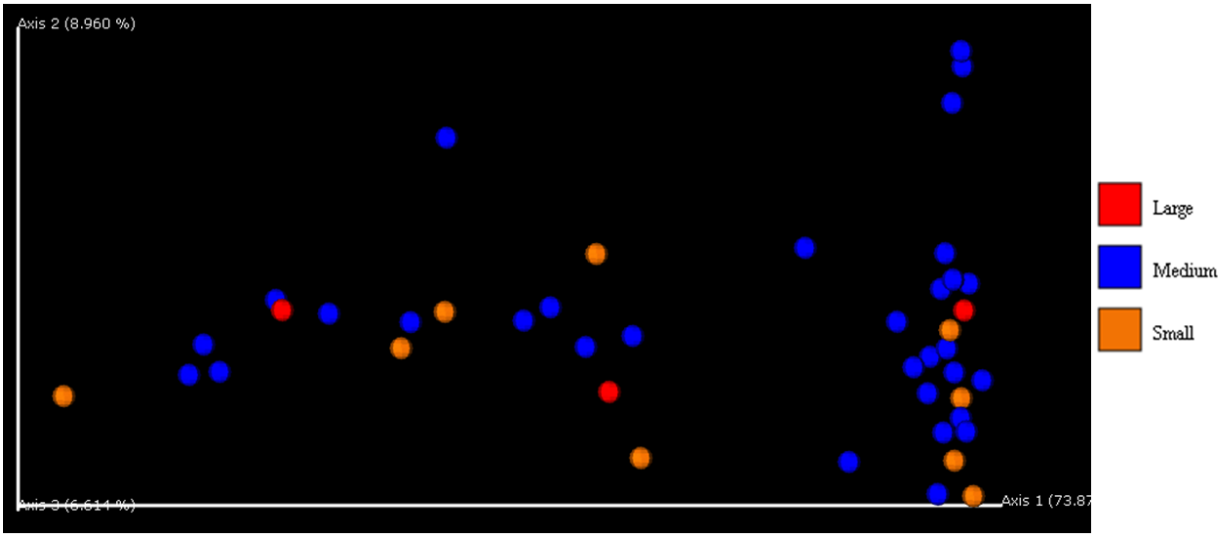

Figure 59. *Beta diversity significance weighted UniFrac distance by proportion.* This graph shows a quantitative measure of community dissimilarity that incorporates phylogenetic relationships between the features in the samples and groups.

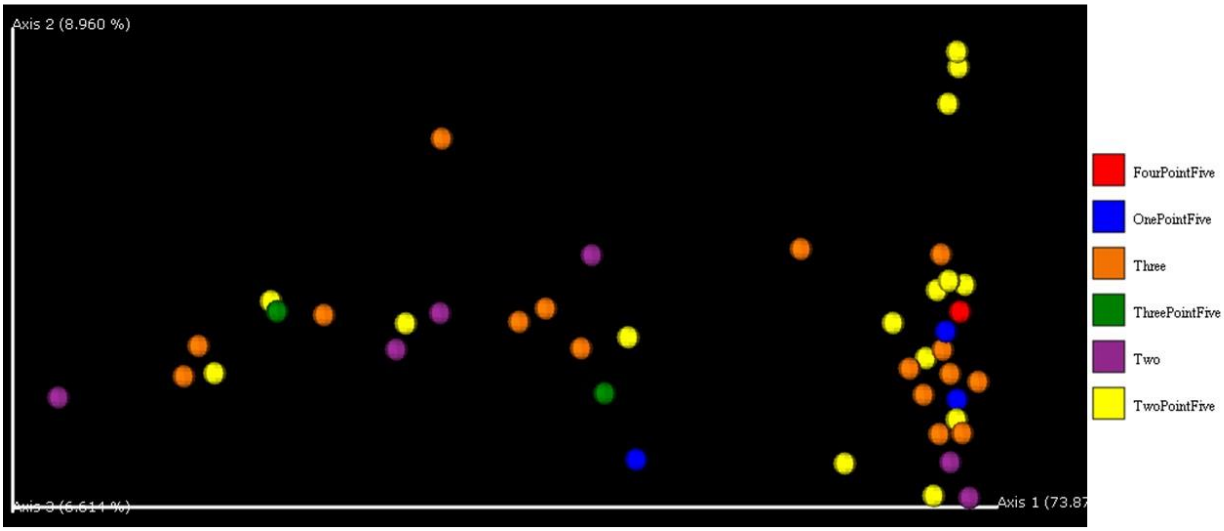

Figure 60. *Beta diversity significance weighted UniFrac distance by size.* This graph shows a quantitative measure of community dissimilarity that incorporates phylogenetic relationships between the features in the samples and groups.

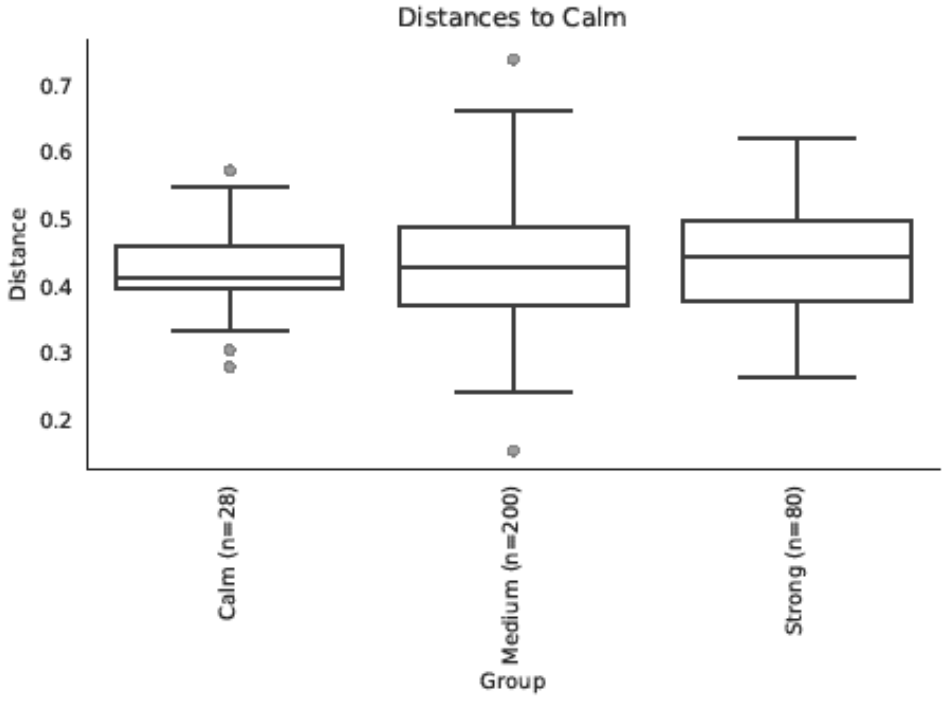

Figure 61. *Pairwise distance boxplots within the current strength category and calm.*

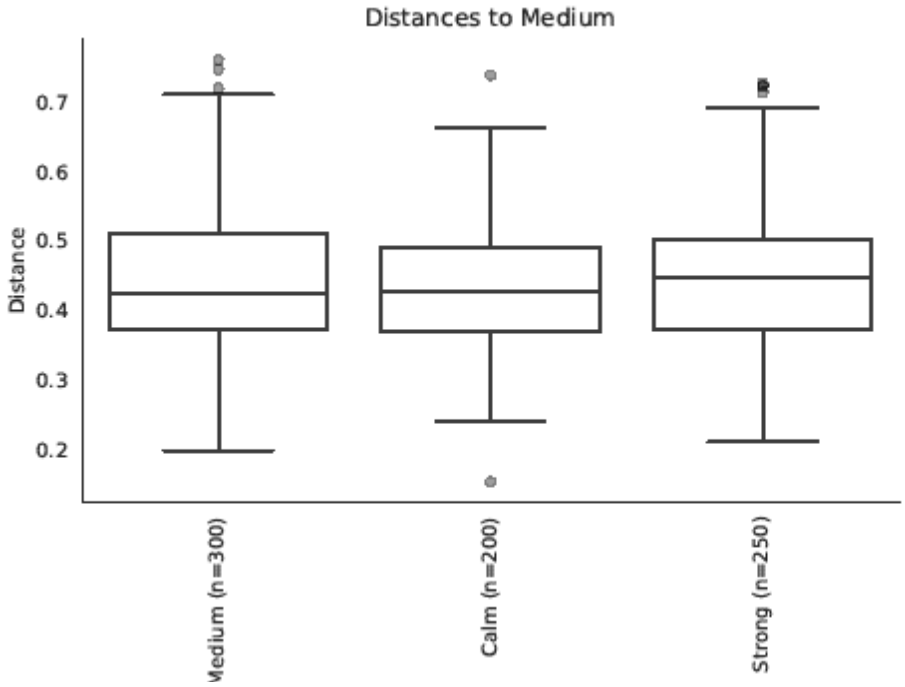

Figure 62. *Pairwise distance boxplots within the current strength category and medium.*

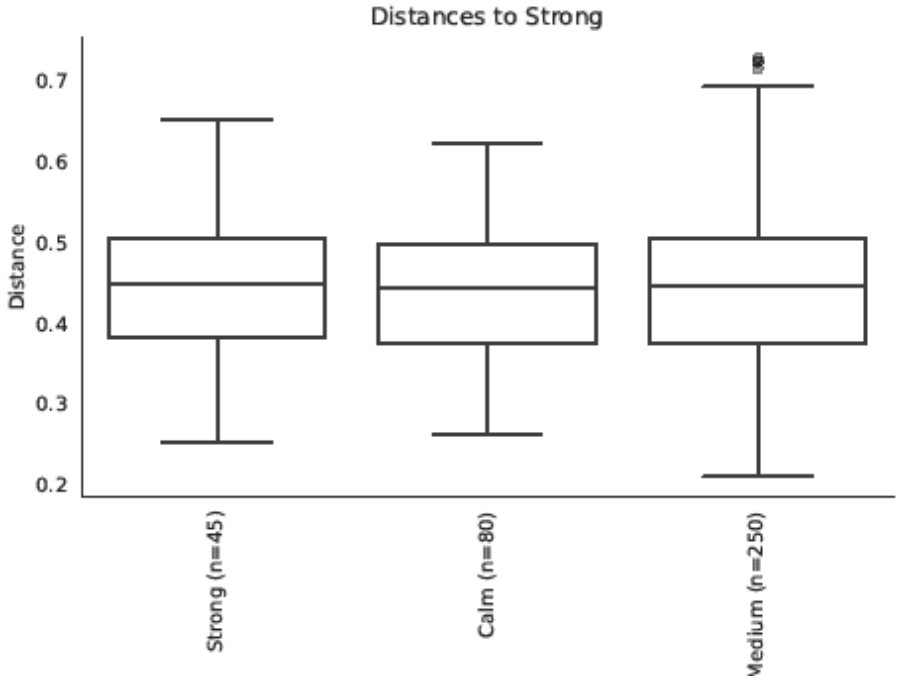

Figure 63. *Pairwise distance boxplots within the current strength category and strong.*

method name	PERMANOVA
test statistic name	pseudo-F
sample size	43
number of groups	3
test statistic	0.993805
p-value	0.471
number of permutations	999

Figure 64. *PERMANOVA by current.* This table shows the statistical analysis done with PERMANOVA and the current category.

Group 1	Group 2	Sample size	Permutations	pseudo-F	p-value	q-value
Calm	Medium	33	999	0.75871588	0.74	0.74
Calm	Strong	18	999	1.10493569	0.354	0.531
Medium	Strong	35	999	1.15745772	0.291	0.531

Figure 65. *PERMANOVA by current categories.* This table shows the statistical analysis done with PERMANOVA and the current category divided into groups.

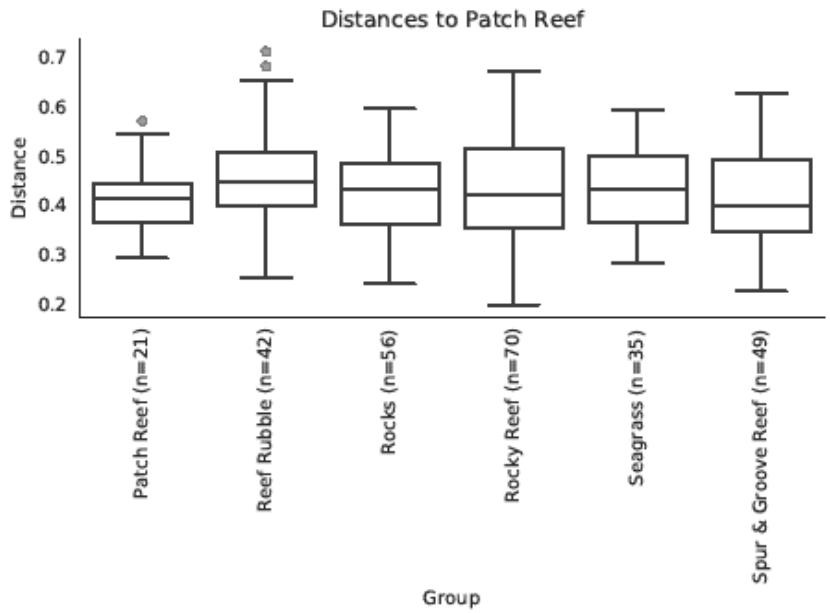

Figure 66. *Pairwise distance boxplots within the habitat category and patch reef.*

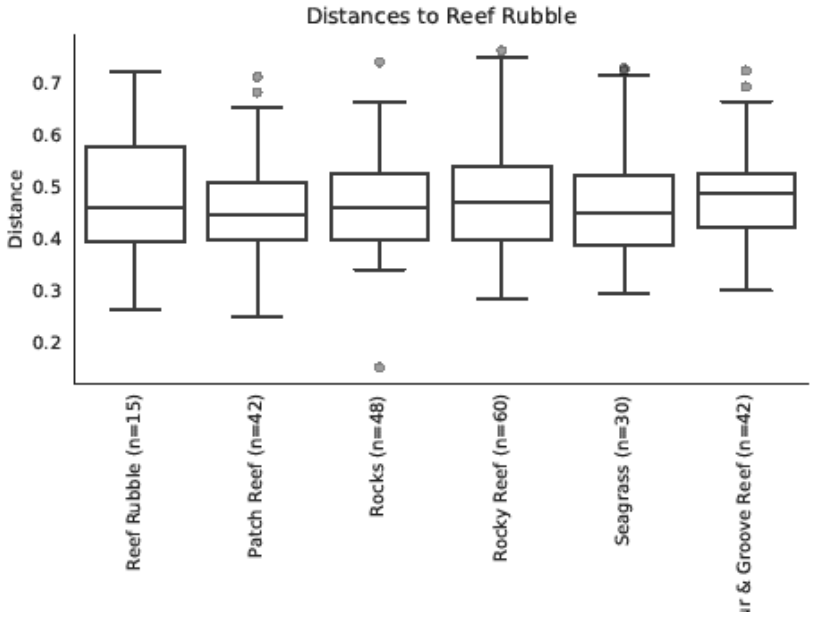

Figure 67. *Pairwise distance boxplots within the habitat category and reef rubble.*

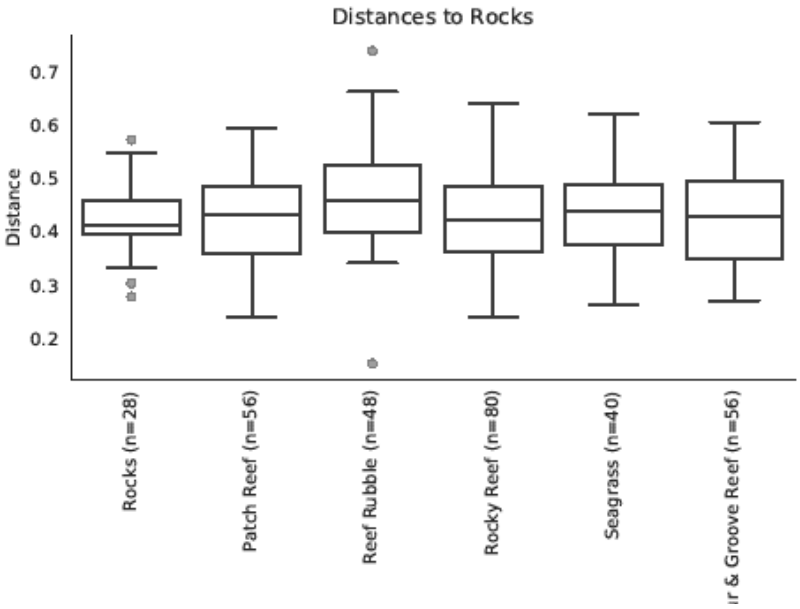

Figure 68. *Pairwise distance boxplots within the habitat category and rocks.*

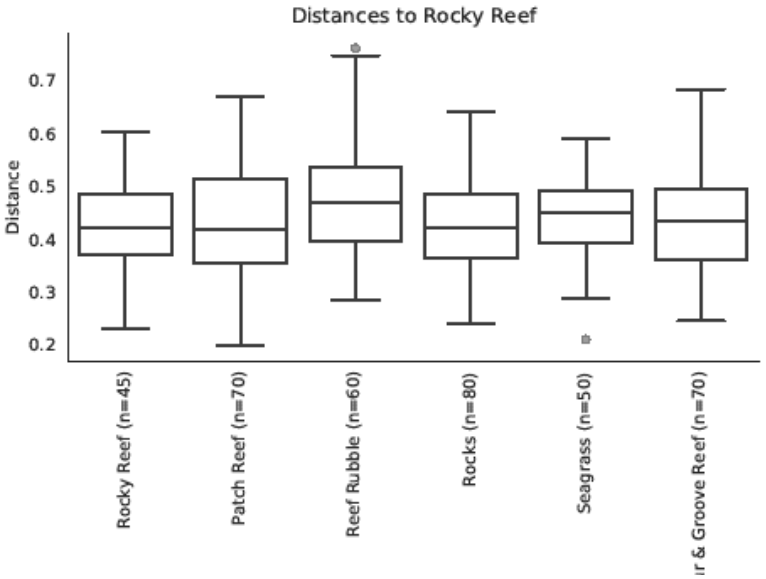

Figure 69. *Pairwise distance boxplots within the habitat category and rocky reef.*

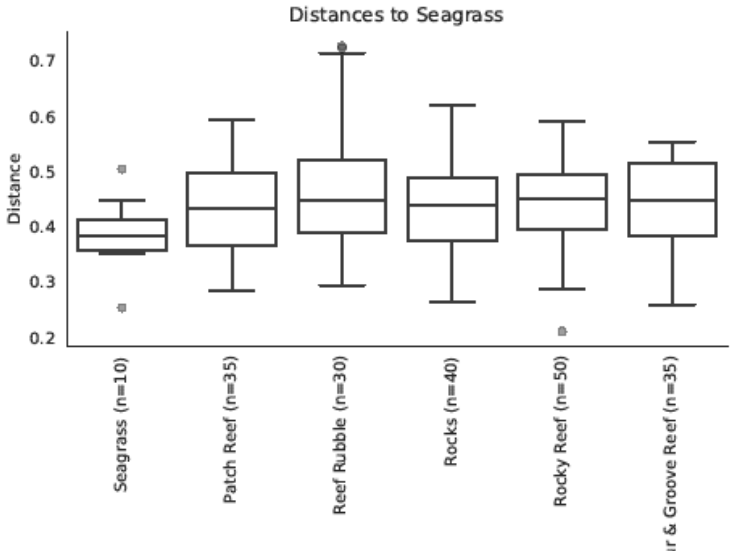

Figure 70. *Pairwise distance boxplots within the habitat category and seagrass.*

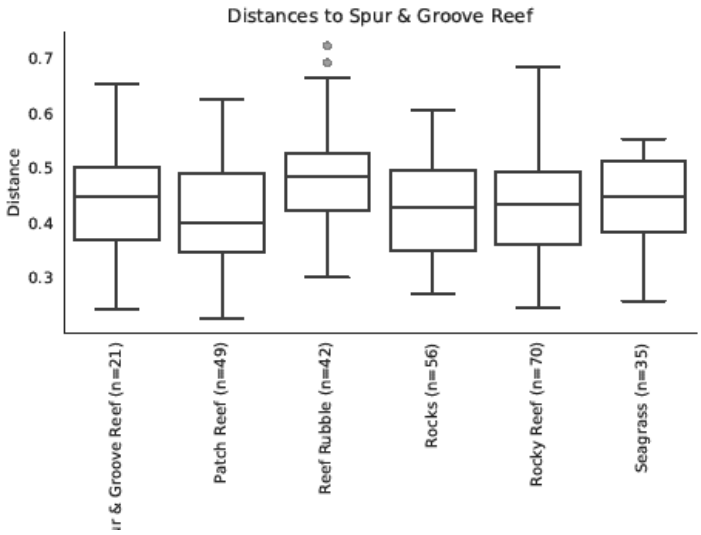

Figure 71. *Pairwise distance boxplots within the habitat category and spur and groove reef.*

method name	PERMANOVA
test statistic name	pseudo-F
sample size	43
number of groups	6
test statistic	1.33551
p-value	0.045
number of permutations	999

Figure 72. *PERMANOVA by habitat.* This table shows the statistical analysis done with PERMANOVA and the habitat category.

Group 1	Group 2	Sample size	Permutations	pseudo-F	p-value	q-value
Patch Reef	Reef Rubble	13	999	1.438563	0.172	0.286667
	Rocks	15	999	1.056581	0.401	0.546818
	Rocky Reef	17	999	1.173627	0.302	0.453
	Seagrass	12	999	1.888892	0.024	0.13
	Spur & Groove Reef	14	999	0.658183	0.839	0.839
Reef Rubble	Rocks	14	999	1.489868	0.115	0.215625
	Rocky Reef	16	999	1.781223	0.05	0.13
	Seagrass	11	999	1.873051	0.045	0.13
	Spur & Groove Reef	13	999	1.56524	0.111	0.215625
Rocks	Rocky Reef	18	999	0.690031	0.811	0.839
	Seagrass	13	999	1.770784	0.031	0.13
	Spur & Groove Reef	15	999	0.833184	0.668	0.770769
Rocky Reef	Seagrass	15	999	1.779518	0.052	0.13
	Spur & Groove Reef	17	999	0.888286	0.537	0.67125
Seagrass	Spur & Groove Reef	12	999	1.706816	0.029	0.13

Figure 73. *PERMANOVA by habitat categories.* This table shows the statistical analysis done with pairwise PERMANOVA and the habitat category and its groupings.

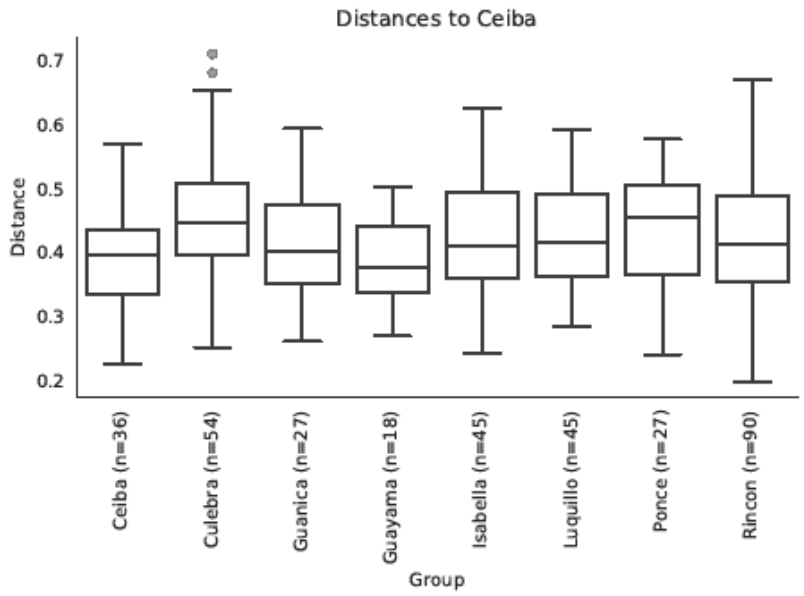

Figure 74. *Pairwise distance boxplots within the location category and Ceiba.*

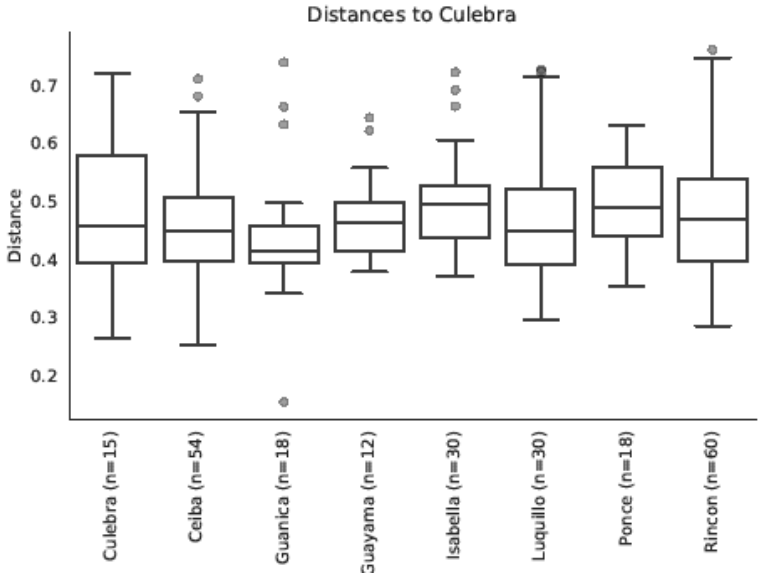

Figure 75. *Pairwise distance boxplots within the location category and Culebra*.

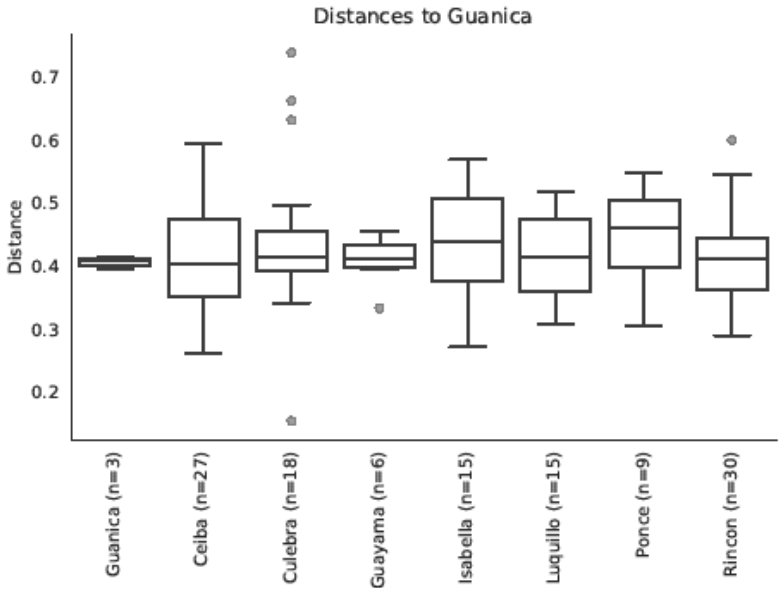

Figure 76. *Pairwise distance boxplots within the location category and Guánica.*

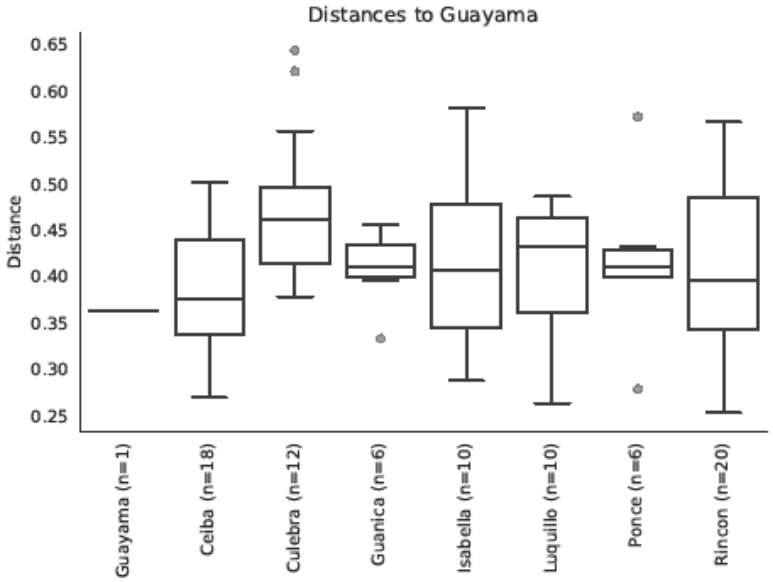

Figure 77. *Pairwise distance boxplots within the location category and Guayama.*

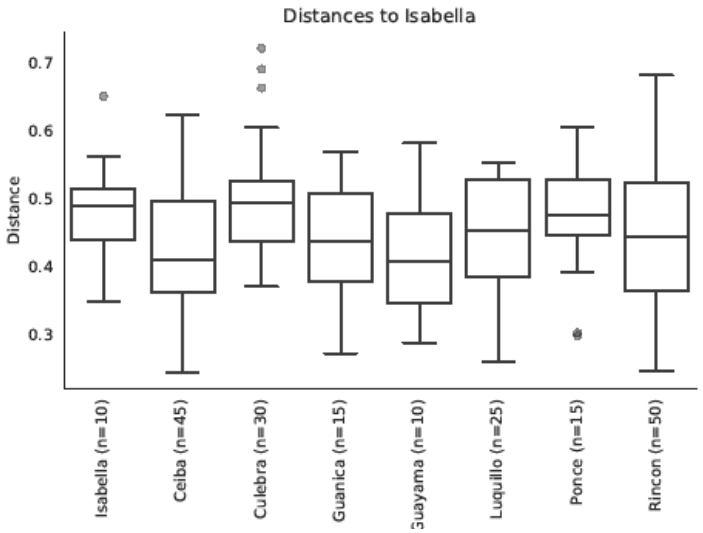

Figure 78. *Pairwise distance boxplots within the location category and Isabela.*

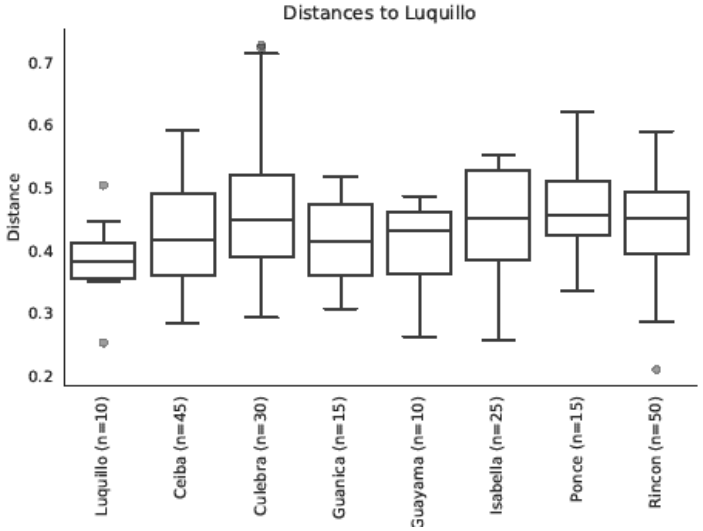

Figure 79. *Pairwise distance boxplots within the location category and Luquillo.*

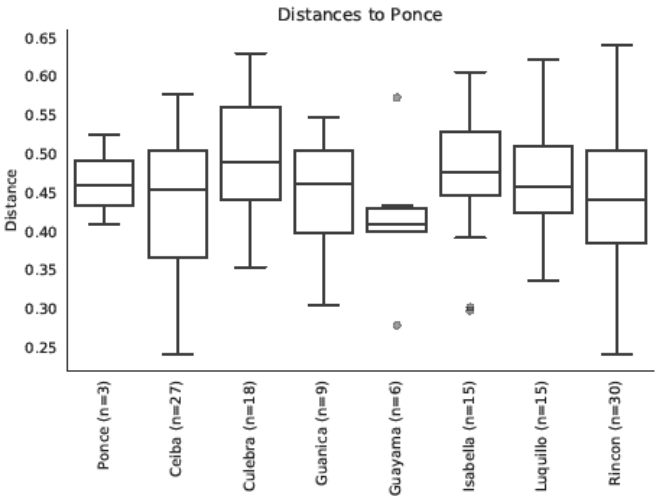

Figure 80. *Pairwise distance boxplots within the location category and Ponce.*

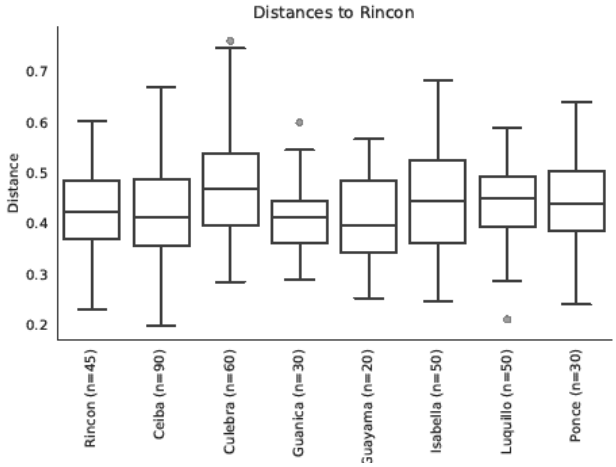

Figure 81. *Pairwise distance boxplots within the location category and Rincón.*

method name	PERMANOVA
test statistic name	pseudo-F
sample size	43
number of groups	8
test statistic	1.26628
p-value	0.064
number of permutations	999

Figure 82. *PERMANOVA by location.* This table shows the statistical analysis done with PERMANOVA and the location category.

Group 1	Group 2	Sample size	Permutations	pseudo-F	p-value	q-value
Ceiba	Culebra	15	999	1.795809	0.055	0.284667
	Guánica	12	999	1.211706	0.241	0.449867
	Guayama	11	999	0.979635	0.352	0.556889
	Isabela	14	999	0.668397	0.816	0.816
	Luquillo	14	999	2.18838	0.004	0.112
	Ponce	12	999	1.423844	0.151	0.422
	Rincón	19	999	1.298919	0.188	0.422
Culebra	Guánica	9	999	0.930467	0.544	0.662261
	Guayama	8	999	1.256066	0.358	0.556889
	Isabela	11	999	1.181207	0.283	0.49525
	Luquillo	11	999	1.873051	0.034	0.259
	Ponce	9	999	1.27413	0.207	0.422
	Rincón	16	999	1.781223	0.037	0.259
Guánica	Guayama	5	999	1.246876	0.196	0.422
	Isabela	8	999	0.752686	0.715	0.772593
	Luquillo	8	999	1.375532	0.188	0.422
	Ponce	6	999	1.293054	0.188	0.422
	Rincón	13	999	0.75842	0.696	0.772593
Guayama	Isabela	7	999	0.668536	0.745	0.772593
	Luquillo	7	999	1.480112	0.211	0.422
	Ponce	5	999	0.962173	0.497	0.652909
	Rincón	12	999	0.937973	0.47	0.652909
Isabela	Luquillo	10	999	1.341236	0.172	0.422
	Ponce	8	999	0.948109	0.513	0.652909
	Rincón	15	999	0.736638	0.736	0.772593
Luquillo	Ponce	8	999	2.05015	0.012	0.168

	Rincón	15	999	1.779518	0.061	0.284667
Ponce	Rincón	13	999	0.975751	0.503	0.652909

Figure 83. *PERMANOVA by location categories.* This table shows the statistical analysis done with PERMANOVA and the location category by individual groupings.

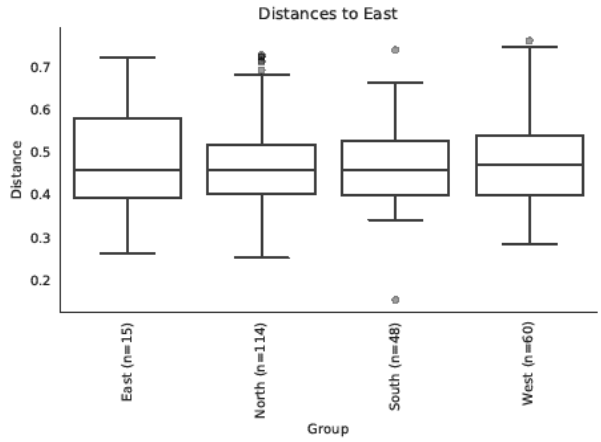

Figure 84. *Pairwise distance boxplots within the location category and East.*

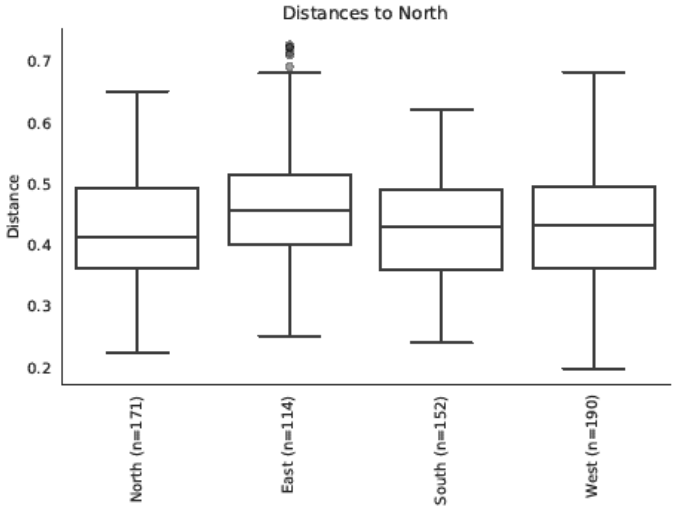

Figure 85. *Pairwise distance boxplots within the location category and North.*

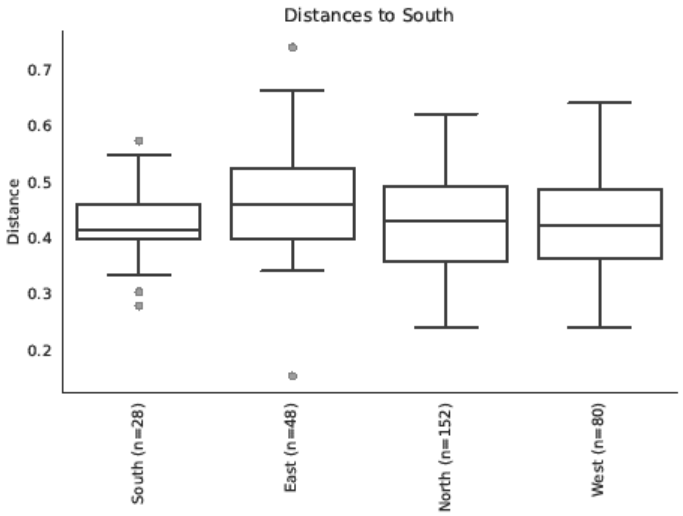

Figure 86. *Pairwise distance boxplots within the location category and South.*

Figure 87. *Pairwise distance boxplots within the location category and west.*

method name	PERMANOVA
test statistic name	pseudo-F
sample size	43
number of groups	4
test statistic	1.3735
p-value	0.068
number of permutations	999

Figure 88. *PERMANOVA by cardinal location.* This table shows the permanova statistical analysis done with the cardinal location category.

Group 1	Group 2	Sample size	Permutations	pseudo-F	p-value	q-value
East	North	25	999	1.950922	0.029	0.093
	South	14	999	1.489868	0.1	0.2
	West	16	999	1.781223	0.031	0.093
North	South	27	999	1.073693	0.365	0.438
	West	29	999	1.22679	0.24	0.36
South	West	18	999	0.690031	0.8	0.8

Figure 89. *PERMANOVA by cardinal location categories.* This table shows the pairwise permanova statistical analysis done with the cardinal location category and the different groups.

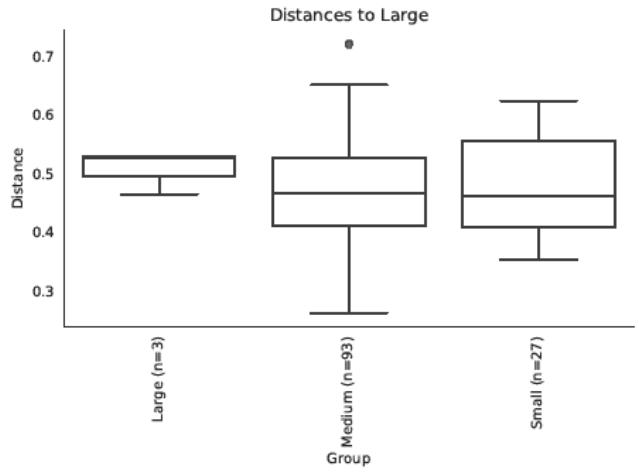

Figure 90. *Pairwise distance within the proportion size category and large*.

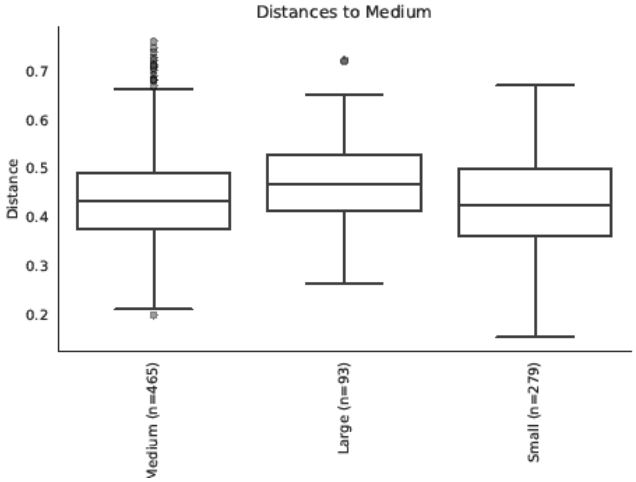

Figure 91. *Pairwise distance within the proportion size category and medium.*

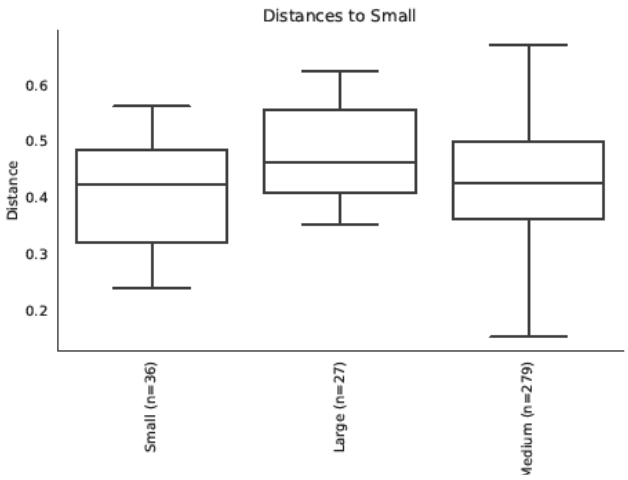

Figure 92. *Pairwise distance within the proportion size category and small.*

method name	PERMANOVA
test statistic name	pseudo-F
sample size	43
number of groups	3
test statistic	1.34816
p-value	0.132
number of permutations	999

Figure 93. *PERMANOVA by size proportion.* This table shows the permanova statistical analysis done with the size proportion category.

Group 1	Group 2	Sample size	Permutations	pseudo-F	p-value	q-value
Large	Medium	34	999	1.176873	0.275	0.275
	Small	12	999	1.732696	0.064	0.192
Medium	Small	40	999	1.390986	0.138	0.207

Figure 94. *PERMANOVA by size proportion category.* This table shows the pairwise permanova statistical analysis done with the size proportion category and its groupings.

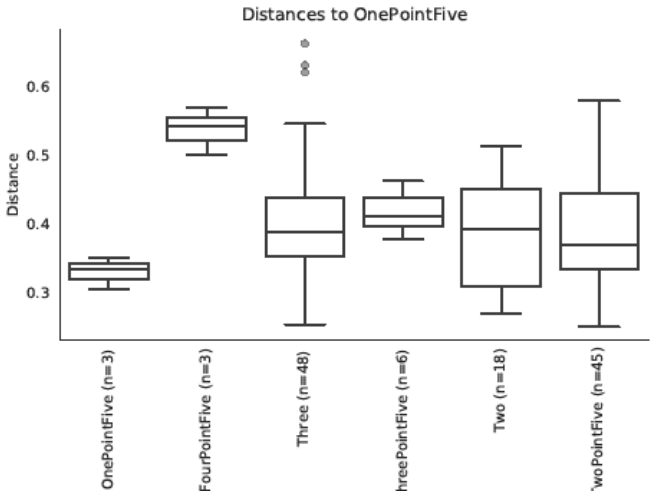

Figure 95. *Pairwise distance within the size category and one point five*.

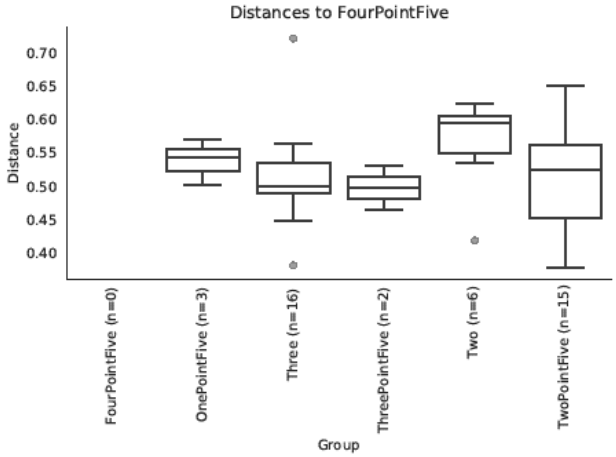

Figure 96. *Pairwise distance within the size category and four point five.*

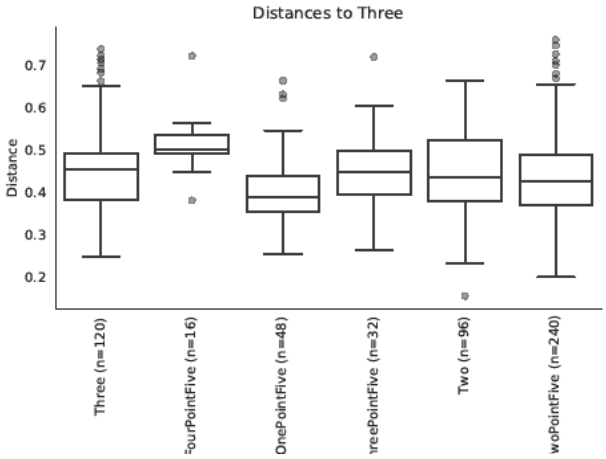

Figure 97. *Pairwise distance within the size category and three.*

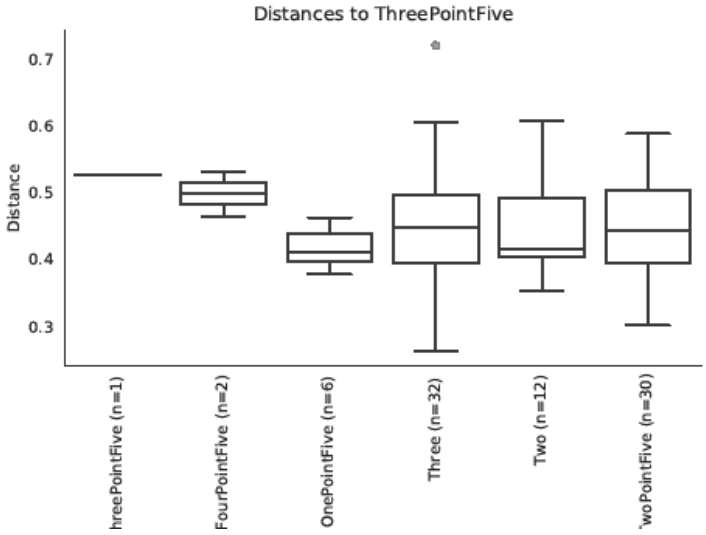

Figure 98. *Pairwise distance within the size category and three point five.*

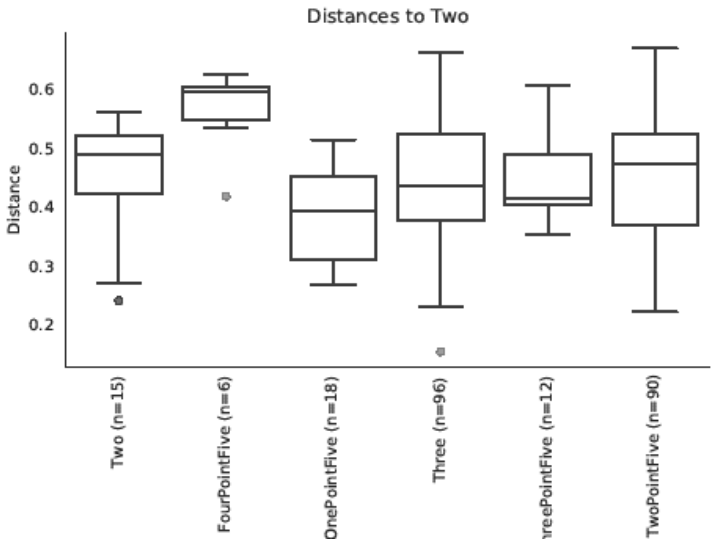

Figure 99. *Pairwise distance within the size category and two.*

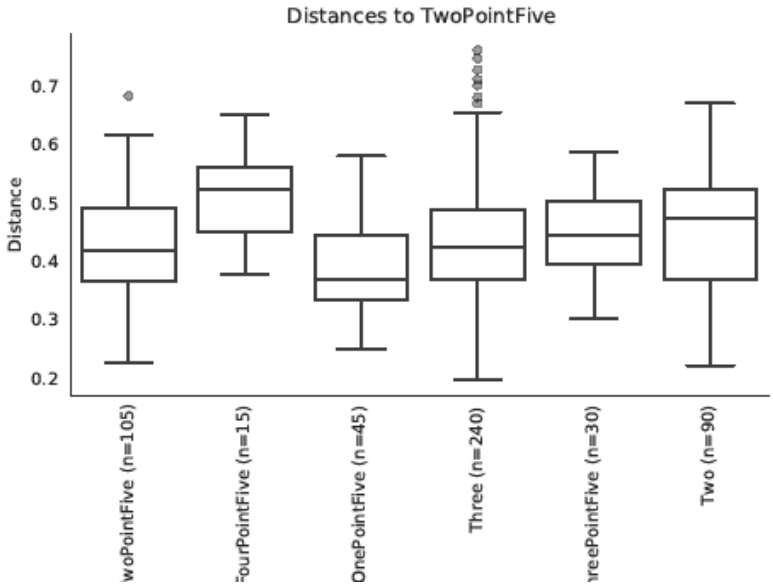

Figure 100. *Pairwise distance within the size category and two point five.*

method name	PERMANOVA
test statistic name	pseudo-F
sample size	43
number of groups	6
test statistic	1.04421
p-value	0.36
number of permutations	999

Figure 101. *PERMANOVA by size.* This table shows the permanova statistical analysis done with the size category.

Group 1	Group 2	Sample size	Permutations	pseudo-F	p-value	q-value
FourPointFive	OnePointFive	4	999	3.497431	0.269	0.807
	Three	17	999	1.449353	0.126	0.7
	ThreePointFive	3	999	0.86364	0.681	0.908571
	Two	7	999	1.886876	0.14	0.7
	TwoPointFive	16	999	1.755409	0.196	0.735
OnePointFive	Three	19	999	0.818118	0.662	0.908571
	ThreePointFive	5	999	1.005198	0.503	0.908571
	Two	9	999	0.633363	0.922	0.922
	TwoPointFive	18	999	1.019989	0.432	0.908571
Three	ThreePointFive	18	999	0.63314	0.823	0.908571
	Two	22	999	0.607589	0.848	0.908571
	TwoPointFive	31	999	0.792434	0.677	0.908571
ThreePointFive	Two	8	999	0.73987	0.785	0.908571
	TwoPointFive	17	999	0.876615	0.581	0.908571
Two	TwoPointFive	21	999	1.603256	0.073	0.7

Figure 102. *PERMANOVA by size categories.* This table shows the pairwise permanova statistical analysis done with the size proportion category and its groupings.

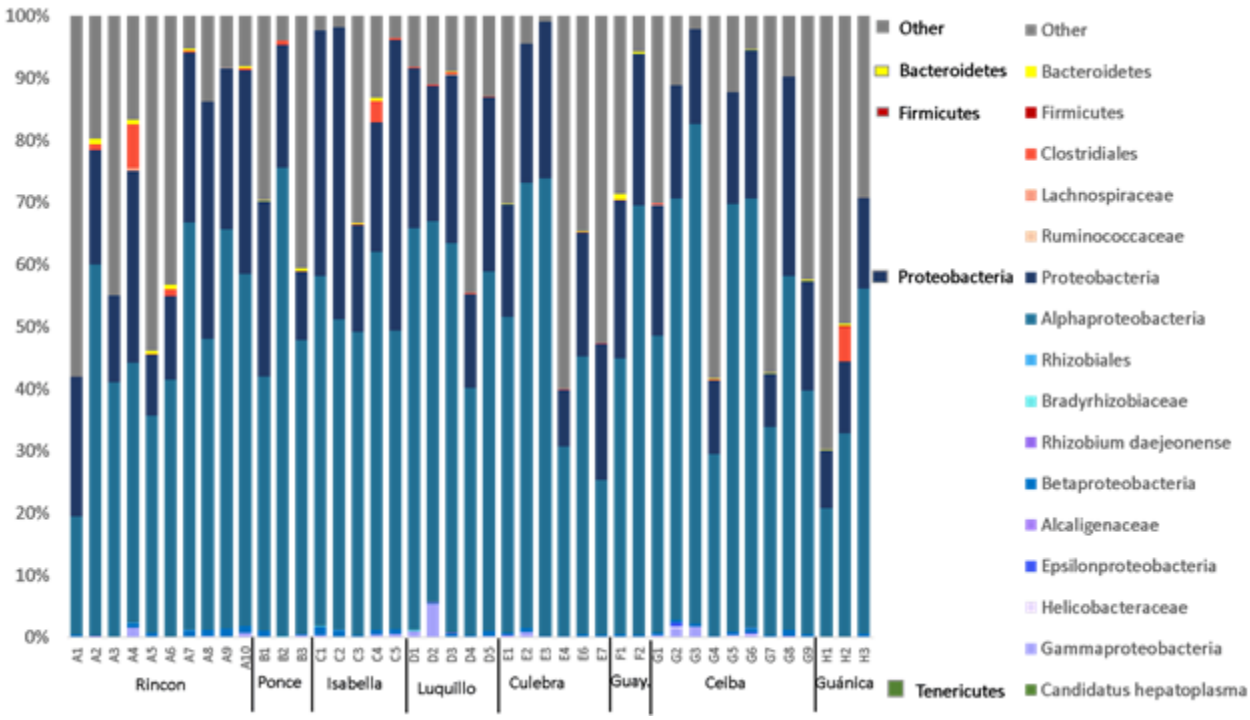

Figure 103. *Taxonomic classification of urchin intestine*. Intestinal microbiome of *D. antillarum* (n=44) collected in the coastal waters of eight different municipalities across Puerto Rico. Microbiome data was generated using 16S metagenomic sequencing. Bars indicate the percentage of microbiota present in each animal sample, which was generated using QIIME2. Chi-squared analysis was used to test differences between taxonomic grouping percentages and municipalities.

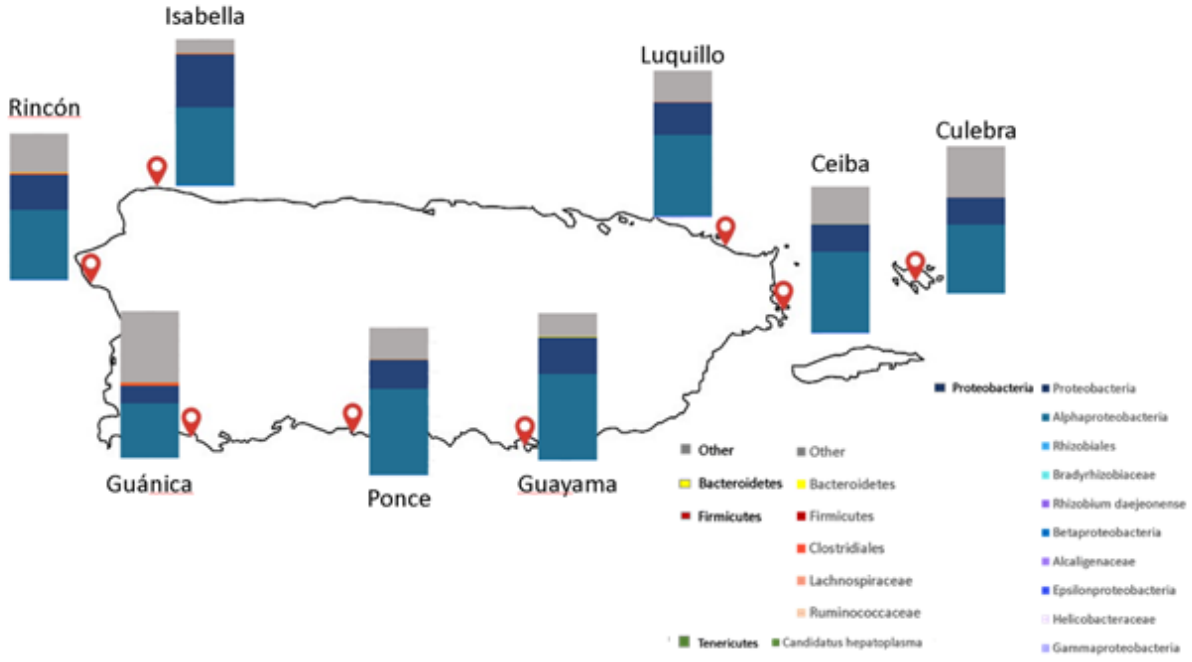

Figure 104. *Intestinal microbiomes of D. antillarum by sampling location correlate with surface water currents in Puerto Rico.* Bars indicate the average percentage of microbiota in each sample set collected at each marked location (red pin). A total of 44 samples were collected from Rincón (n=10), Guánica (n=3), Ponce(n=3), Isabela (n=5), Luquillo (n=5), Culebra (n=7), Ceiba (n=9), Guayama (n=2). Here is shown non-log-transformed data.

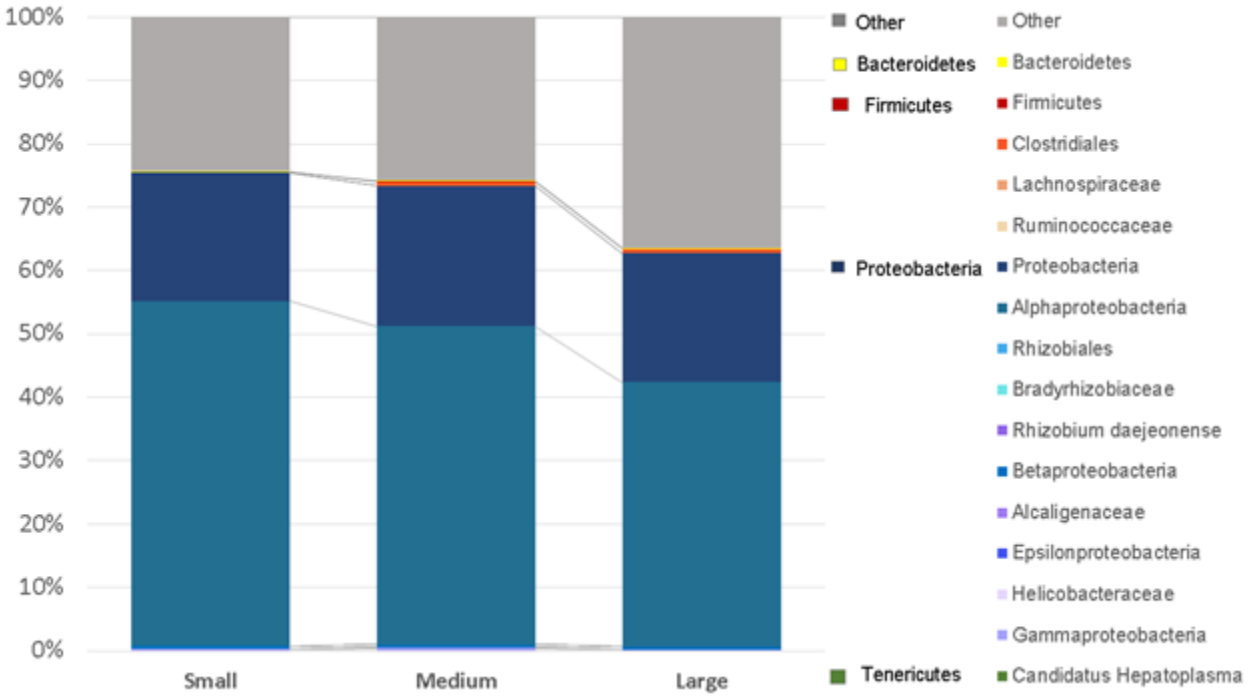

Figure 105. *Intestinal microbiome correlates with animal size.* Animal body diameter size is categorized by small (1.5 - 2 in), medium (2.5 - 3 in) and large (3.5 - 4.5 in). Bars indicate the percentage of microbiota present in each sample set by taxonomic grouping, which was generated using QIIME2. Animal sample numbers for each category include small (n=8), medium (n=31) and large (n=4). Here is shown non-log-transformed data.

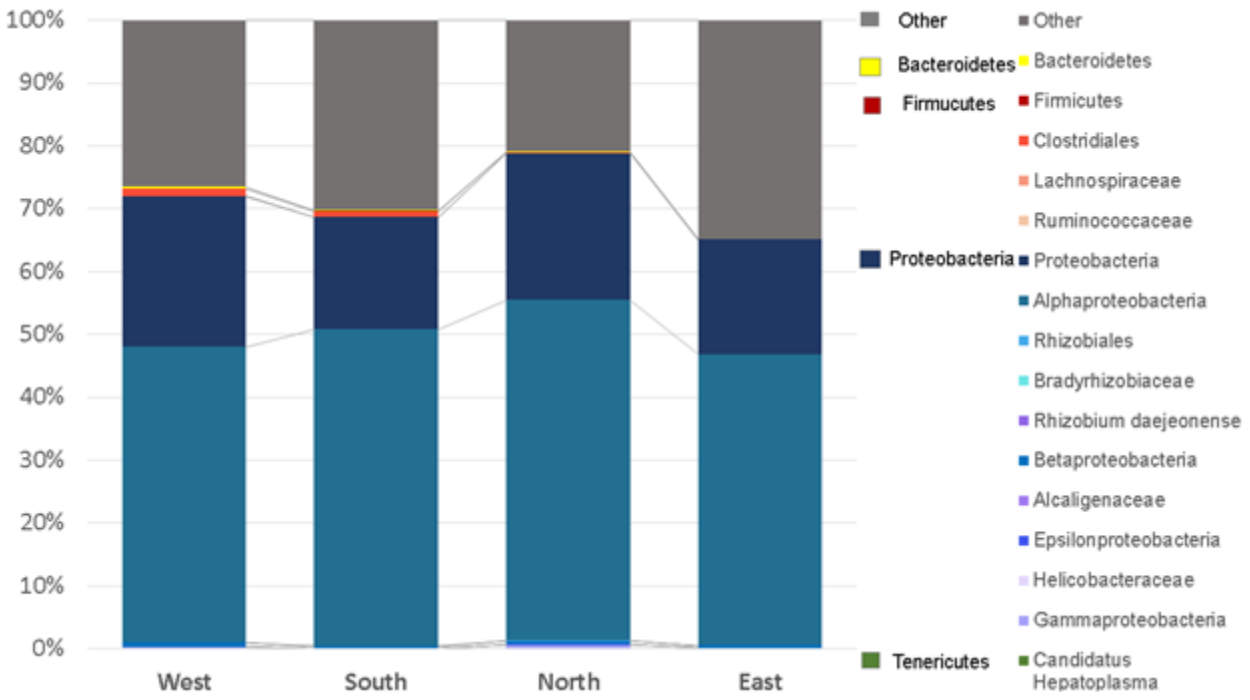

Figure 106. *Intestinal microbiome of D. antillarum (does not) OR correlate(s) with animal collection sites in Puerto Rico.* Collection sites are categozied into west (Rincón), south (Guánica, Ponce, Guayama), North (Luquillo, Isabela) and East (Ceiba, Culebra). Animal numbers for each cardinal grouping include West (n = 10), South (n = 8), North (n = 18) and East (n = 7). Bars indicate the percentage of microbiota present in each sample set by cardinal grouping, which was generated using QIIME2. Here is shown non-log-transformed data.

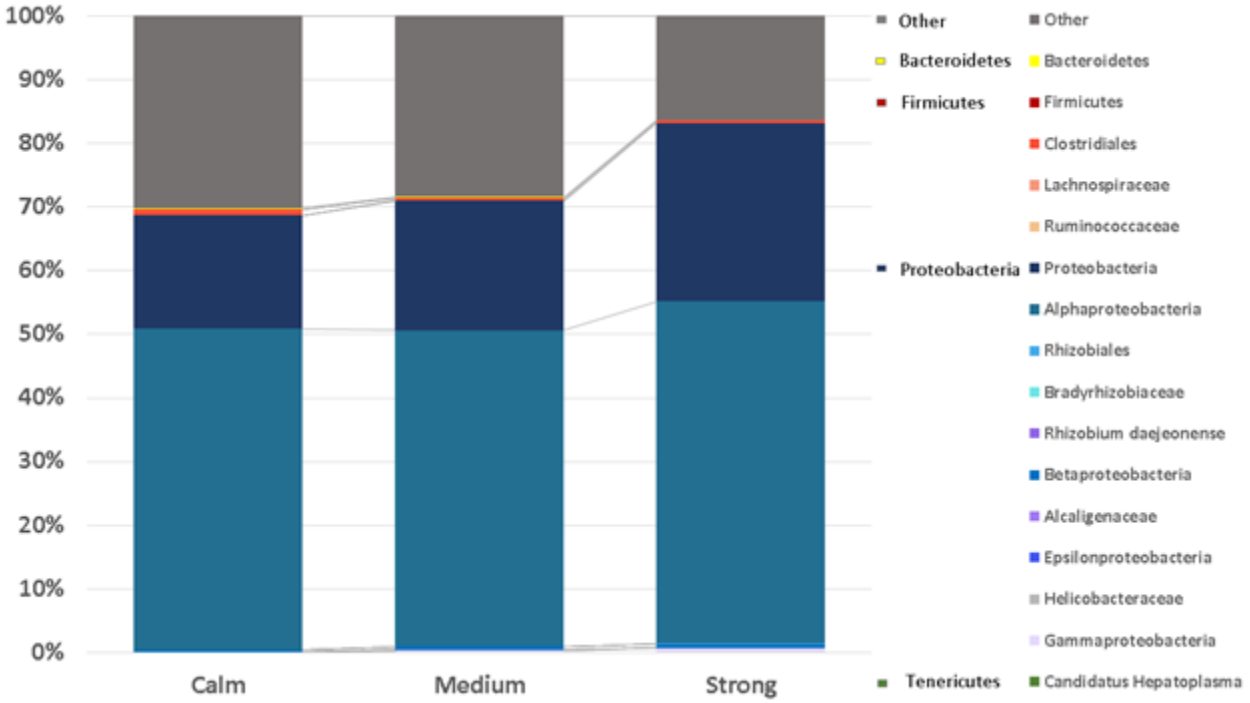

Figure 107. *Intestinal microbiome of D. antillarum (does not) OR correlate(s) with surface water currents in Puerto Rico.* Surface water current is categorized by Calm waters in the South to the Caribbean Sea, Strong waters to the North facing the Atlantic Ocean and Medium waters in the East and West side being in between both bodies of water. Bars indicate the percentage of microbiota present in each sample set by surface current classification, which was generated using QIIME2. Animal sample numbers for each surface current grouping includes calm (n = 8), medium (n = 26) and strong (n = 10). Here is shown non-log-transformed data.

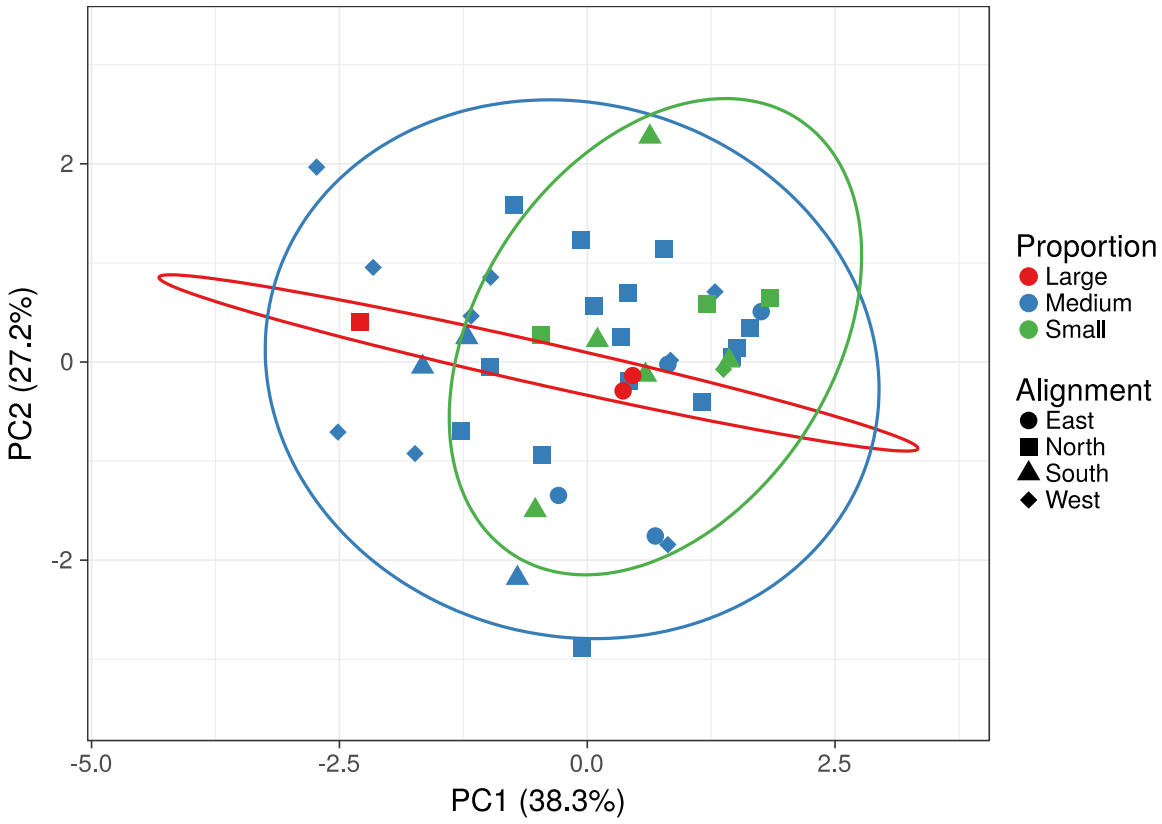

Figure 108. *Principal component plot analysis of the proportion and alignment categories.* Ellipses and circular shapes represent the clustering of sample. Shape and color correspond to the category of the samples.

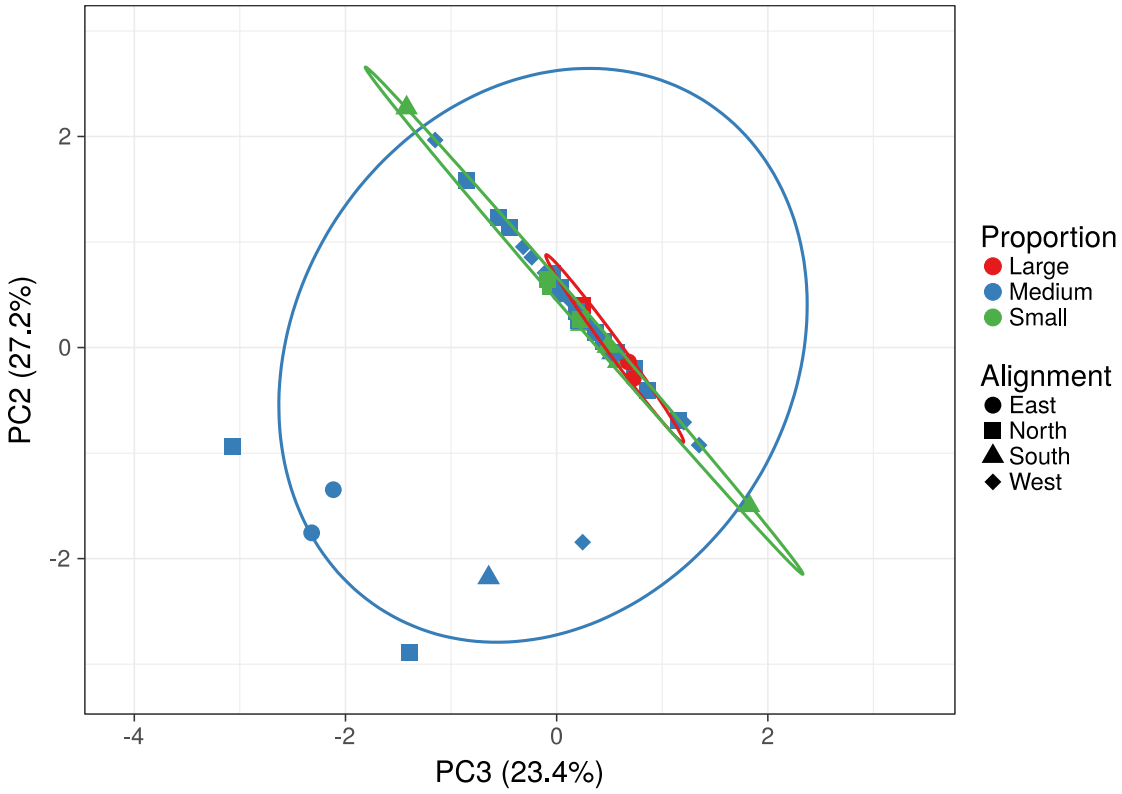

Figure 109. *Principal component analysis of the proportion and alignment categories.* Ellipses and circular shapes represent the clustering of sample. Shape and color correspond to the category of the samples.

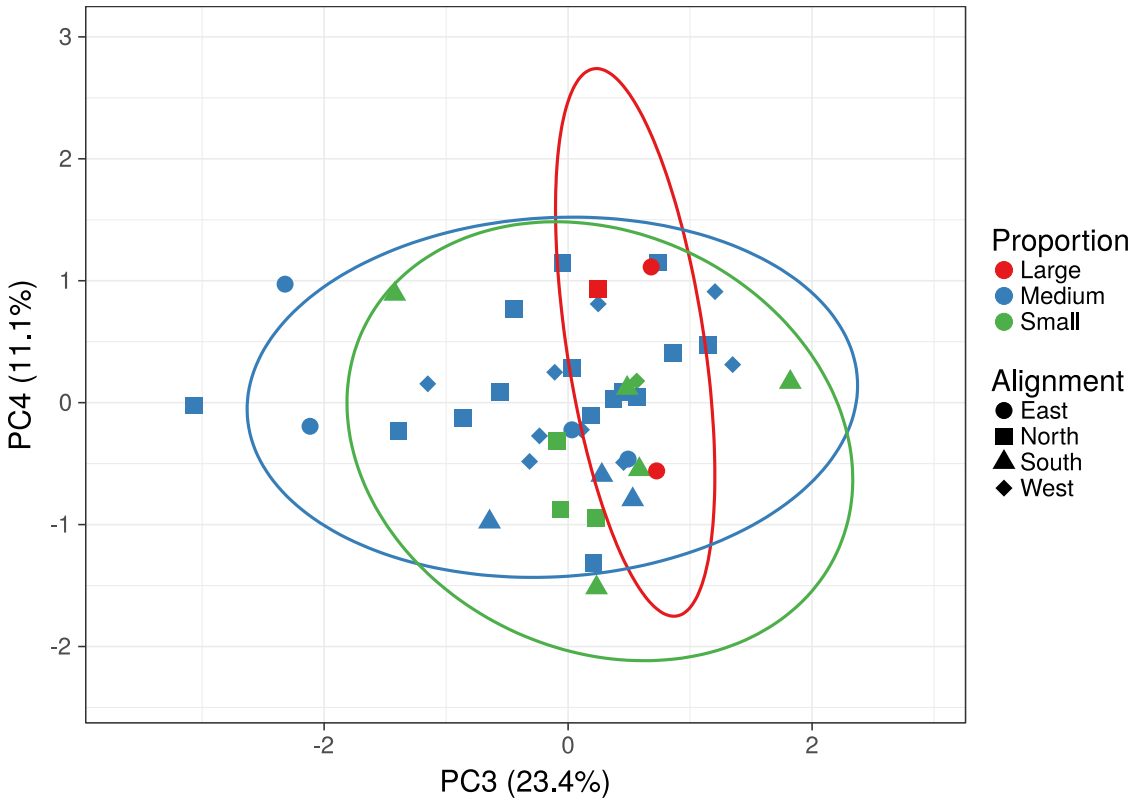

Figure 110. *Principal component analysis of the proportion and alignment categories.* Ellipses and circular shapes represent the clustering of sample. Shape and color correspond to the category of the samples.

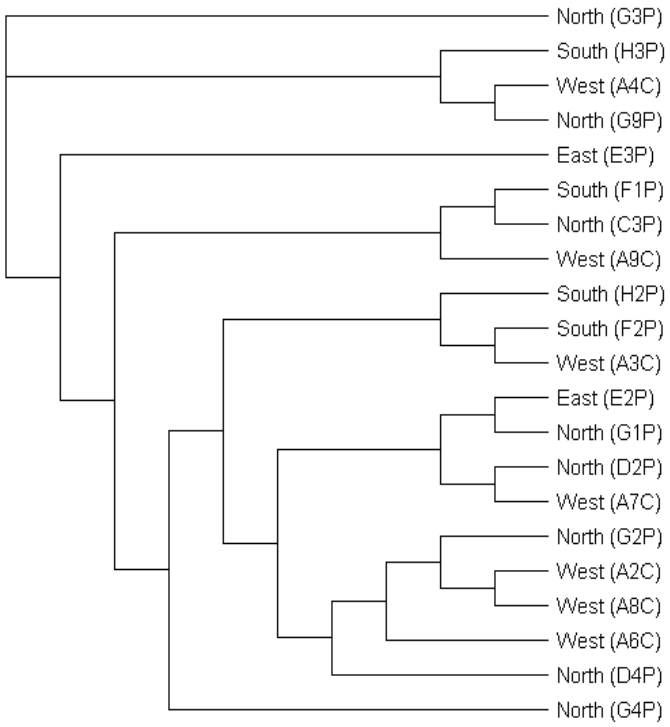

Figure 111. *Phylogenetic tree and cardinal location.* This figure shows the phylogenetic tree along with the cardinal alignments of each sample.

Figure 112. *Reads generated by QIIME2 and 16sRNA data.* Sample statistics that correspond to the 44 samples of the study that were determined after importing them into QIIME2.

sample-id	total-input-reads	total-retained-reads	reads-truncated	reads-too-short-after-truncation	reads-exceeding-maximum-ambiguous-bases
#q2:types	numeric	numeric	numeric	numeric	numeric
A1	25955	25955	0	0	0
A10	26004	26004	0	0	0
A2	33302	33302	0	0	0
A3	42288	42286	0	0	2
A4	50716	50714	0	0	2
A5	17121	17121	0	0	0
A6	17557	17557	0	0	0
A7	27149	27149	0	0	0
A8	33789	33787	0	0	2
A9	33306	33306	0	0	0
B1	29117	29117	0	0	0
B2	64552	64549	0	0	3
B3	31475	31475	0	0	0
C1	33643	33643	0	0	0
C2	20780	20780	0	0	0
C3	26676	26676	0	0	0
C4	17745	17745	0	0	0
C5	52198	52195	0	0	3
D1	28905	28905	0	0	0
D2	43438	43436	0	0	2
D3	36125	36125	0	0	0

D4	51098	51098	0	0	0
D5	20661	20661	0	0	0
E1	27323	27323	0	0	0
E2	24413	24413	0	0	0
E3	35136	35135	0	0	1
E4	44815	44815	0	0	0
E5	80863	80856	0	0	7
E6	37497	37496	0	0	1
E7	30610	30610	0	0	0
F1	26009	26009	0	0	0
F2	36007	36006	0	0	1
G1	31147	31147	0	0	0
G2	28338	28337	0	0	1
G3	32782	32782	0	0	0
G4	22983	22983	0	0	0
G5	27080	27080	0	0	0
G6	50354	50353	0	0	1
G7	30036	30036	0	0	0
G8	32059	32059	0	0	0
G9	37029	37029	0	0	0
H1	22735	22735	0	0	0
H2	33728	33728	0	0	0
H3	28731	28730	0	0	1

Figure 113. *Statistics generated by QIIME2 and 16sRNA data after the filtering step*. Table statistics determined after deblur filtering statistics of the variable 16S rRNA gene region.

sample-id	reads-raw	fraction-artifact-with-minsize	fraction-artifact	fraction-missed-	unique-reads-derep	reads-derep	unique-reads-deblur	reads-deblur	unique-reads-hit-	reads-hit-artifact	unique-reads-	reads-chimeric	unique-reads-hit-	reads-hit-reference	unique-reads-	reads-missed-
E5	80856	0.999802	0	0	7	16	7	13	0	0	0	0	0	0	0	0
D2	43436	0.609771	0	0	1649	16950	400	5435	0	0	111	304	143	4827	0	0
G6	50353	0.60622	0	0	1590	19828	242	5938	0	0	54	266	109	5524	0	0
C5	52195	0.572315	0	0	1472	22323	245	6575	0	0	48	309	97	6068	0	0
B2	64549	0.563944	0	0	1668	28147	291	9920	0	0	77	269	87	9365	0	0
D5	20661	0.498282	0	0	827	10366	168	3371	0	0	36	122	101	3192	0	0
C3	26676	0.477096	0	0	1218	13949	205	4556	0	0	49	175	121	4324	0	0
E3	35135	0.468649	0	0	1074	18669	125	6398	0	0	32	222	55	6095	0	0
A3	42286	0.465568	0	0	1468	22599	161	7805	0	0	32	302	80	7409	0	0

F2	36006	0.446648	0	0	1726	19924	331	6071	0	0	102	306	93	5453	0	0
A8	33787	0.445763	0	0	1543	18726	256	5522	0	0	67	273	115	5096	0	0
E1	27323	0.436738	0	0	1118	15390	256	5439	0	0	59	129	113	5145	0	0
A6	17557	0.422282	0	0	962	10143	230	2865	0	0	54	136	102	2603	0	0
A10	26004	0.421512	0	0	1479	15043	345	4511	0	0	91	300	147	4013	0	0
A2	33302	0.417573	0	0	2038	19396	507	5872	0	0	122	296	188	5166	0	0
C4	17745	0.415046	0	0	1100	10380	307	3283	0	0	73	140	117	2903	0	0
C2	20780	0.393936	0	0	926	12594	109	3621	0	0	26	254	63	3333	0	0
E6	37496	0.387055	0	0	1884	22983	227	7126	0	0	56	214	106	6807	0	0
G1	31147	0.374418	0	0	1668	19485	325	6310	0	0	83	154	132	5911	0	0
B3	31475	0.37201	0	0	1849	19766	369	6473	0	0	78	184	141	6012	0	0
E7	30610	0.366482	0	0	1389	19392	171	6380	0	0	49	221	89	6104	0	0

G8	32059	0.360336	0	0	1563	20507	244	6195	0	0	58	101	126	5979	0	0
G4	22983	0.359788	0	0	1221	14714	224	4897	0	0	68	201	105	4608	0	0
G2	28337	0.359001	0	0	1765	18164	352	5585	0	0	92	283	114	5008	0	0
A4	50714	0.357613	0	0	2883	32578	555	7858	0	0	156	541	168	6839	0	0
F1	26009	0.356723	0	0	1404	16731	229	4537	0	0	47	139	111	4257	0	0
E2	24413	0.354156	0	0	1456	15767	291	4900	0	0	80	216	110	4470	0	0
A7	27149	0.35412	0	0	1550	17535	238	5161	0	0	56	226	121	4820	0	0
A5	17121	0.34484	0	0	966	11217	190	3805	0	0	56	117	97	3614	0	0
H2	33728	0.340074	0	0	1896	22258	324	6751	0	0	102	336	136	6249	0	0
G5	27080	0.336484	0	0	1521	17968	204	5597	0	0	58	139	101	5370	0	0
E4	44815	0.32922	0	0	1956	30061	218	10503	0	0	49	237	98	10135	0	0
A9	33306	0.320363	0	0	1971	22636	232	6450	0	0	66	214	106	6125	0	0

A1	25955	0.315161	0	0	1344	17775	164	5757	0	0	45	150	86	5546	0	0
B1	29117	0.315039	0	0	1586	19944	184	6017	0	0	52	266	89	5677	0	0
D4	51098	0.313554	0	0	2916	35076	428	11225	0	0	104	458	154	10427	0	0
D3	36125	0.312692	0	0	2090	24829	420	7666	0	0	80	261	139	6987	0	0
H3	28730	0.31253	0	0	1651	19751	202	6321	0	0	49	110	97	6109	0	0
H1	22735	0.303981	0	0	1293	15824	198	5509	0	0	41	110	116	5317	0	0
G9	37029	0.298172	0	0	2155	25988	268	7912	0	0	73	256	114	7508	0	0
D1	28905	0.286871	0	0	1755	20613	508	7055	0	0	142	426	146	6186	0	0
G3	32782	0.278568	0	0	1870	23650	214	7168	0	0	65	285	86	6743	0	0
G7	30036	0.278133	0	0	1710	21682	184	6519	0	0	42	89	100	6363	0	0
C1	33643	0.264007	0	0	1731	24761	189	7056	0	0	40	385	96	6574	0	0